Connections of the amygdaloid structures integrating olfactory and vomeronasal information in mice

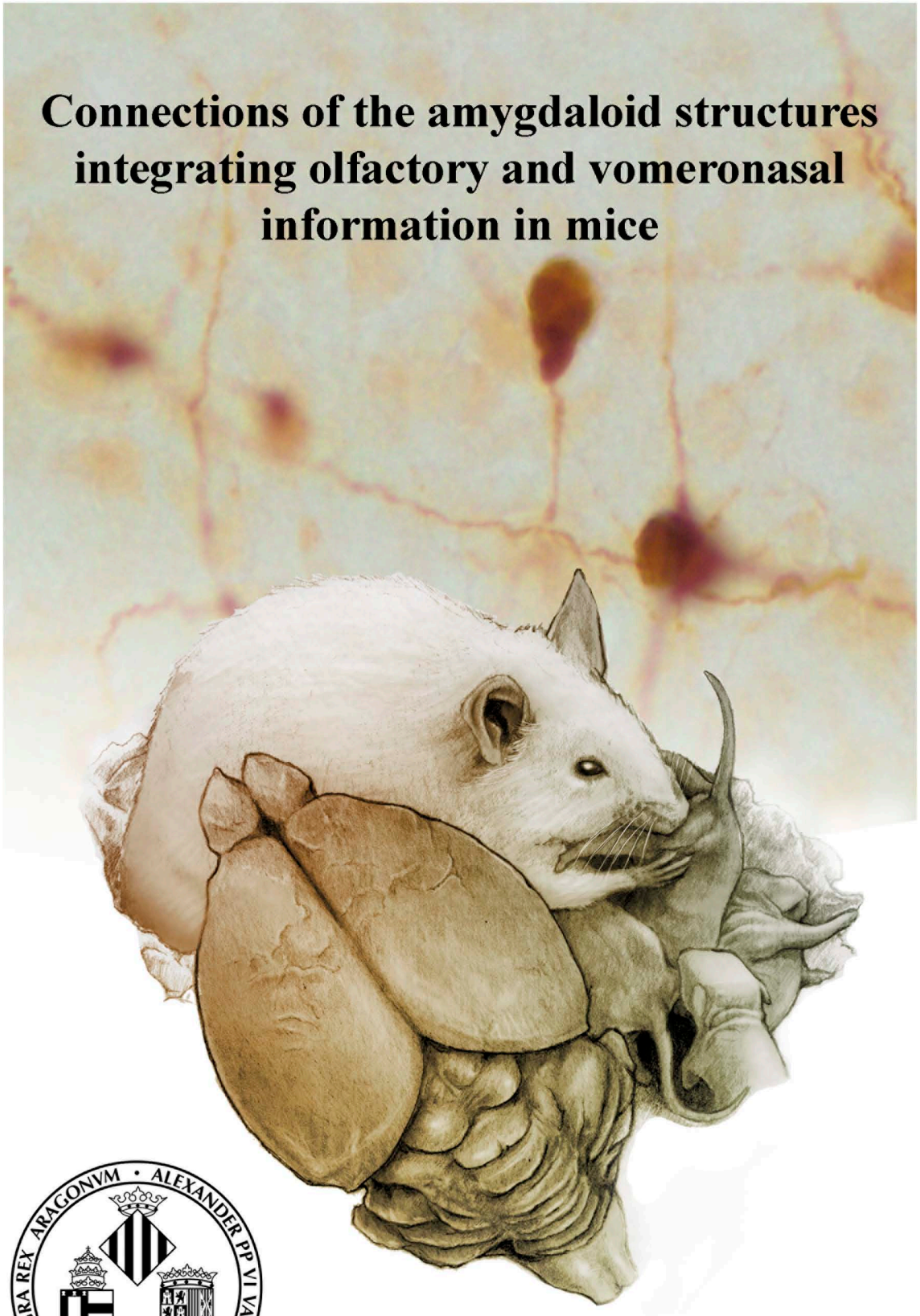

Doctorando: **Bernardita Cádiz Moretti**

Director de Tesis: **Enrique Lanuza Navarro**

Programa de Doctorado en Neurociencia

VNIVERSITAT DE VALÈNCIA

VNIVERSITAT DE VALÈNCIA

Connections of the amygdaloid structures integrating olfactory and vomeronasal information in mice

(Estudio de las conexiones de las estructuras amigdalinas que integran la información vomeronasal y olfatoria en ratón)

Doctorando: **Bernardita Cádiz Moretti**

Director de Tesis: **Enrique Lanuza Navarro**

Programa de Doctorado en Neurociencias

Depto. de Biología Celular y Parasitología

D. Enrique Lanuza Navarro, Doctor en Biología y Profesor Titular del Departamento de Biología Celular y Parasitología de la Universitat de València,

C E R T I F I C A

que Dña. **Bernardita José Cádiz Moretti**, licenciada en Ciencias con mención en Biología por la Universidad de Chile, y Máster en Neurociencias Básicas y Aplicadas por la Universitat de València, ha realizado bajo su dirección el trabajo titulado "**Estudio de las conexiones de las estructuras amigdalinas que integran la información vomeronasal y olfatoria en ratón**" para optar al Grado de Doctor en Biología en el Programa de Doctorado en Neurociencias.

Para que conste, en cumplimiento de la legislación vigente, hagos constar que dicho trabajo recibe mi **INFORME FAVORABLE** y firmo el presente certificado a 6 de noviembre de 2014

Dr. Enrique Lanuza Navarro

The author of this thesis is a scholarship recipient of the “Becas Chile” program of the Government of Chile.

This work has been funded by the Spanish Ministry of Science-FEDER (BFU 2010-16656 and BFU 2013-47688-P) and the Junta de Comunidades de Castilla-La Mancha (PEIC11-0045-4490).

The artwork of the cover is authored by Hugo Saláis López, predoctoral student of the Neuroscience programme at the Dept. of Functional Biology, to whom the author is greatly indebted.

ACKNOWLEDGMENTS

First of all, I would like to thank my tutor, Quique, for giving me the opportunity to join his laboratory and do my PhD work with him. I am really grateful for his dedication and patience, because despite his amount of work, he has always had a moment to answer all my questions. I would also like to thank to Fernando, whose ideas and knowledge were vey helpful for the development of this work. In addition, I would like to thank Dori, because of her dedication to keep this laboratory always on the move and order. And of course, I would like to thank all my laboratory mates, Lluis, Marcos, Ana, Ceci and Hugo, for all the time they spent teaching and helping me. Thanks to the newest ones too, Pau, Maria and Guille. With all this group of people that form this laboratory, we spent nice moments discussing about brain circuitries, their functions and possible roles in behaviours. All of them made me feel at ease.

I would like to thank my family, despite the distance, they supported me in this adventure. To all my friends, the ones that I left in Chile and those that I met here, because they join me during these last four years.

Finally, apart from all scientific knowledge, I appreciate all the things that I have learned at a personal level and my personal growth.

INDEX

ABBREVIATIONS

I	layer I
IA	Layer IA
IB	Layer IA
II	layer II
IIA	layer IIA
IIB	layer IIB
2Cb	2nd Cerebellar lobule
III	layer 3
3V	3rd ventricle
4V	4th ventricle
7n	facial nerve or its root
8n	vestibulocochlear nerve
8vn	vestibular root of the vestibulocochlear nerve
AA	anterior amygdaloid area
AAD	anterior amygdaloid area, dorsal part
AAV	anterior amygdaloid area, ventral part
aca	anterior commissure, anterior part
Acb	accumbens nucleus
AcbC	accumbens nucleus, core
AcbSh	accumbens nucleus, shell
aci	anterior commissure, intrabulbar part
ACo	anterior cortical amygdaloid nucleus
acp	anterior comissure, posterio
AH	anterior hypothalamic area
AHA	anterior hypothalamic area, anterior part
AHC	anterior hypothalamic area, central part
AHi	amygdalohippocampal area
AHP	anterior hypothalamic area, posterior part
AI	agranular insular cortex
AID	agranular insular cortex, dorsal part
AIP	agranular insular cortex, posterior part
AIV	agranular insular cortex, ventral part
AO	anterior olfactory nucleus
AOB	accessory olfactory bulb
AOM	anterior olfactory nucleus, medial part
AON	anterior olfactory nucleus
AOP	anterior olfactory nucleus, posterior part
APir	amygdalopiriform transition area
Aq	aqueduct
Arc	arcuate hypothalamic nucleus
BAOT	bed nucleus of the accessory olfactory tract
BLA	basolateral amygdaloid nucleus, anterior part
BLP	basolateral amygdaloid nucleus, posterior part
BLV	basolateral amygdaloid nucleus, ventral part

BMA	basomedial amygdaloid nucleus, anterior part
BMP	basomedial amygdaloid nucleus, posterior part
BST	bed nucleus of the *stria terminalis*
BSTIA	BST, intraamygdaloid division
BSTLP	BST, lateral division, posterior part
BSTLV	BST, lateral division, ventral part
BSTMA	BST, medial division, anterior part
BSTMPI	BST, medial division, posterointermediate part
BSTMPL	BST, medial division, posterolateral part
BSTMPM	BST, medial division, posteromedial part
BSTMV	BST, medial division, ventral part
BSTS	bed nucleus of stria terminalis, supracapsular part
CA1	field CA1 of hippocampus
CA3	field CA3 of hippocampus
Ce	central amygdaloid nucleus
CeC	central amygdaloid nucleus, capsular part
CeL	central amygdaloid nucleus, lateral division
CeM	central amygdaloid nucleus, medial division
Cl	claustrum
CM	central medial thalamic nucleus
cp	cerebral peduncle
CPu	caudate putamen
csc	commissure of the superior colliculus
cst	commissural stria terminalis
CxA	cortex-amygdala transition zone
D3V	dorsal 3rd ventricle
DEn	dorsal endopiriform nucleus
DG	dentate gyrus
dlot	dorsal lateral olfactory tract
DM	dorsomedial hypothalamic nucleus
DP	Dorsal peduncular cortex
DR	dorsal raphe nucleus
DTT	dorsal *tenia tecta*
E/OV	ependymal and subendymal layer/olfactory ventricle
ec	external capsule
Ect	ectorhinal cortex
eml	external medullary lamina
EPl	external plexiform layer of the olfactory bulb
EPlA	external plexiform layer of the accessory olfactory bulb
f	fornix
FC	Frontal cortex
fi	fimbria of the hippocampus
fmi	forceps minor of the corpus callosum
fr	fasciculus retroflexus
Gl	glomerular layer of the olfactory bulb
GlA	glomerular layer of the AOB
GrA	granule cell layer of the AOB
GrO	granular cell layer of the olfactory bulb
HDB	nucleus of the horizontal limb of the diagonal band
I	intercalated nuclei of the amygdala

ic	internal capsule
ICj	islands of Calleja
IF	interfascicular nucleus
IL	infralimbic cortex
IM	intercalated amygdaloid nucleus, main part
IMD	intermediodorsal thalamic nucleus
IP	interpeduncular nucleus
IPAC	interstitial nucleus of the posterior limb of the anterior commissure
IPl	internal plexiform layer of the olfactory bulb
LA	lateroanterior hypothalamic nucleus
La	lateral amygdaloid nucleus
LaDL	lateral amygdaloid nucleus, dorsolateral part
LaVL	lateral amygdaloid nucleus, ventrolateral part
LaVM	lateral amygdaloid nucleus, ventromedial part
LC	locus coeruleus
Ld	lambdoid septal zone
LDTg	laterodorsal tegmental nucleus
LEnt	lateral entorhinal cortex
LGP	lateral globus pallidus
LH	lateral hypothalamic area
LHb	lateral habenular nucleus
LPB	lateral parabrachial nucleus
LPO	lateral preoptic area
LO	lateral orbital cortex
lo	lateral olfactory tract
LOT	nucleus of the lateral olfactory tract
LPO	lateral preoptic area
LSD	lateral septal nucleus, dorsal part
LSI	lateral septal nucleus, intermediate part
LSV	lateral septal nucleus, ventral part
LV	lateral ventricle
mcp	middle cerebellar peduncle
MCPO	magnocellular preoptic nucleus
MD	mediodorsal thalamic nucleus
ME	median eminence
Me	medial amygdaloid nucleus
MeA	medial amygdaloid nucleus, anterior subdivision
me5	mesencephalic trigeminal tract
MeAD	medial amygdaloid nucleus, anterodorsal subdivision
MeAV	medial amygdaloid nucleus, anteroventral subdivision
MeP	Medial amygdaloid nucleus, posterior subdivision
MePD	medial amygdaloid nucleus, posterodorsal subdivision
MePV	medial amygdaloid nucleus, posteroventral subnucleus
MGD	medial geniculate nucleus, dorsal part
MGM	medial geniculate nucleus, medial part
MGV	medial geniculate nucleus, ventral part
MHb	medial habenular nucleus
Mi	mitral cell layer of the olfactory bulb
MiA	mitral cell layer of the AOB
mfb	medial forebrain bundle

ml	medial lemniscus
mlf	medial longitudinal fasciculus
MM	medial mammillary nucleus, medial part
MnR	median raphe nucleus
MO	medial orbital cortex
MOE	Main olfactory epithelium
Mo5	motor trigeminal nucleus
MOB	main olfactory bulb
MPA	medial preoptic area
MPB	medial parabrachial nucleus
MPO	medial preoptic nucleus
MS	medial septal nucleus
mt	mammillothalamic tract
mtg	mammillotegmental tract
ns	nigrostriatal bundle
OB	Olfactory bulb
opt	optic tract
ox	optic chiasm
Pa	paraventricular hypothalamic nucleus
PAG	periaqueductal gray
PB	parabrachial nucleus
pc	posterior commissure
Pe	periventricular hypothalamic nucleus
PF	parafascicular thalamic nucleus
PH	posterior hypothalamic area
PIL	posterior intralaminar thalamic nucleus
Pir	piriform cortex
PLCo	posterolateral cortical amygdaloid nucleus
PMCo	posteromedial cortical amygdaloid nucleus
PMD	premammillary nucleus, dorsal part
PMV	premammillary nucleus, ventral part
PnC	pontine reticular nucleus, caudal part
Po	posterior thalamic nuclear group
PP	peripeduncular nucleus
Pr5VL	principal sensory trigeminal nucleus, ventrolateral part
PRh	perirhinal cortex
PrL	prelimbic cortex
pv	periventricular fiber system
PV	paraventricular thalamic nucleus
PVA	paraventricular thalamic nucleus, anterior part
PVP	paraventricular thalamic nucleus, posterior part
Py	piramidal cell layer of the hippocampus
py	pyramidal tract
RCh	retrochiasmatic area
Re	reuniens thalamic nucleus
Rh	rhomboid thalamic nucleus
RLi	rostral linear nucleus of the raphe
RMC	red nucleus, magnocellular part
S	subiculum
s5	sensory root of the trigeminal nerve

scp	superior cerebellar peduncle
SG	suprageniculate thalamic nucleus
SHi	septohippocampal nucleus
SI	*substantia innominata*
SL	semilunar nucleus
sm	*stria medullaris*
SNC	*substantia nigra, compact part*
SNR	*substantia nigra, reticular part*
sox	supraoptic decussation
sp5	spinal trigeminal tract
SPF	subparafascicular thalamic nucleus
SPFPC	Subparafascicular thalamic nucleus, parvicellular part
st	*stria terminalis*
str	superior thalamic radiation
Su5	supratrigeminal nucleus
SuM	supramammillary nucleus
SuMM	supramammillary nucleus, medial part
TC	tuber cinereum area
Tu	olfactory tubercle
unc	*uncinate fasciculus*
VDB	nucleus of the vertical limb of the diagonal band
VEn	ventral endopiriform nucleus
VL	ventrolateral thalamic nucleus
VMH	ventromedial hypothalamic nucleus
VNO	Vomeronasal organ
VO	ventral orbital cortex
VP	ventral pallidum
vsc	ventral spinocerebellar tract
VTA	ventral tegmental area
VTT	ventral *tenia tecta*
ZI	*zona incerta*
ZID	zona incerta, dorsal part
ZIV	zona incerta, ventral part

1. GENERAL INTRODUCTION

1. GENERAL INTRODUCTION

The detection of environmental chemicals gives valuable information about the external conditions in which an organism is living, and enables it to generate proper behavioural responses for its survival. The environmental chemicals are detected by chemical sensory organs present from the most primitive forms of life to the most complex ones. These molecules are sensed by the olfactory systems in vertebrates. Most tetrapods present two olfactory systems, the olfactory and vomeronasal (Ubeda-Bañon et al. 2011). These systems have been identified in some teleost fishes, such as the lungfishes (Gonzalez et al. 2010), in amphibians such as Xenopus and Bufo (Taniguchi et al. 2008), in lizards (Martinez-Garcia et al. 1991) and snakes (Lanuza and Smeets, 1993) among the reptiles, in marsupials such as opossum (Martinez-Marcos and Halpern, 2006; Martinez-Marcos and Halpern, 1999) and in placental mammals such as mice (Cadiz-Moretti et al. 2013; Kang et al. 2009) and rats (Pro-Sistiaga et al. 2007). On the other hand, birds do not have a vomeronasal system (Ubeda-Bañon et al. 2011), while in primates the vomeronasal system is poorly developed (platyrrhini), vestigial (hominidae) or lost (catarrhini) (Ubeda-Bañon, et al 2011).

In rodents, the olfactory stimuli play an essential role in the acquisition of socio-sexual information about conspecifics, possible predators and food. These chemical molecules are sensed by its main sensorial system, which is chemosensation (rodents are macrosmatic mammals). The chemosensory organs include the main olfactory epithelium (MOE), which is activated mainly by volatile stimuli and the vomeronasal organ (VNO), which is activated by non-volatile stimuli (Gutiérrez-Castellanos et al. 2010). Recent studies have shown that the non-volatile stimuli detected by the vomeronasal organ contained important information for the proper development of social and reproductive behaviours in rodents (Chamero et al. 2012). In fact, the molecules detected by the vomeronasal system trigger innate behavioural responses, suggesting that some chemical cues have an intrinsic biological value for the species, such as sexual pheromones (Gutiérrez-Castellanos et al. 2010).

One of the main conclusion of the previous works done by our group and others in the field of olfactory and pheromone research, is that the main and accessory systems interact in the detection of chemical substances present in the environment and play a

complementary role in the generation of appropriate behavioural responses (Baum and Kelliher, 2009; Keller et al. 2009; Martínez-García et al. 2009). In this complementary role a key aspect is the learning process in which odorants become associated with unconditioned stimuli with either positive (e.g., sexual pheromones, food) or negative (e.g., predator odours) value. A particularly interesting type of learning is that involving chemical signals that posses a positive emotional value, such as sexual pheromones. It has been suggested that the sexual pheromones detected by the vomeronasal system, may act as unconditioned stimuli that are associated with neutral odorants detected by the olfactory systems, which would act as conditioned stimuli (Moncho-Bogani et al. 2002; Roberts et al. 2010). This kind of learning probably takes place in the amygdala, as it has been shown for the case of olfactory fear conditioning (Cousens and Otto, 1998), although the amygdaloid nuclei involved are unknown. For the olfactory-vomeronasal association to occur, the information detected by the vomeronasal organ and the main olfactory epithelium should eventually converge.

The MOE projects to the main olfactory bulb (MOB), while the VNO projects to the accessory olfactory bulb (AOB). Anatomical tracing experiments have shown that the MOB and AOB send afferent projections to cortical and non-cortical nuclei of the amygdala, converging in some of these nuclei such as the ventral part of the anterior amygdaloid area, the medial amygdaloid nucleus (Me), cortex-amygdala transition zone (CxA) and anterior cortical amygdaloid nucleus (ACo) (Pro-Sistiaga et al. 2007; Kang et al. 2009; Cadiz-Moretti et al. 2013). Therefore, it is likely that the association between vomeronasal and olfactory stimuli (e.g. pheromones and odours) may occur in some of these amygdaloid nuclei. These nuclei are possible candidates areas where this kind of appetitive learning can take place.

Our study is focused on the anatomical bases underliying these kind of appetitive emotional learning. Our initial hypothesis is that the corticomedial amygdala (which received the strongest projections arising from the olfactory and vomeronasal bulbs) is the main candidate to play a key role in this learning process.

Within the corticomedial amygdala, the medial amygdaloid nucleus (Me) is the main area of convergence of vomeronasal and olfactory stimuli. It has been extensively studied since it is considered a key structure in the neural circuit that controls sociosexual behaviours. The Me is a heterogeneous structure presenting three

subdivisions, the anterior, posteroventral and posterodorsal parts. These subdivisions present differential efferent connections within the encephalon (Pardo-Bellver et al. 2012) and more specifically, with brain structures implicated in reproductive and defensive behaviours (Canteras et al. 1995). It is also sexually dimorphic (Simerly et al. 1990). Regardless to its well characterized efferent connections, there is very little information about the afferent projections to the Me, and no previous study has been focused in the inputs to the Me subnuclei. The remaining amygdaloid nucleus where the vomeronasal and olfactory converge, such as the cortex-amygdala transition zone (CxA) and the anterior cortical amygdaloid nucleus (ACo) have been scarcely studied.

Our work is focused on the description of the afferent connections to the three subdivisions of the Me, together with the description of the afferent connections of the CxA and ACo. With these studies, we try to enlight important information regarding to the anatomical connections of these nuclei with the encephalon and the possible role of these circuitries in the associative learning of odours and pheromones and its effects in sociosexual behaviours.

This doctoral thesis is organized in three chapters. In chapter 1, we describe the efferent projections arising from the AOB and MOB to the amygdala and the amygdaloid nuclei where these projections converge. This chapter has already been published (Cadiz-Moretti et al. 2013). In chapter 2, we describe the afferent connections of the three subdivisions of the Me and discuss its functions implications. This chapter is now accepted for publication in the journal of Brain, Structure and Function. In chapter 3, we describe the afferent connections to the CxA and ACo and discuss its functional implications. This last chapter is going to be submitted to a neuroscience journal.

1.1 References

Baum MJ, Kelliher KR (2009) Complementary roles of the main and accessory olfactory systems in mammalian mate recognition. Annu Rev Physiology 71:141-160.

Cadiz-Moretti B, Martinez-Garcia F., Lanuza E (2013) Neural Substrate to Associate Odorants and Pheromones: Convergence of Projections from the Main and Accessory Olfactory Bulbs in Mice. In: Chemical Signals in Vertebrates 12, East ML, Dehnhard M, editors. Springer Science: New York. p 3-16.

Canteras NS, Simerly RB, Swanson LW (1995) Organization of projections from the medial nucleus of the amygdala: a PHAL study in the rat. J Comp Neurol 360:213-245.

Chamero P, Leinders-Zufall T, Zufall F (2012) From genes to social communication: molecular sensing by the vomeronasal organ. Trends Neurosci 35:597-606.

Cousens G, Otto T (1998) Both pre- and posttraining excitotoxic lesions of the basolateral amygdala abolish the expression of olfactory and contextual fear conditioning Behav Neurosci 112:1092-1103.

Gonzalez A, Morona R, Lopez JM, Moreno N, Northcutt RG (2010) Lungfishes, like tetrapods, possess a vomeronasal system. Front Neuroanat 4:10.3389/fnana.2010.00130. eCollection 2010.

Gutiérrez-Castellanos N, Martínez-Marcos A, Martínez-García F, Lanuza E (2010) Chemosensory function of the amygdala. In: Vitamins & Hormones - Pheromones, Litwack G, editor. Elsevier Acad. Press.: London. .

Kang N, Baum MJ, Cherry JA (2009) A direct main olfactory bulb projection to the 'vomeronasal' amygdala in female mice selectively responds to volatile pheromones from males. Eur J Neurosci 29:624-634.

Keller M, Baum MJ, Brock O, Brennan PA, Bakker J (2009) The main and the accessory olfactory systems interact in the control of mate recognition and sexual behavior. Behav Brain Res 200:268-276.

Lanuza E, Halpern M (1998) Efferents and centrifugal afferents of the main and accessory olfactory bulbs in the snake Thamnophis sirtalis. Brain Behav Evol 51:1-22.

Martínez-García F, Novejarque A, Lanuza E (2009) Evolution of the amygdala in vertebrates. In: Evolutionary Neuroscience, J Kaas, editor. Elsevier Academic Press: Oxford (U.K.). p 313-392.

Martinez-Garcia F, Olucha FE, Teruel V, Lorente MJ, Schwerdtfeger WK (1991) Afferent and efferent connections of the olfactory bulbs in the lizard Podarcis hispanica. J Comp Neurol 305:337-347.

Martinez-Marcos A, Halpern M (2006) Efferent connections of the main olfactory bulb in the opossum (Monodelphis domestica): a characterization of the olfactory entorhinal cortex in a marsupial. Neurosci Lett 395:51-56.

Martinez-Marcos A, Halpern M (1999) Differential projections from the anterior and posterior divisions of the accessory olfactory bulb to the medial amygdala in the opossum, Monodelphis domestica. Eur J Neurosci 11:3789-3799.

Moncho-Bogani J, Lanuza E, Hernandez A, Novejarque A, Martinez-Garcia F (2002) Attractive properties of sexual pheromones in mice. Innate or learned? Physiol Behav 77:167-176.

Pardo-Bellver C, Cadiz-Moretti B, Novejarque A, Martinez-Garcia F, Lanuza E (2012) Differential efferent projections of the anterior, posteroventral, and posterodorsal subdivisions of the medial amygdala in mice. Front Neuroanat 6:33.

Pro-Sistiaga P, Mohedano-Moriano A, Ubeda-Banon I, Del Mar Arroyo-Jimenez M, Marcos P, Artacho-Perula E, Crespo C, Insausti R, Martinez-Marcos A (2007) Convergence of olfactory and vomeronasal projections in the rat basal telencephalon. J Comp Neurol 504:346-362.

Roberts SA, Simpson DM, Armstrong SD, Davidson AJ, Robertson DH, McLean L, Beynon RJ, Hurst JL (2010) Darcin: a male pheromone that stimulates female memory and sexual attraction to an individual male's odour BMC Biol 8:75-7007-8-75.

Simerly RB, Chang C, Muramatsu M, Swanson LW (1990) Distribution of androgen and estrogen receptor mRNA-containing cells in the rat brain: an in situ hybridization study. J Comp Neurol 294:76-95.

Taniguchi K, Saito S, Oikawa T, Taniguchi K (2008) Phylogenic aspects of the amphibian dual olfactory system. J Vet Med Sci 70:1-9.

Ubeda-Banon I, Pro-Sistiaga P, Mohedano-Moriano A, Saiz-Sanchez D, de la Rosa-Prieto C, Gutierrez-Castellanos N, Lanuza E, Martinez-Garcia F, Martinez-Marcos A (2011) Cladistic analysis of olfactory and vomeronasal systems. Front Neuroanat 5:3.

2. MATERIAL AND METHODS

2. MATERIAL AND METHODS

Animals

For this work, 105 adult female mice (Mus musculus) from the CD1 strain (experiment 1 from Charles River, LÁrbresle Cedex, Francia and experiments 2 and 3 from Janvier, Le Genest Saint-Isle, France), which were 8-27 weeks old and weighed 24.7-53.2 g were used. They were kept in cages with food and water *ad libitum* in a 12 h light:dark cycle at 25-26 °C. The mice were treated according to the guidelines of the European Union Council Directive of June 3rd, 2010 (6106/1/10 REV1). The Committee of Ethics on Animal Experimentation of the University of Valencia approved the experimental procedures.

Surgery and tracer injections

The first 29 animals were anaesthetised with intraperitoneal (IP) injections of a 3:2 ketamine (75 mg/kg, Merial laboratories, Barcelona, Spain) and medotomedine (1 mg/kg, Pfizer, Alcobendas, Madrid, Spain) solution, complemented with atropine (Sigma, St. Louis, MO, USA; 0.04 mg/kg, IP) to reduce cardio-respiratory depression. The remaining 76 animals were anaesthetized with a newly acquired vapour anaesthetic system. They received isofluorane (2-2.5%) delivered in oxygen (1-1.3 L/min) (MSS Isoflurane Vaporizer, Medical Supplies and Services, UK) using a mouse anaesthetic mask and a subcutaneous butorfanol injection (5 mg/kg, Turbugesic, Pfizer, New York, USA,) as analgesic. After fixing the mouse head in the stereotaxic apparatus (David Kopf, 963-A, Tujunga CA, USA), a small hole was drilled above the target zone.

Experiment 1: To study the projections arising from the AOB and the MOB, 37 animals received iontophoretic injections of dextranamine (10,000 MW, lysine fixable, Invitrogen, Carlsbad, CA, USA) conjugated with tetramethylrhodamine and biotin (TBDA) diluted at 5% in diluted in phosphate buffer (PB; 0.01 M, pH 8.0).

Experiment 2: To study the afferents to the three subdivisions of the medial amygdaloid nucleus, 28 mice received iontophoretic injections of the fluorescent retrograde tracer Fluoro-Gold (FG) (Hydroxystilbamidine bis(methanesulfonate), Sigma-Aldrich, Cat # 39286) diluted at 2% in distilled water.

Experiment 3: To study the afferents to the cortex-amygdala transition zone and the anterior cortical amygdaloid nucleus, 40 mice received iontophoretic injections of FG. In addition, to minimize the number of animals, and to study the efferent connections of the CxA and ACo, the anterograde tracer Biotin-conjugated dextranamine (BDA, 10,000 MW, lysine fixable, Invitrogen, Carlsbad, CA, USA) was delivered in the contralateral hemisphere, diluted at 5% in PB (0.01M, pH 8.0) (the results of the anterograde projections of these nuclei will be present in other study).

The tracers were delivered from glass micropipettes (10–50 μm diameter tips for experiment 1 and 20-30 μm for experiment 2 and 3) by means of positive current pulses (7on/7off seconds) with the following parameters: 3–5 μA during 10 to 15 min for **experiment 1;** 3 μA during 3 min for the **experiment 2;** and in **the experiment 3**, 2 μA during 2-3 minutes for the CxA injections and 2-3 μA during 3-6 minutes for the ACo injections. To avoid diffusion of the tracer along the pipette track, a mild retention current (-0.8 to – 0.1μA) was applied during the entrance and withdrawal of the micropipette and in addition, after finishing the injection, the tip was left in place for 2 minutes in experiment 1 and 10 minutes in experiments 2 and 3. Injection coordinates relative to Bregma were adapted to the CD1 mice from the atlas of the mouse brain (Paxinos and Franklin, 2004). The coordinates for each injection site were the following: **Experiment 1**: ventral MOB: AP 4.25 mm; L 0.95 mm and DV -3.22 mm; AOB: AP 3.57 mm; L 0.95 mm and DV -0.90 mm. **Experiment 2**: MeA: AP -1.40 to -1.45 mm, L -2.0 to -2.1mm, DV -5.55 to -5.60 mm; MePV: AP -1.9mm, L -2.05 to -2.10 mm, DV -5.48; MePD: AP -1.9mm, L - 2.1mm and DV -5.18mm. **Experiment 3**: rostral CxA: AP -0.09 to -0.2 mm, L -2.89 to -2.94 mm, DV -6.04 mm; caudal CxA: AP -1.4 mm, L - 2.8 mm, DV -6.02; ACo: AP -0.8 to – 1.5 mm, L - 2.55 to -2.8 mm and DV -5.97 to -6.02 mm.

After the injection, the wound was closed with Histoacryl (Braun, Tuttlinger, Germany) and in the case of those animals anaesthetized with the ketamine/medotomedine solution, an intramuscular injection of atipamezol (Pfizer, Alcobendas, Madrid, Spain; 1 mL/kg) was used to revert the medotomedine effects. During the whole procedure, animals rested on a thermic blanket to maintain their body temperature, and they received eye drops (Siccafluid, Thea S.A Laboratories, Spain) to prevent eye ulceration.

Histology

After 3-5 days of survival for experiment 1, 6-8 days for experiment 2 and 3, animals were deeply anaesthetised with an overdose of sodium pentobarbital (Sigma, 90 mg/kg) for experiment 1 or sodium pentobarbital (intraperitoneal, 100mg/kg, Eutanax, Laboratorios Normon S.A. Madrid, Spain) for experiments 2 and 3. Then, they were perfused transcardially with saline solution (0.9%) followed by 4% paraformaldehyde diluted in PB (0.1 M, pH 7.6). Following perfusion, brains were removed from the skull, postfixed for 4 h in the same fixative and cryoprotected with 30% sucrose in PB (0.1M, pH 7.6) until they sank. Using a freezing microtome, parasagittal sections (30 μm) from the bulbs and frontal sections (40 μm) from the rest of the brain were obtained. In both cases, sections were collected in four parallel series.

For the detection of the TBDA or BDA tracers, endogenous peroxidase was inactivated with 1% H_2O_2 in Tris buffer saline (TBS; 0.05 M, pH 7.6) for 15 min and then sections were incubated for 90 min in ABC complex (Vectastain ABC kit, 6 Vector Labs, PK-6100, Burlingame, CA, USA) diluted 1:50 in TBS-Tx (Triton X-100 0.3% in TBS 0.05 M pH 7.6) at room temperature. After rinsing thoroughly with buffer, peroxidase activity was developed with 0.025% diaminobenzidine in PB (0.1 M, pH 8.0) and 0.01% H_2O_2 and 0.1% nickel ammonium sulphate, obtaining a black precipitated product.

In those cases were the FG tracer was injected, first the location of the injection was checked using fluorescence microscopy and then one of the series of each brain was processed for FG immunoperoxidase. To do so, endogenous peroxidase activity was first inactivated with 1% H_2O_2 in TBS (0.05M, pH 7.6) for 15 min (in the cases where a contralateral injection of BDA was performed, this step was not repeated, since the BDA tracer was previously detected). Then, the sections were incubated in a blocking solution of TBS-Tx containing 8% of normal goat serum (NGS) and 4% of bovine serum albumin (BSA), for 2 hours at room temperature. After that, the sections in were sequentially incubated in: rabbit anti-Fluorescent Gold (Millipore, Cat # AB153) diluted 1:3000 in TBS-Tx with 4% NGS and 2% BSA overnight at 4°C; biotinyled goat anti-rabbit IgG (Vector, Cat # BA-1000) diluted 1:200 in TBS-Tx with 4% NGS for 2 hours at room temperature; and ABC Elite diluted 1:50 in TBS-Tx for 2 hours at room temperature. Finally the resulting peroxidase labelling was revealed with 0.0025%

diaminobenzidine in PB (0.1M, pH 8.0) with 0.01% H_2O_2, obtaining a brown precipitated product.

The anti-FG antibody has been previously validated in many papers (e.g. Gutierrez-Castellanos et al. 2014; summarized in the *Journal of Comparative Neurology* antibody database). We also checked that the omission of the primary antibody resulted in no labelling in our brain tissue.

Series were mounted onto gelatinised slides, dehydrated with graded alcohols, cleared with xylene and coverslipped with Entellan (Merck Millipore, Cat # 1079610100). To facilitate the identification of the neural structures containing the anterograde labelled fibres in experiment 1, before the tissue was coverslipped, it was counterstained with the Nissl method. In the experiments 2 and 3, to facilitate the identification of the neural structures containing retrogradely labelled cells, in most cases a second series of sections was processed for FG immunohistochemistry and counterstained with Nissl staining (experiment 2) or was stained with the Nissl method (experiment 3).

In addition, the histochemistry of the acetil cholinesterase was studied in the amygdala from mouse brain series that were available on the laboratory stock samples.

Image acquisition and processing

We observed the sections using an Olympus CX41RF-5 microscope and photographed them using a digital Olympus XC50 camera. Fluorescent images of the FG injection sites were captured with a Leitz DMRB microscope with epifluorescence (Leica EL-6000) equipped with a specific filter for FG (Leica, A) and a digital Leica DFC 300 FX camera. Using Adobe Photoshop 7.0 (AdobeSystems, MountainView, CA, USA) pictures were flattened by subtracting background illumination and brightness and contrast were optimized. No further changes were performed. Finally, illustrations were designed with Adobe Photoshop 7.0 and Illustrator.

3. RESULTS

3.1 Chapter 1

Neural Substrate to Associate Odorants and Pheromones: Convergence of Projections from the Main and Accessory Olfactory Bulbs in Mice

3.1.1 Introduction

Rodents possess two long-distance chemosensory organs, the nasal or main olfactory epithelium (MOE) and the vomeronasal organ (VNO). Chemosensory stimuli detected by them play a key role in socio-sexual (Brennan and Kendrick 2006) and antipredatory behaviour (Papes et al. 2010). The MOE mainly detects air-borne volatiles while the VNO seems specialised (with some exceptions) in detecting non-volatile chemicals (Krieger et al. 1999) possessing an intrinsic biological value, such as sexual pheromones or predator-derived chemosignals. Thus, in the context of socio-sexual behaviour, vomeronasal stimuli apparently trigger innate behavioural responses (Martínez-García et al. 2009; Keller et al. 2009).

The MOE and VNO project to the main (MOB) and accessory (AOB) olfactory bulbs respectively. In the 1970´s, tract-tracing experiments described that the main and accessory olfactory bulbs (OB) projected to adjacent but non-overlapping telencephalic nuclei (Scalia and Winans 1975; Skeen and Hall 1977). Traditionally, the structures considered as receiving only main olfactory projections are the piriform cortex (Pir), the olfactory tubercle (Tu), cortex-amygdala transition zone (CxA), anterior cortical amygdala (ACo), the nucleus of the lateral olfactory tract (LOT) and the posterolateral cortical amygdala (PLCo). The nuclei traditionally considered as vomeronasal recipients are the bed nucleus of the accessory olfactory tract (BAOT), the posteromedial part of the medial division of the bed nucleus of the stria terminalis (BSTMPM), the anterior amygdaloid area (AA), the medial amygdaloid nucleus (anterior, MeA, and posterior, MeP, subdivisions) and the posteromedial cortical amygdala (PMCo). These observations led to the dual olfactory hypothesis, which stated that these two pathways act independently in the chemical information processing (see, for a review, Halpern 1987).

This view has been seriously challenged by recent data. Thus, tract-tracing experiments conducted in rats (Mohedano-Moriano et al. 2007; Pro-Sistiaga et al. 2007) and mice (Kang et al. 2009, 2011a), have demonstrated the existence of convergent projections from the MOB and AOB to several cortical and non-cortical amygdaloid structures (Gutiérrez-Castellanos et al. 2010). Functional experiments also indicate that both chemosensory systems play a complementary role in eliciting adequate behavioural

responses (Martínez-García et al. 2009; Keller et al. 2009). This interaction can be observed in a particular case of emotional learning in which airborne olfactory stimuli are associated with sexual pheromones detected by the vomeronasal organ. Male-derived involatile pheromones elicit an unconditioned attraction in female mice (even if the females have no previous experience with males or male-derived chemical signals; Roberts et al. 2010). In contrast, male-derived volatile odorants do not attract inexperienced females. Following experience with male-soiled bedding, which contains involatile pheromones and volatile odorants, females acquire a learned attraction to volatile male odours (Moncho-Bogani et al. 2002). Therefore, in this case, male pheromones act like appetitive unconditioned stimuli for females and, following chemosensory experience, become associated with male-derived volatiles, what results in a conditioned attraction for those volatiles (Moncho-Bogani et al. 2002; Martínez-Ricós et al. 2008).

In this context, we have started a neuroanatomical study of the neural centres receiving direct projections from both the main and accessory olfactory bulbs in the mouse brain, as a way to explore the brain regions where olfactory-vomeronasal associative learning might first occur.

3.1.2 Results

3.1.2.1 Injections in the Accessory Olfactory Bulb

Six injections involved in the AOB. Three of them were centred in the AOB (with no MOB involvement), one of which was restricted to the glomerular and mitral layer (Fig. 1A). This injection is described as a representative case. Importantly, in this AOB injection no labelled fibres appeared in the dorsolateral olfactory tract (dlot) (Figs. 1B, C), and no retrogradely labelled cells were observed.

Anterogradely labelled fibres originated by the AOB injection ran caudally in the inner part of the lateral olfactory tract (*lo*) to reach the anterior piriform cortex (Pir), nuclei of the lateral (LOT) and accessory (BAOT) olfactory tracts, anterior amygdala (AA), medial amygdala (Me) and several nuclei of the cortical amygdala.

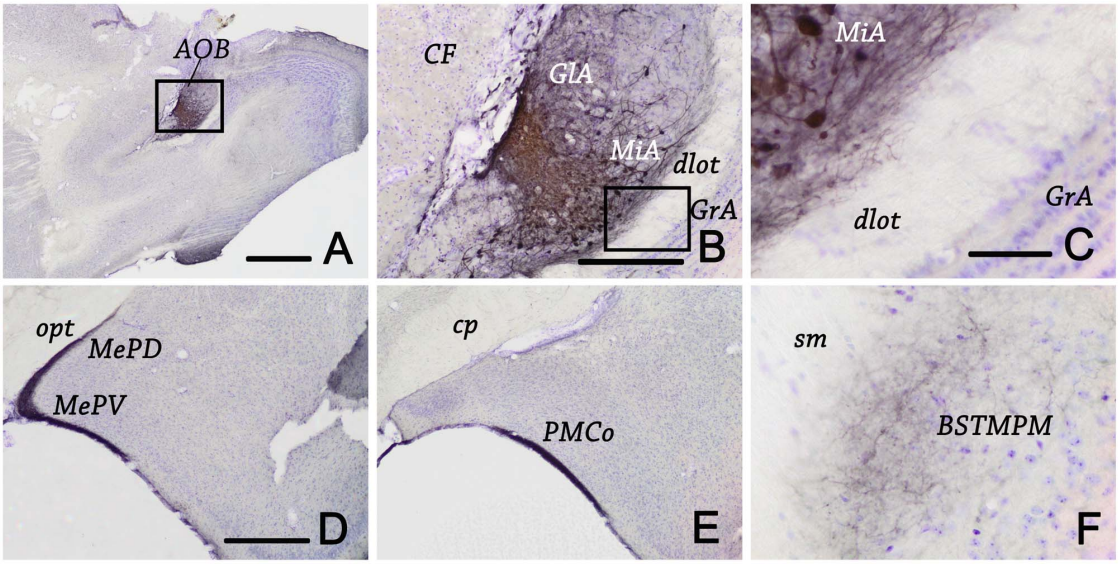

Fig. 1 Photomicrographs of Nissl counterstained parasagittal (A-C) and frontal (D-F) sections, illustrating the injection site of TBDA in the AOB (A-C) and the resulting anterograde labelling (D-F) in some of the vomeronasal nuclei. Rectangles in A and B correspond to B and C, respectively. For abbreviations, see list. Scale bar: 1 mm for A; 500 μm for B; 250 μm for D, E; 50 μm for C, F.

In the anterior Pir labelled fibres were observed in the edge between the *lo* and layer IA (Figs. 2A, B). Labelled fibres display abundant varicosities and most of them are oriented parallel to the pial surface. In addition, in the anterior ventral Pir (where the *lo* runs below the pial surface, see Martínez-García et al. 2012) a number of fibres were observed crossing the layers II and III (Fig. 2c). In the posterior Pir (at the level of the AA and CxA), labelled fibres are not present anymore. At the medioventral edge of the Pir, in the limit with the adjacent the striato-pallidal territory, some labelled fibres were observed running towards the ventral external capsule (Fig. 2D).

In the rostral CxA, next to the ventral and dorsal AA (ventral part of the anterior amygdaloid area (AAV) and dorsal part of the anterior amygdaloid area (AAD), varicose fibres were seen in layers IA and IB (Figs. 2D, E, F), and a number of fine fibres crossed layer II (Fig. 2D). At this level, vertically oriented fine and thick fibres crossed through the AAD, entering the ventral tip of the external capsule (Figs. 2D, E). Labelled, fine fibres were seen scattered throughout the AAV and AAD (Figs. 2D, E).

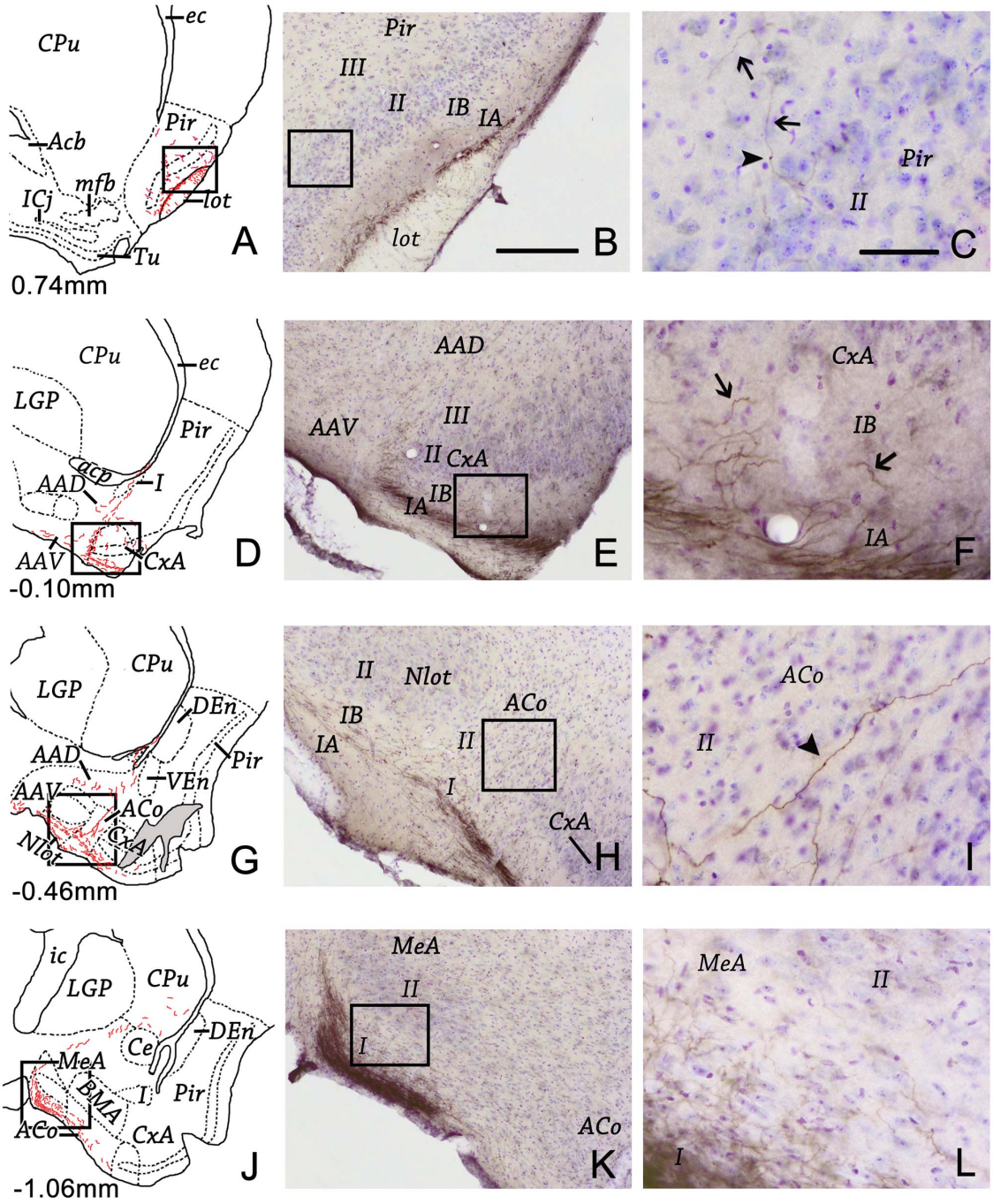

Fig. 2 Line drawings and photomicrographs of Nissl counterstained frontal sections illustrating the anterogradely labelled fibres in the telencephalon resulting from the AOB injection shown in Fig. 2.1. The drawings A, D, G illustrate the labelling in traditional olfactory recipients (with indication of the coordinate relative to bregma). For abbreviations, see list. Rectangles in A, D, G, J correspond to B, E, H, K, respectively. Rectangles in B, E, H, K, correspond to C, F, I, L respectively. Scale bar = 250µm for B, E, H, K; 50 µm for C, F, I, L. Arrows indicate fibres and arrowheads varicosities.

At the level of the ACo, labelled varicose fibres appeared in its layer I (sublayers IA and IB; Figs. 2G, H). Some fibres crossed layer II (Fig. 2I) tangentially to the pial surface. In the LOT, scattered varicose fibres were present in the layers IA and IB, whereas in the BAOT a compact bundle of labelled fibres was observed (not shown).

In the anterior subdivision of the Me (MeA) we observed a dense plexus of terminal (fine and varicose) fibres in layer I (Fig 2J, K, L), some of which reached layer II. Dorsal to the MeA, a few labelled fibres took a dorsal course to reach the ventral zone of the caudoputamen (CPu) (Fig. 2J). In the posterior subdivisions of the Me (MeP) a dense field of anterogradely labelled, fine, varicose fibres occupied layer I (Fig. 1D), with a few fibres reaching layer II. From the posterodorsal subdivisions of the Me (MePD) labelled fibres were seen to enter the stria terminalis (st) and ran rostrally up to the medial bed nucleus of the stria terminalis (BST), where they gave rise to a terminal field specifically innervating its posteromedial part of the medial division (Fig. 1F).

Finally, a dense terminal plexus of labelled fibres was observed in layers IA and IB of the PMCo (Fig. 1E).

3.1.2.2 Main Olfactory Bulb Injections

We obtained six injections in the MOB. Two of them were restricted to the ventral MOB, and were located in the glomerular, external plexiform and mitral layers (as a shown in a representative case in Figs. 3A and 3B), and are described here as examples.

From the injection site, labelled fibres entered the lateral olfactory tract (Fig. 3C) to reach the Pir, olfactory tubercle (Tu), AA, parts of the cortical amygdala, LOT and Me. Occasionally, some retrogradely labelled cells were observed in the Pir, nucleus of the horizontal limb of the band diagonal (HDB) and magnocellular preoptic nucleus (MCPO).

Throughout the Pir, a dense plexus of beaded and varicose labelled fibres was observed in layer IA (Figs. 3D, E, G). Only occasionally labelled fibres were observed in layer IB. No labelled fibres appeared in layers II and III. In the Tu, anterogradely labelled

fibres ran parallel to the pial surface (Fig. 3F), most of which restricted to layer IA, with some occasional fibres reaching the layer IB.

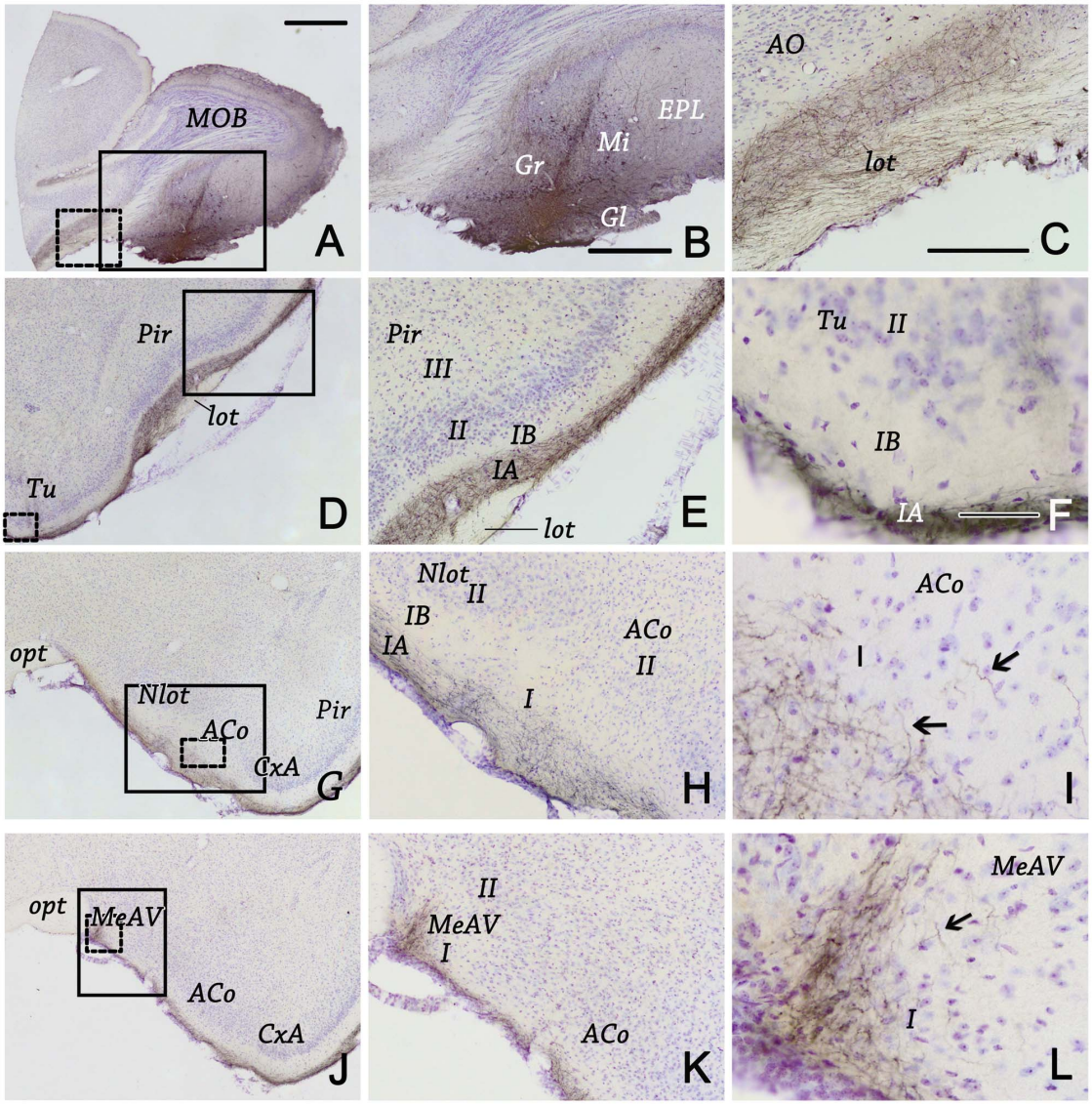

Fig. 3 Photomicrograph of Nissl counterstain of parasagittal (A-C) and frontal sections (D-L), illustrating the injection site in the ventral MOB (A,B) and the anterograde labelling in the traditionally considered vomeronasal (D-I) and olfactory (J-L) nuclei. Continuous rectangles in A, D, G, J, correspond to B, E, H, K, respectively. Discontinuous rectangles in A, D, G, J, correspond to C, F, I, L, respectively. For abbreviations, see list. Scale bar = 1 mm for A; 500 μm for B, D, G, J; 250 μm for C, E, H, K; 50 μm to F, I, L. Arrows indicate fibres.

When the lateral olfactory tract reaches the amygdaloid formation, labelled varicose fibres were observed in layer IA of the CxA and in the superficial portion of the AAV (Figs. 3G and 4A-C). At the medial edge of the CxA, in the limit with the AAV, a few

fibres were observed to run dorsally into the AAD (Fig. 4A). Within the cortical amygdaloid nuclei, thick varicose labelled fibres formed dense plexuses in layer IA of the ACo and the LOT (Figs. 3G, H, I), where some fibres occasionally entered layer IB. Caudally in the cortical amygdala, both fine and thick beaded and varicose labelled fibres were present in layer IA of the PLCo, restricted to the most superficial zone (Fig. 4H).

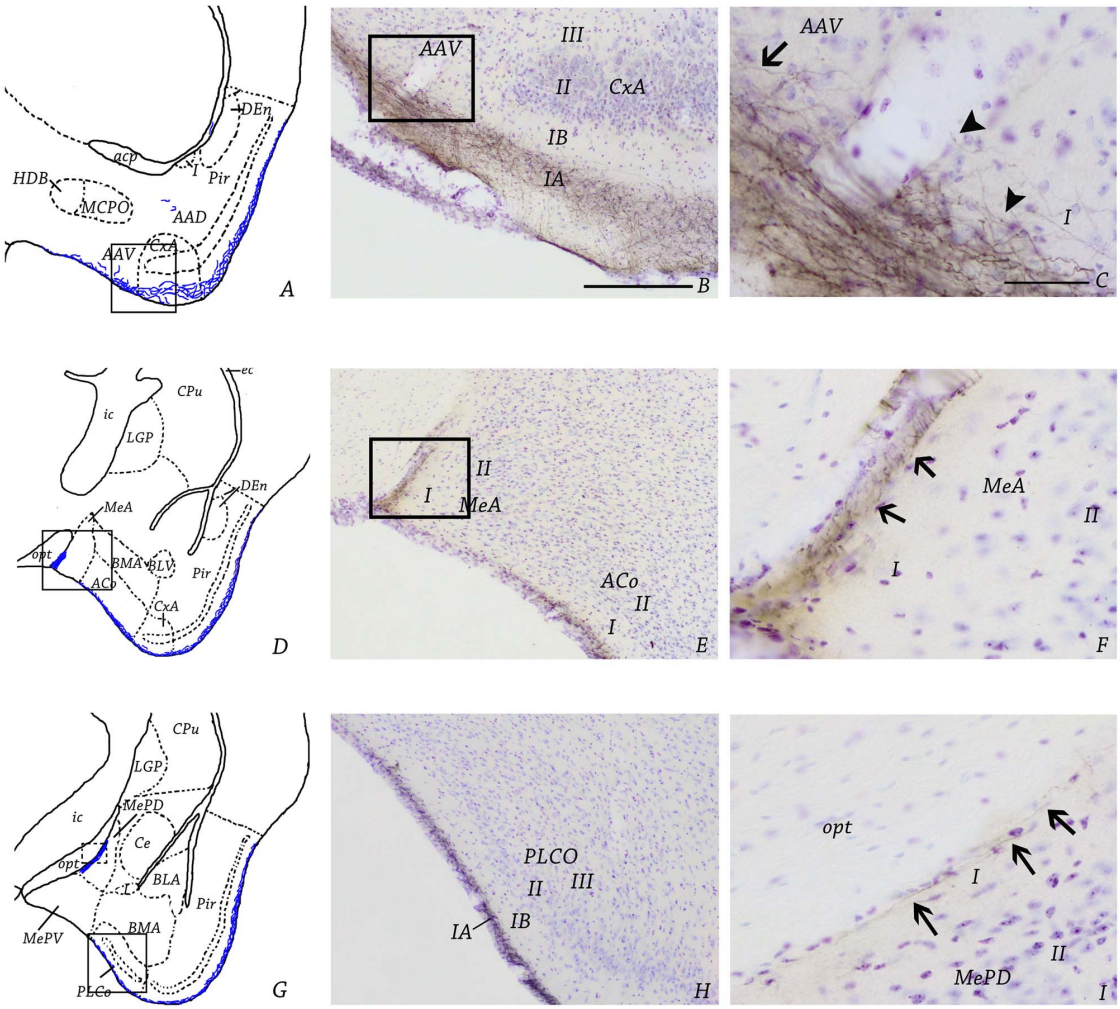

Fig. 4 Line drawings and photomicrographs of Nissl-stained frontal sections illustrating the anterogradely labelled fibres in the telencephalon of a MOB injection (same animal of Fig. 2.3). Photomicrographs show the labelling in traditionally considered vomeronasal recipients (except for H that is a traditionally olfactory recipient). Continuous rectangles in A, D, G correspond to B, E, H, respectively. Discontinuous rectangle in G corresponds to I. Rectangles in B, E correspond to C, F. For abbreviations, see list. Scale bar: 250 μm in B, E, H; 50 μm in C, F, I. Arrows indicate fibres and arrowheads varicosities.

In the medial amygdala, a number of thin labelled fibres were observed to reach the superficial aspect of the ventral part of the MeA (Figs. 3J, K, L and Figs. 4D, E, F). This anterograde labelling is particularly dense at the rostralmost levels of the MeA. The plexus of anterograde labelling in the MeA did not show continuity with the fibres present in the ACo (Figs. 4D, E). In the posterior medial amygdala, a few fine fibres were observed in layer I of the MePD (Figs. 4G, I), whereas no labelling was found in the MePV.

3.1.3 Discussion

Traditionally, the vomeronasal and olfactory systems have been considered to process chemosensory information independently, given their differential and non-convergent projections to the basal telencephalon (Skeen and Hall 1977; Scalia and Winans 1975). This idea is known as the dual olfactory hypothesis (reviewed in Halpern 1987). The results of the present study confirm and extend previous results reported in mice and rats of convergent projections of the main and accessory olfactory bulbs to portions of the amygdala and olfactory cortex, thus contradicting the dual olfactory hypothesis. Our results indicate that the AOB projects to areas traditionally considered being olfactory recipients, such as the CxA, ACo and LOT in the amygdala and a particular zone of the Pir, while the MOB projects to areas traditionally considered as vomeronasal, such as the AAV, MeA and MePD.

The Pir is the main projection target of the MOB, and therefore is usually viewed as the primary olfactory cortex (but see Martínez-García et al. 2012). Our results show fibres originated in the AOB innervating layers I, II and III in a small restricted area of the Pir: the anterior ventral Pir (surrounding the *lo*). It is important to note that the distribution of anterograde labelling in the Pir following AOB injections (fibres oriented perpendicularly to the brain surface that entered layers II and III) is very different from that observed after MOB injections (fibres oriented parallel to the brain surface concentrated in layer IA), and therefore it is unlikely that these fibres might arise from inadverted contamination of the MOB. In addition, these results agree with schematic drawings shown by Mohedano-Moriano et al. (2007) in rats (Table 1), as well as with the description of collaterals fibres entering the Pir after AOB injections in mice (Kang et al. 2011a; Table 1).

Table 1. Comparison of the present results with recent studies of AOB and MOB projections performed in rats (Mohedano-Moriano et al. 2007; Pro-Sistiaga et al. 2007) and mice (Kang et al. 2009, 2011a). *Collaterals* refer to reported axon collaterals entering the structure in a flat-mount view. * Layers IA and IB not specified in the original paper. - Not mentioned in the original paper. MOB, main olfactory bulb; accessory (AOB) olfactory bulbs; MeA, anterior medial amygdale, MePD, posterodorsal medial amygdala; MePV, posteroventral medial amygdale; Nlot, nucleus of the lateral olfactory tract; Pir, piriform cortex; PMCo, posteromedial cortical amygdale; PLCo, posterolateral cortical amygdale.

Nucleus	**Layers where it can be seen labelling from AOB**			**Layers where it can be seen labelling from MOB**		
	Rat	**Mouse**	**Present work**	**Rat**	**Mouse**	**Present work**
Pir	Line drawing	Collaterals	IA-IB II-III	IA	IA	IA-IB
CxA	IA-II	-	IA-IB	IA-II	-	IA
AAV	I	I*	I	I	I*	I
LOT	I-II-III	I*	IA-IB	IA-IB	I*	IA-IB
ACo	IB-III	Collaterals	IA-IB II-III	IA	I*	IA
BAOT	I-II	I-II	I-II	IA	I*	IA
MeA	I-II-III	I-II	I-II	I	IA-II	I
MePV	I-II	-	I	No	No	No
MePD	I-II	I-II	I	No	IA-II	I
PMCo	IA-IB	IA-IB	IA-IB	No	No	No
PLCo	IA-IB	No	No	IA	I*	IA-IB

In the latter study only the fibres in layer I were described probably because the authors used flat-mount preparations of the telencephalon. In any case, the authors did not discuss the observed fibres in the Pir. However, this evidence suggests that this particular zone of the Pir is the first cortical area where vomeronasal and olfactory information converge.

With regard to the projections of the AOB to the amygdala, our results fully agree with those reported by Kang et al. (2009; 2011a), the only differences being that they did not report fibre labelling in the CxA, and that they described fibres in deep MeA. In rats, Pro-Sistiaga et al. (2007) and Mohedano-Moriano et al. (2007) reported AOB-originated projections in the same structures that we found in the present study (with the

exception of a few fibres in the PLCo that we could not observe), thus suggesting that rats and mice have similar patterns of olfactory projections, although some differences might exist regarding the layers innervated, as summarised in Table 1.

We have also observed fibre labelling through the AAD that apparently reached the ventral tip of the external capsule (Fig. 2D). We could not identify the target structures of these fibres. In rats, similar anterograde labelling has been reported (Mohedano-Moriano et al. 2007) and was interpreted as part of the stria terminalis (st) pathway to the BSTMPM. However, at the levels where this labelling appears the st is not present yet. An alternative explanation would be that these fibres are actually retrogradely labelled axons from neurons of the diagonal band that project back to the bulb (Shipley and Adamek 1984), although we did not observed retrograde labelled cell bodies in this nucleus.

The amygdaloid targets of the MOB projection described in the present report are fully consistent with the results of previous works (Kang et al 2009; Pro-Sistiaga et al. 2007), again with minor differences regarding the layers innervated in each structure, as summarised in Table 1. The only result of our work not previously reported is the presence of a few labelled fibres located deep in the AAV and in the AAD. Since this labelling is similar to that found in injections that only affected the granular layer of the MOB (not shown) that gave rise to abundant retrograde labelling, it is possible that it actually corresponds to retrogradely labelled axons.

Therefore, according to our results and other previous works, the amygdala contains several associative areas where chemosensory information coming from the AOB and MOB converge, including the CxA, ACo, MeA and MePD (Fig. 5). The CxA and ACo are structures receiving predominantly olfactory projections and a minor input from the AOB in layers I and II (also reaching layer III in the ACo) (Table 1).

The MeA and MePD are areas receiving predominantly vomeronasal projections and also a minor afferent from the MOB (layers I and II). Since the inputs to the inner layers are closest to the cell body, they presumably have a higher modulatory strength than those reaching the distal dendrites. Taking these considerations into account, we consider the four mentioned areas more relevant for the association of olfactory and

vomeronasal information than the AAV, LOT and BAOT, where fibres coming from the MOB and AOB are superficial and may also be axons en passant (Table 1).

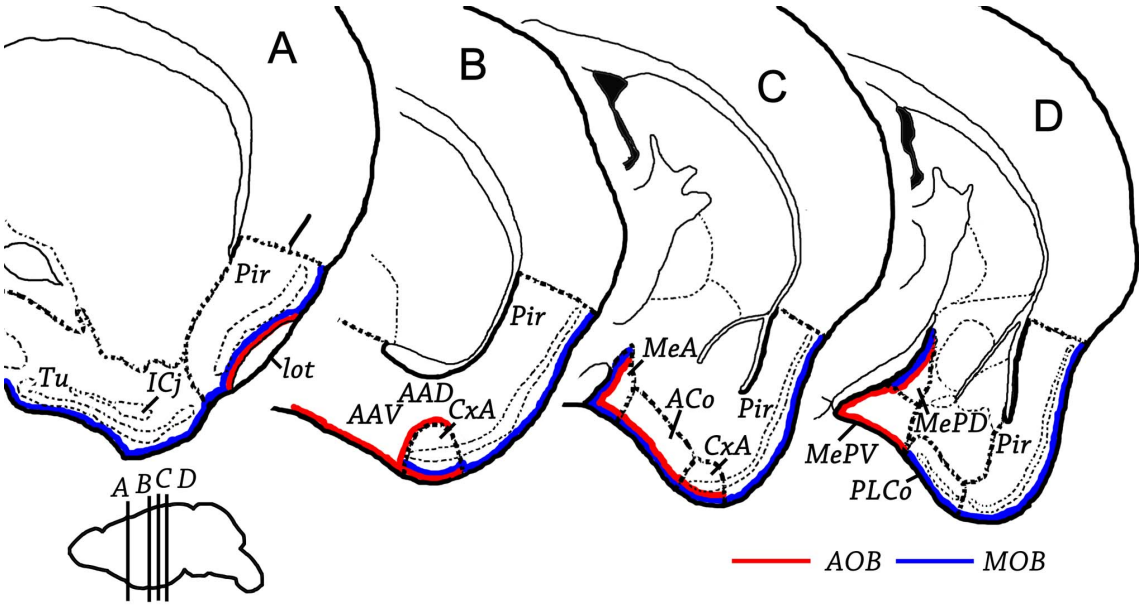

Fig. 5 Semi-schematic diagram showing the convergence from the AOB (red) and MOB (blue) projections.

Although the present studies were performed in female mice, previous works showed no differences in the pattern of the AOB projections between male and female mice (von Campenhausen and Mori 2000). Regarding the MOB efferent projections, most of the previous works in mice were performed in males (e.g., Shipley and Adamek 1984; Kang et al. 2011a), and our results have not revealed any difference with these previous reports. Consistent with these observations, no sexual differences have been found in the AOB or MOB projections in rats (Dr. Martinez-Marcos, University of Castilla-LaMancha, personal communication). In addition, the reported similarities between mice and rats make it unlikely that the described convergent projections from the AOB and MOB to amygdaloid structures are different in males, although experimental confirmation of this possibility awaits further study. Noteworthy, a recent study has revealed a sexual dimorphism in the distribution within the MOB of the mitral cells that project to the medial amygdala, but no sex difference was found in the pattern of projections from the MOB to the medial amygdala (Kang et al. 2011b).

The direct convergence of projections from the main and accessory olfactory bulbs in the amygdala, as well as in a particular area of the anterior piriform cortex, suggests that these structures are likely implicated in the complementary role played by these two kinds of chemosensory information (Keller et al. 2009). In particular, it has been shown that non-volatile molecules detected by the vomeronasal system, which elicit unconditioned responses (e.g, sexual attraction), become associated by means of chemosensory experience with volatile molecules detected by the main olfactory system (Martínez-García et al. 2009). By this learning mechanism, animals may learn to respond to volatiles, which can be detected at a distance, and consequently track the source of the volatile molecules (e.g., a possible mate). A similar learning process might take place in the case of vomeronasal-detected predator signals (Papes et al. 2010) and associated volatiles, allowing the animals to avoid predators at a distance. This learning process has obvious advantages for the animal.

The medial nucleus of the amygdala is involved in sex-specific and sex-steroid olfactory preference (Dibenedictis et al. 2012). Studies of c-fos expression performed in female mice have shown that the cell bodies of this area are activated after exposure to male-derived chemicals (Moncho-Bogani et al. 2005; Kang et al. 2009), and electrolytic lesions of the MeP abolish the preference of females for male-derived urinary chemicals (Dibenedictis et al. 2012). Similar results have been reported in male hamsters (Maras and Petrulis 2006). This evidence, as well as the convergent projections of the vomeronasal (pheromones) and olfactory (volatiles) information in the medial amygdala, makes this structure a likely candidate to be involved in the association between odours and pheromones. With regard to the CxA and ACo, no information is available about their possible roles in pheromone detection, although it has been shown that the ACo expresses c-fos in female mice following chemoinvestigation of male-derived volatiles (Moncho-Bogani et al. 2005; Kang et al. 2009). Further studies are needed to clarify the role of these associative chemosensory structures.

3.1.4 References

Brennan, P.A. and Kendrick, K.M. (2006) Mammalian social odours: Attraction and individual recognition. Philos. Trans. R. Soc. Lon. B Biol. Sci. 361, 2061–2078.

Dibenedictis, B.T., Ingraham, K.L., Baum, M.J. and Cherry, J.A. (2012) Disruption of urinary odor preference and lordosis behavior in female mice given lesions of the medial amygdala. Physiol. Behav. 105, 554–559.

Gutiérrez-Castellanos, N., Martínez-Marcos, A., Martínez-García, F. and Lanuza, E. (2010) Chemosensory functions of the amygdala. Vitam. Horm. 83, 165–193.

Halpern, M. (1987) The organization and function of the vomeronasal system. Annu. Rev. Neurosci. 10, 325–362.

Kang, N., Baum, K.J. and Cherry, J.A. (2009) A direct main olfactory bulb projection to the "vomeronasal" amygdala in female mice selectively responds to volatile pheromones from males. Eur. J. Neurosci. 29, 624–634.

Kang, N., Baum, K.J. and Cherry, J.A. (2011a) Different profiles of main and accessory olfactory bulb mitral/tufted cell projections revealed in mice using an anterograde tracer and a whole-mount, flattened cortex preparation. Chem. Senses 36, 251–260.

Kang, N., McCarthy, E.A., Cherry, J.A. and Baum, K.J. (2011b) A sex comparison of the anatomy and function of the main olfactory bulb–medial amygdala projection in mice. Neuroscience 172, 196–204.

Keller, M., Baum, M.J., Brock, O., Brennan, P.A. and Bakker, J. (2009) The main and accessory olfactory systems interact in the control of mate recognition and sexual behavior. Behav. Brain Res. 200, 268–276.

Krieger, J., Schmitt, A., Löbel, D., Gudermann, T., Schultz, G., Breer, H. and Boekhoff, I. (1999) Selective activation of G protein subtypes in the vomeronasal organ upon stimulation with urine-derived compounds. J. Biol. Chem. 274, 4655–4662.

Maras, P.M. and Petrulis, A. (2006) Chemosensory and steroid-responsive regions of the medial amygdala regulate distinct aspects of opposite-sex odor preference in male Syrian hamsters. Eur. J. Neurosci. 24, 3541–3552.

Martínez-García, F., Martinez-Ricós, J., Agustín-Pavón, C., Martínez-Hernández, J., Novejarque, A. and Lanuza, E. (2009) Refining the dual olfactory hypothesis: Pheromone reward and odour experience. Behav. Brain Res. 200, 277–286.

Martínez-García, F., Novejarque, A., Gutiérrez-Castellanos, N. and Lanuza, E. (2012) Piriform cortex and amygdala. In: Watson, C., Paxinos, G., Puelles, L. (Eds.), *The Mouse Nervous System*. Academic Press: Amsterdam, pp. 140–220.

Martínez-Ricós, J., Agustín-Pavón, C., Lanuza, E. and Martínez- García, F. (2008) Role of vomeronasal system in intersexual attraction in female mice. Neurosci. 153, 383–395.

Mohedano-Moriano, A., Pro-Sistiaga, P., Ubeda-Bañon, I., Crespo, C., Insausti, R. and Martinez-Marcos, A. (2007) Segregated pathways to the vomeronasal amygdala: differential projections from the anterior and posterior divisions of the accessory olfactory bulb. Eur. J. Neurosci. 25, 2065–2080.

Moncho-Bogani, J., Lanuza, E., Hernández, A., Novejarque, A. and Martínez-García, F. (2002) Attractive properties of sexual pheromones in mice: innate or learned? Physiol. Behav. 77, 167–176.

Moncho-Bogani, J., Martínez-García, F., Novejarque, A. and Lanuza, E. (2005) Attraction to sexual pheromones and associated odorants in female mice involves activation of the reward system and basolateral amygdala. Eur. J. Neurosci. 21, 2186–2198.

Papes, F., Logan, D.W. and Stowers, L. (2010) The vomeronasal organ mediates interspecies defensive behaviors through detection of protein pheromone homologs. Cell 141, 692–703.

Pro-Sistiaga, P., Mohedano-Moriano, A., Ubeda-Bañon, I., Arroyo-Jimenez, M., Marcos, P., Artacho-Pérula, E., Crespo C., Insausti R. and Martinez-Marcos, A. (2007) Convergence of olfactory and vomeronasal projections in the rat basal telencephalon. J. Comp. Neurol. 504:346–362.

Roberts, S.A., Simpson, D.M., Armstrong, S.D., Davidson A.J., Robertson, D.H., McLean, L., Beynon, R.J., Hurst, J.L. (2010) Darcin: a male pheromone that stimulates female memory and sexual attraction to an individual male's odour. BMC Biol. 8, 75.

Scalia, F. and Winans, S.S. (1975) The differential projections of the olfactory bulb and accessory olfactory bulb in mammals. J. Comp. Neurol. 161, 31–56.

Shipley, M.T. and Adamek, G.D. (1984) The connections of the mouse olfactory bulb: a study using orthograde and restrograde transport of wheat germ agglutinin conjugated to horseradish peroxidase. Brain Res. Bull. 12, 669–688.

Skeen, L.C. and Hall, W.C. (1977) Efferent projections of the main and the accessory olfactory bulb in the tree shrew (*Tupaia glis*). J. Comp. Neurol. 172, 1–36.

Von Campenhausen, H. and Mori, K. (2000) Convergence of segregated pheromonal pathways from the accessory olfactory bulb to the cortex in the mouse. Eur. J. Neurosci. 12, 33–46.

3.2 Chapter 2

Afferent projections to the different medial amygdala subdivisions: a retrograde tracing study in the mouse

3.2.1 Introduction

The medial amygdaloid nucleus of the amygdala (Me) is one of the main structures receiving the projections originated in the accessory olfactory bulb (Scalia and Winans 1975), and it was very early identified as a relevant structure for the control of sexual behaviour in male hamsters (Lehman et al. 1980). In addition, the Me has been proposed to be a key node of the sexually dimorphic network mediating sociosexual behaviours in rodents (Newman 1999) and other vertebrates (Goodson 2005). In fact, it is enriched in neurons expressing steroid hormone receptors.

The efferent projections of the Me have been previously characterized in several rodent species (Gomez and Newman 1992; Canteras et al. 1995; Coolen and Wood 1998; Usunoff et al. 2009; Maras and Petrulis 2010a; Pardo-Bellver et al. 2012), and the pattern of projections differs between the anterior (MeA), posteroventral (MePV) and posterodorsal (MePD) subdivisions of the Me. The anatomical data suggest that the posterodorsal part is mainly involved in reproductive behaviours, whereas the posteroventral part plays a role in the expression of defensive behaviours, in particular elicited by predator-derived chemicals (Choi et al. 2005).

However, recent findings about the type of information perceived by the vomeronasal organ have revealed that, in addition to reproductive-related signals and predator-derived cues (Papes et al. 2010; Isogai et al. 2011), it detects chemical signals from competitors (Chamero et al. 2007), stress-related signals (Nodari et al. 2008) and illness cues (Riviere et al. 2009). Therefore, the view of the medial amygdala as a relevant nucleus processing sexually relevant signals versus chemicals from predators should be revised taking into account these other possible types of information. Moreover, the Me also receives direct projections from the main olfactory bulb (Scalia and Winans, 1975; Pro-Sistiaga et al. 2007; Kang et al. 2009; 2011; Cádiz-Moretti et al. 2013), and therefore it is also a critical node to integrate olfactory and vomeronasal information.

To fully understand how the Me process the information derived from the different types of vomeronasally-detected chemicals, it is necessary to identify the rest of the neural inputs received by this nucleus, and in particular by its subdivisions. However, the afferents to the Me have not been properly studied in any mammalian species taking into account its anatomical subdivisions. In fact, our knowledge about the inputs to the

Me derive from a number of anterograde tracing studies of some of the structures giving rise to projections to the Me (see, for a review, Pitkanen 2000), and a few injections of retrograde tracers encompassing several of the Me subdivisions (Ottersen and Ben-Ari 1979). Anatomical information is available mainly for rats (and, to a lesser extent, for hamsters). By contrast, very little information is available for mice, a species used in a large number of behavioural experiments to understand the role of the vomeronasal system (Halpern and Martínez-Marcos 2003). These studies have benefited from the availability of genetically modified mice with alterations of key genes for the function of the vomeronasal organ, which have yielded relevant new information on the neural basis of sociosexual behaviours (Tirindelli et al. 2009; Zufall and Leinders-Zufall 2007).

With the aim to comprehensively describe the neuroanatomical substrate of the inputs relaying information to the different subdivisions of the medial amygdala, in the present study, we have traced the afferent projections to the anterior, posterodorsal and posteroventral subdivisions of the Me by using the retrograde tracer fluorogold.

3.2.2 Results

For the description of the results we follow the cytoarchitecture and nomenclature by Paxinos and Franklin (2004) with a few modifications that are discussed where needed. For the amygdaloid complex (see Table 2), we follow the architecture proposed by Martínez-García et al. (2012) and the functional grouping of the chemosensory amygdala proposed by Gutierrez-Castellanos et al. (2010): olfactory nuclei, receiving inputs only from the main olfactory bulb (MOB); vomeronasal nuclei, receiving inputs only from the accessory olfactory bulb (AOB); and mixed nuclei, receiving inputs from both bulbs, with either olfactory or vomeronasal predominance.

Retrograde labelling with FG typically appears as granular staining of the cell body. Staining intensity ranged from a few granules surrounding the neuronal nucleus to darkly stained somata with labelling extending into the proximal dendritic tree.

On the other hand, the extent and boundaries of the injection sites are difficult to discern in immunoperoxidase material, apparently because high concentrations of FG make immunostaining hazy. In contrast, fluorescence microscopy neatly delineates the injections. Therefore, each injection was photographed under fluorescence microscopy

to map its location and extent (Fig. 6). In addition, retrograde labelling in structures adjoining the injection sites were analysed in fluorescence material.

In this section we will describe the distribution and relative density of retrogradely labelled cells after the three kinds of injections performed.

Table 2. Semiquantitative rating of the density of the retrograde labelling resulting after tracer injections in three subnuclei of the medial amygdaloid nucleus.
++++ very dense; +++ dense; ++ moderate; + scarce; - very scarce; 0 not found.

		MeA	**MePV**	**MePD**
OLFACTORY SYSTEM				
Accessory Olfactory Bulb	MiA rostral/MiA caudal	++++	++++	++++/++
Main Olfactory Bulb	Mi	-	0	-
Olfactory Cortex	DTT/VTT	++/+	+/0	-/0
	Pir	++	+	-
	DEn/VEn	++/++	++/+	+/-
AMYGDALA AND BST				
Vomeronasal	PMCo	++++	++++	++
Vomeronasal predominance	MeA	**injection**	++++	++++
	MeAV/MeAD	++++	+++/++	-/++
	MePV	+++	**injection**	++++
	MePD	++	+++	**injection**
	BAOT	++++	++++	+++
	AAV/AAD	++	++/+	-/-
Olfactory	PLCo	+++	+++	++
	APir	++	+	-

		MeA	**MePV**	**MePD**
Olfactory predominance	ACo	+++	+++	+++
	CxA	++	+	0
	LOT	+	-	+
Basolateral complex	BLA	-	-	0
	BLP	-	+	-
	BLV	-	+	0
	BMA	+++	++	++
	BMP	+++	++	-
	LaDL/LaVM/LaVL	-/+/+	-/+/-	0/0/0
Amygdalohippocampal transition area	AHi	++	++	+++
Central	CeC	0	-	0
	CeL	-	0	0
	CeM	+	+	+
	I	+	+	-
	IM	+	+	-
BSTL	BSTLP	-	0	0
	BSTLV	-	-	0
BSTM	BSTMA	-	-	0
	BSTMV	-	0	0
	BSTMPM	++	++	++++
	BSTMPI	+++	+++	++
	BSTMPL	+	-	0
	BSTIA	+++	++	++

CORTEX AND HIPPOCAMPAL FORMATION				
	AI	++	-	0
	PrL	+	-	0
	CI	-	0	-
	MO	+	+	-
	LO	-	0	0
	IL	+	-	-
	DP	+	+	-
	PRh	-	0	-
Hippocampal formation	LEnt	++	+	+
	CA1	+++	+++	++
	S	++	++	+
SEPTUM/STRIATUM				
Lateral septal complex	LSI	+	+	+
	LSD	-	0	0
	LSV	-	-	-
	SHi	++	+	-
Medial septum/Diagonal band	MS	++	++	+
	HDB/MCPO	++	+	+
	VDB	++	+	-
Striato-pallidum	VP	-	+	
	SL	+++	++	+
	SI	++	++	+
	IPAC	-	0	0

		MeA	MePV	MePD
THALAMUS				
	PVA/PV	++/+	++/+	+/-
	PVP	+++	+++	++
	Re	++	++	+
	MD	-	0	0
	MHb	-	-	0
	ZI	+	-	+
	pv	+++	++	++
	SPF	+++	++	++
	SPFPC	++	++	++
	PIL	+++	+++	+++
	SG	++	+	-
	PP	+++	+++	++
	MGM	+	+	-
HYPOTHALAMUS				
Preoptic	MPA	-	0	-
	MPO	+	+	++
	LPO	-	0	-
Anterior	AH	+	+	+
	Pa	-	0	-
Tuberal	VMH	++	++	+
	DM	-	-	0
	LH	+	+	+
	Arc	-	0	-
	TC	-	+	-
Mammilary	PMD/PMV	0/+	0/+++	0/++++

		MeA	MePV	MePD
	SuM	-	+	-
	PH	++	++	+
BRAINSTEM AND MIDBRAIN				
	PAG	-	-	-
	VTA	-	0	0
	RLi	-	0	0
	DR	+	+	+
	IP	-	0	0
	MnR	-	-	-
	PB	++	++	+

3.2.2.1 Retrograde labelling after FG injections into the anterior subdivision of the medial amygdaloid nucleus (MeA)

Nine injections were aimed at the MeA, four of which were restricted to this subnucleus (see Figs. 6A-C and 6I). In addition, five more injections were centred in the MeA but extended to some neighbouring structures such as the substantia innominata (M1242), the anterior amygdaloid area (M1248), the MePD (cases M1316 and M1314) or the MePV (M1317). The pattern of labelling was similar in all four restricted injections (case M1310 is illustrated in Fig. 7), and the labelling in non-restricted injections is fully consistent with the pattern described.

In general, the density of labelled cells was high in areas of the olfactory systems and in several nuclei of the amygdala and bed nucleus of the stria terminalis (BST), moderate in the hippocampal formation and scarce in the neocortex. Within the subcortical telencephalon, labelled cells were also present in the septum and basal forebrain. In addition, several populations of labelled cells were seen in several nuclei of the thalamus, hypothalamus as well as in some midbrain and brainstem centres.

Retrograde labelling in the olfactory systems

As expected, injections of FG in the MeA gave rise to very dense retrograde labelling throughout the mitral cell layer of the accessory olfactory bulb (MiA) (Figure 7A, Table

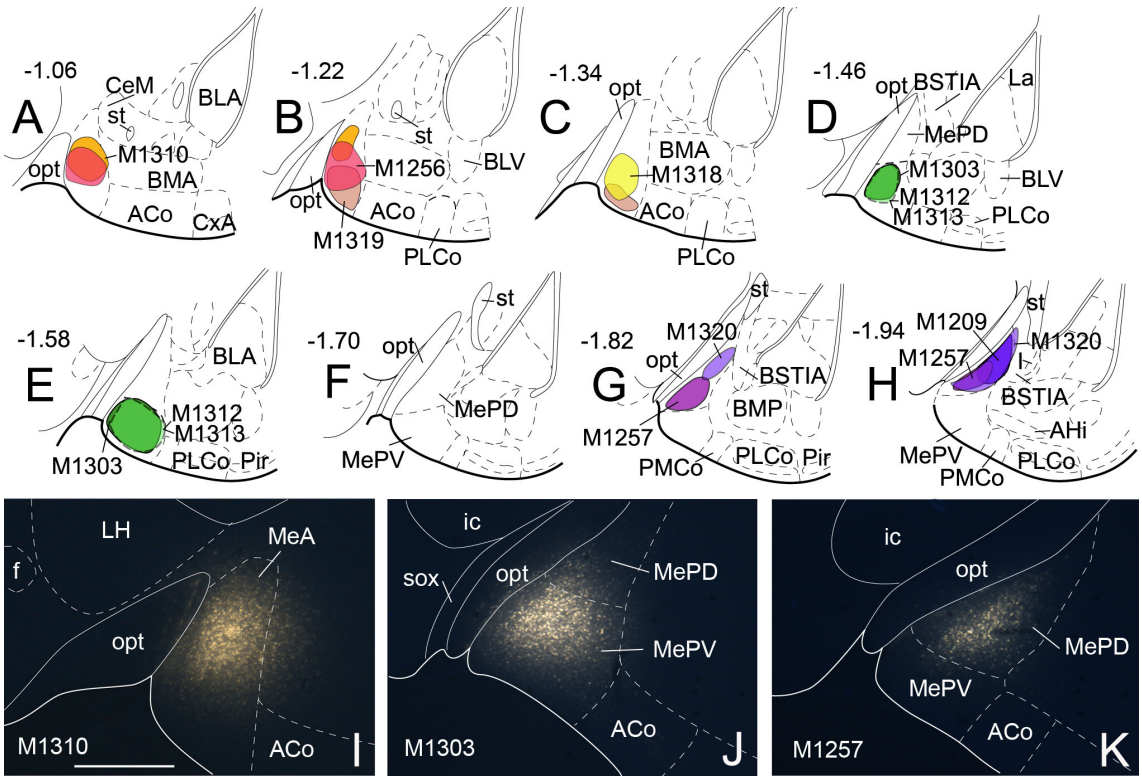

Fig. 6 Injection sites in the anterior, posteroventral and posterodorsal subdivisions of the medial amygdaloid nucleus in mice. (A–H) Schematic drawings representing the extent of the tracer injections in the anterior medial amygdaloid nucleus (MeA), posteroventral medial amygdaloid nucleus (MePV) and posterodorsal medial amygdaloid nucleus (MePD). The MeA injections are represented in panels **A-C**; MePV injections are shown in panels **D, E** (injections M1312 and M1313 were almost identical, and therefore one drawing illustrates both) and MePD injections are represented in panels **G, H**. Single injections are identified with the animal code. Note that no injection site is present in panel **(F),** shown only for the sake of the rostro-caudal continuity of the figure. **(I-K)** Fluorescent photomicrographs through the amygdala showing representative injections sites of Fluorogold. **(I)** Injection site in MeA, case M1310. **(J)** Injection site in MePV, case M1303. **(K)** Injection site in MePD, case M1257. For abbreviations, see list. Scale bar in I, valid for I-K = 500 µm

2), which represents one of the main sources of inputs to the MeA. In addition, the main olfactory bulb also displayed labelled mitral cells, mainly located in the medial and lateral aspects of the bulb (see Table 2). Labelling density in the MOB is relatively higher in case M1256, in which the injection is centred in the superficial layer of MeA,

and in the non-restricted injection M1242, which involved the external layer of the MeA.

Secondary olfactory centres also showed remarkable retrograde labelling. Thus, a moderate number of labelled cells was observed in the dorsal tenia tecta (DTT, layer III)

(Figure 8A), while the ventral tenia tecta (VTT) showed scarce labelling mainly located in its layer II. The piriform cortex (Pir) showed a heterogeneous pattern of retrograde labelling, from very scarce in the anterior Pir to dense in its caudal portion (Figure 7B-J; Fig. 8C). Labelling was distributed in layers II and III but, occasionally, labelled cells were seen in layer I, just below the lateral olfactory tract (*lo*) (Figure 7B-D). In addition, the endopiriform nucleus, especially its dorsal portion (DEn), also showed retrograde labelling, with a heterogenous antero-posterior distribution (Figure 7B-J, Figure 8C).

Retrograde labelling in the amygdala

The amygdala (together with the BST) presented the densest populations of retrogradely labelled cells, and the most intensely labelled neurons. Labelling was present in the chemosensory nuclei, as well as in deep nuclei belonging to the basolateral/amygdalo-hippocampal or central divisions.

Within the chemosensory amygdala, labelling was dense in the PMCo (Fig. 7H-K), the only vomeronasal nucleus that does not receive direct olfactory projections. In general, this nucleus showed a very dense labelling, with labelled somata located in the cellular layers (layers II and III). Retrogradely labelled neurons appeared heterogeneously distributed: labelling was very dense in the rostral PMCo (adjacent to the MePV, Fig. 7H), moderate in intermediate levels, where labelled cells were located mainly in the lateral aspect of the nucleus (Figure 7I, J), and very dense in the caudal edge of the nucleus (Figure 2K).

With regard to the mixed chemosensory amygdala, within the nuclei with vomeronasal predominance, labelling was present in the different divisions of the Me, the bed nucleus of the accessory olfactory tract (BAOT) and the anterior amygdaloid area (AA) (Table 2). Within the Me very dense labelling was observed in the non-injected portions of the MeA, including the dense-celled regions of the anteroventral (MeAV) and the anterodorsal (MeAD) parts of the MeA, which are rostral to the injection site (Fig. 7F). The MePV showed a heterogeneous pattern of labelling along its antero-caudal axis,

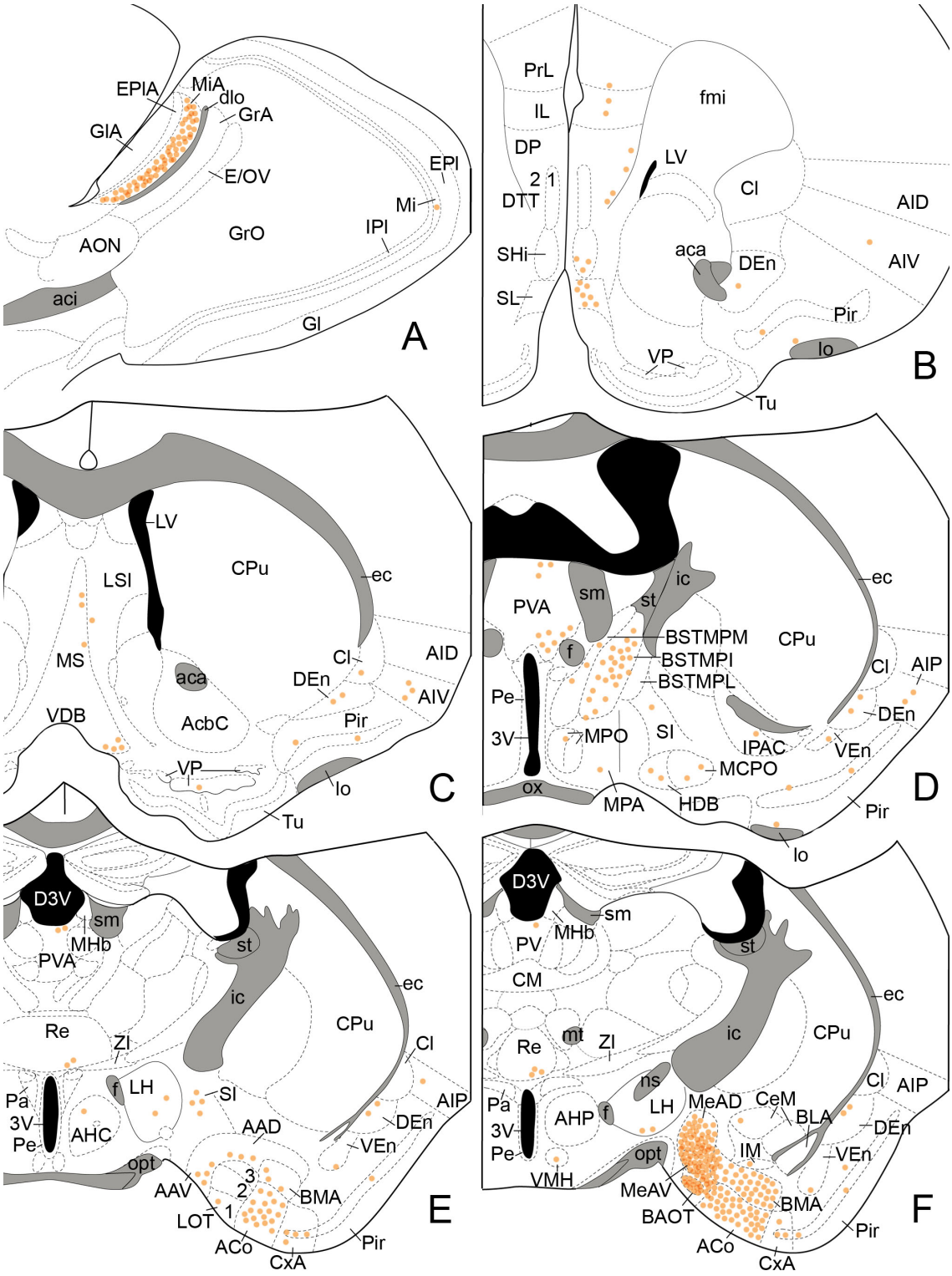
EPIA
MiA
dlo
GrA
GlA
E/OV
EPl
Mi
IPl
GrO
AON
aci
Gl
A
PrL
IL
DP
2 1
DTT
fmi
LV
Cl
AID
SHi
aca
DEn
AIV
SL
Pir
lo
VP
Tu
B
LV
LSI
CPu
ec
MS
Cl
AID
aca
DEn
AIV
VDB
AcbC
Pir
VP
lo
Tu
C
PVA
sm
st
ic
ec
f
BSTMPM
BSTMPI
BSTMPL
CPu
Cl
AIP
Pe
DEn
3V
MPO
SI
IPAC
VEn
MCPO
ox
MPA
HDB
Pir
lo
D
D3V
sm
MHb
PVA
st
ec
ic
CPu
Re
ZI
Cl
f
LH
SI
AIP
Pa
3V
Pe
AHC
AAD
DEn
VEn
opt
AAV
3
2
BMA
LOT
1
ACo
CxA
Pir
E
D3V
sm
MHb
PV
CM
st
ec
Re
mt
ZI
ic
CPu
ns
Cl
AIP
Pa
AHP
f
LH
MeAD
CeM
BLA
3V
DEn
Pe
opt
IM
VEn
VMH
MeAV
BMA
BAOT
Pir
ACo
CxA
F

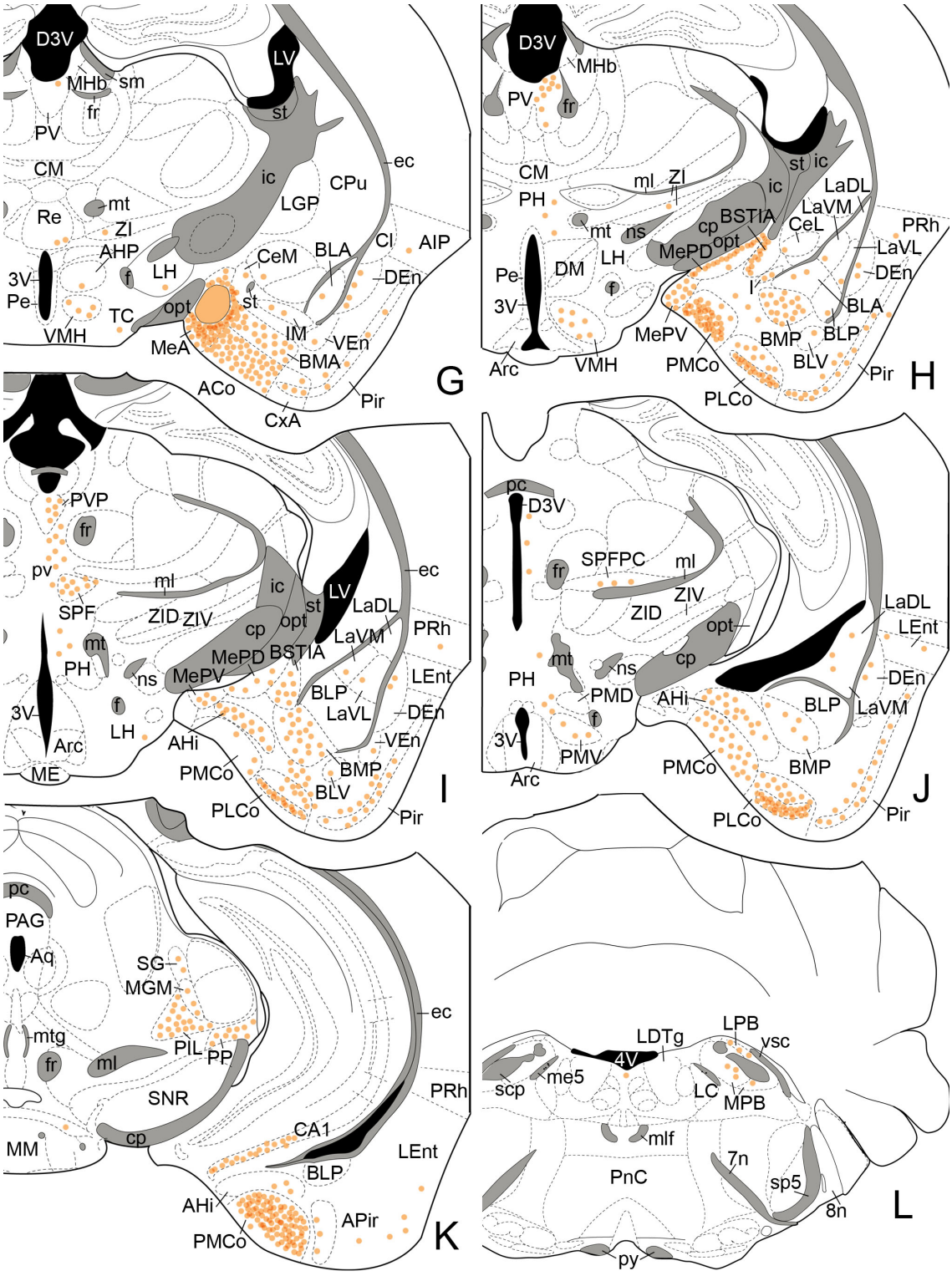

Fig. 7 Semi-schematic drawings of parasagittal (A) and frontal (B-L) sections through the mouse brain showing the distribution of retrogradely labelled somata following a Fluorogold tracer injection in the anterior medial amygdaloid nucleus. The injection site is depicted in panel **(G)**. The semi-schematic drawings are based on the case M1310, which presented the largest restricted injection. **B** is rostral, **L** is caudal. For abbreviations, see list.

very dense at rostral levels (Fig. 8C) and less so caudally (Figure 7H, I). Finally, the MePD presented, in general, moderate labelling with a conspicuous heterogeneity in the distribution of labelled cells (Figure 7H, I). As figure 8C illustrates, at least at rostral levels of the MePD, labelled cells apparently lined up the outer boundary of the cell layer, with deeper regions showing a lower density of stained cells. In addition, the BAOT showed also very dense labelling with darkly stained somata (Figure 7F), whereas the ventral and dorsal divisions of the AA (AAV, AAD) presented a moderate density of retrograde labelling.

Regarding to the olfactory amygdala (Table 2), the posterolateral cortical amygdaloid nucleus (PLCo) displayed a high density of labelled cells (Fig. 7H-J), most cells being located in layer II and to a lesser degree in layer III (see Fig. 8C). By contrast, the amygdalo-piriform transition area (APir) showed a moderate density of labelled cells (Table 2, Figure 7K).

Among the nuclei of the mixed chemosensory amygdala with olfactory predominance (Table 2), the anterior cortical amygdaloid nucleus (ACo) showed a dense population of labelled neurons in the cell layer (Figure 7E-G, Figure 8C). The cortex-amygdala transition zone (CxA) displayed moderate labelling density, with the labelled somata mainly located in layer II (Fig. 7E). Finally, the nucleus of the lateral olfactory tract (LOT) showed just a few retrogradely labelled cells confined to layer I (Fig. 7E).

Within the multimodal or deep amygdala (Table 2), in the basolateral complex, the anterior and posterior parts of the basomedial amygdaloid nucleus (BMA, BMP respectively) showed a heterogeneous labelling density (dense, in average). In both nuclei dense labelling was present in their rostral parts while in their posterior parts the labelling decreased to moderate (Figure 7E-J). In the basolateral amygdaloid nucleus, the anterior (BLA), ventral (BLV) and posterior (BLP) parts showed scarce labelling (Figure 7F-K). In the lateral amygdaloid nucleus labelling was scarce in its ventromedial and ventrolateral parts (LaVM, LaVL) and very scarce in its dorsolateral part (LaDL) (Figure 7H-J). Finally, in the amygdalo-hippocampal area (AHi) labelling was denser in the rostral half than its caudal aspect (Fig. 7I-K).

To complete the description of retrograde labelling in the amygdala, scarce or very scarce labelling was observed in the central amygdaloid nucleus (Table 2), mainly in its

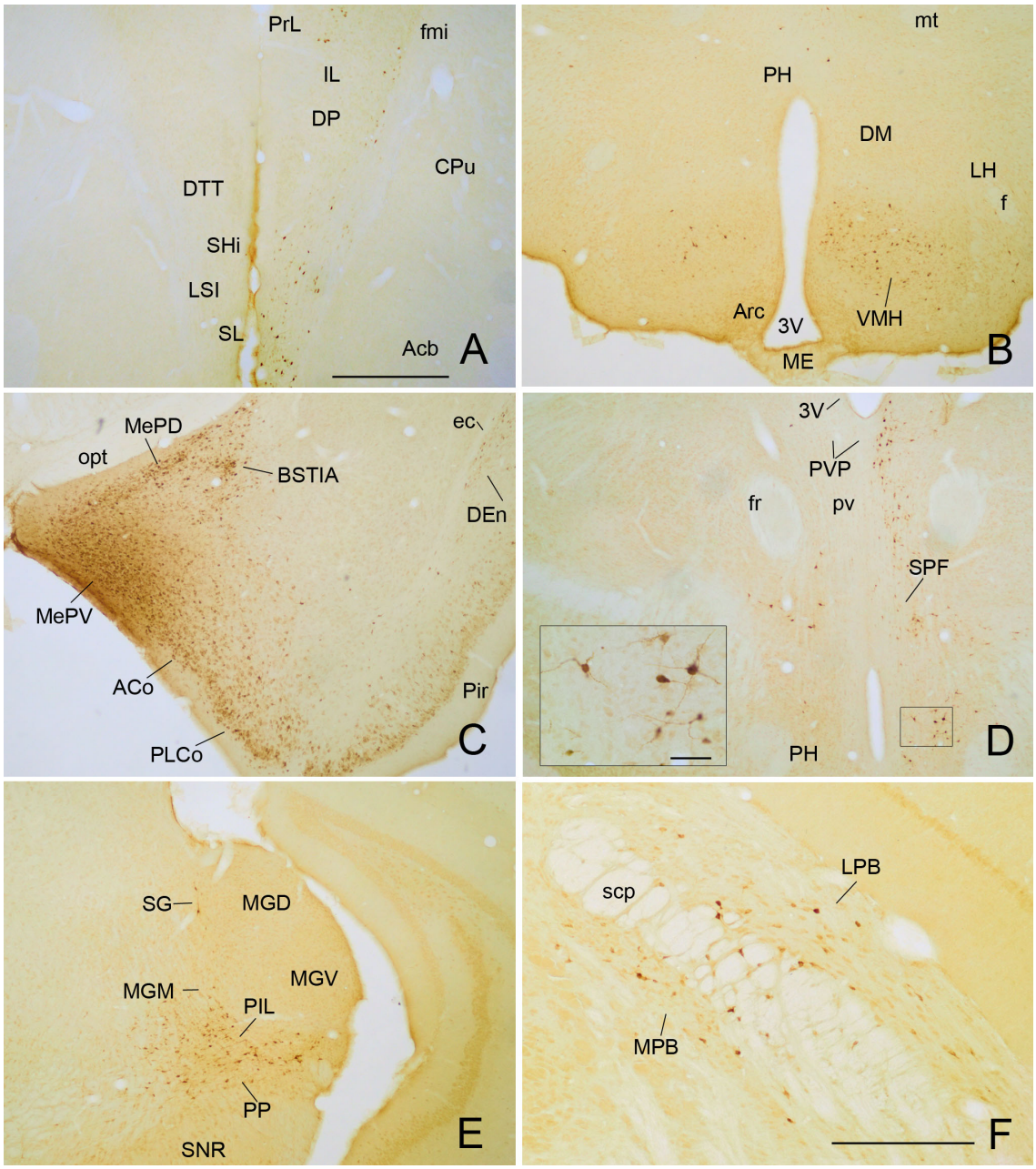

Fig. 8 Photomicrographs of frontal sections illustrating the retrograde labelling through the mouse telencephalon of animals receiving a Fluorogold injection in the anterior medial amygdaloid nucleus. The images correspond to the retrograde labelling presented in the cases M1310 **(A, B, E)** and M1319 **(C, D, F)**. **(A)** Retrograde labelling in the prelimbic and infralimbic areas of the prefrontal cortex and the rostral areas of the septum. **(B)** Retrogradely labelled neurons in the ventromedial hypothalamus. **(C)** Numerous labelled cells in the posterodorsal and posteroventral subnuclei of the medial amygdala, as well as in the anterior and posterolateral cortical amygdaloid nuclei. **(D)** Retrogradely labelled cells in the midline thalamus and posterior hypothalamus. The inset shows the Golgi-like stained neurons observed in the posterior hypothalamic area. **(E)** Retrogradely labelled neurons in the posterior intralaminar thalamic complex. **(F)** Retrograde labelling in the parabrachial nucleus of the brainstem. For abbreviations, see list. Scale bar in A (valid for B-E): 500 µm. Scale bar in F: 250 µm. Scale bar in inset in D: 500 µmmedial division (CeM, Fig. 7F-H), and

in the intercalated nuclei of the amygdala (I), including the main intercalated nucleus (IM; Figs. 7F and 7H).

Labelling in the bed nucleus of the stria terminalis (BST)

Within the BST complex, the posterior part of the medial subdivision presented the strongest labelling (Figure 7D). The posterointermediate part of the medial division of

the BST (BSTMPI) showed dense labelling whereas in the posteromedial (BSTMPM) and posterolateral (BSTMPL) parts labelled cells were relatively scarcer (Fig. 9A, D). Other parts of the BST (results not shown) display a low number of labelled cells, including the ventral (BSTMV) and anterior parts of the medial BST (BSTMA), and the posterior and ventral parts of the lateral BST (BSTLP and BSTLV, respectively; Table 2). Finally, the intraamygdaloid part of the BST (BSTIA) showed dense labelling with the stained cells located more frequently in its medial aspect adjoining the MePD (Figs. 7H, I and 8C).

Retrograde labelling in the Cortex and Hippocampal formation

In the neocortex, labelling was scarce and restricted to the prefrontal and perirhinal regions. Thus labelled neurons were observed in the medial orbital (MO), prelimbic (PrL), infralimbic (IL) and dorsal peduncular cortices (DP) (Figure 7B, Figure 8A, Table 2). Except for case M1257, in which the IL presented a moderate number of labelled cells, the rest of the areas in the medial prefrontal cortex showed very scarce labelling. Likewise, the lateral orbital cortex (LO), claustrum (Cl) and perirhinal cortex (PRh) displayed very few labelled cells (Figure 7D-K). In contrast, a moderate density of labelled cells appeared in the ventral and posterior parts of the agranular insular cortex (AIV, AIP respectively), with labelled somata located in layer V (Figure 7C-G). More caudally, a moderate number of labelled neurons were seen in the lateral entorhinal cortex (LEnt; Figure 7I-K), where labelling was especially dense immediately caudal to the APir.

Regarding to the hippocampus, a dense population of labelled somata appeared restricted to the ventralmost region of the field CA1 of the caudal hippocampus (CA1) (Fig. 7K).

Labelling in the septum and ventral forebrain

In the septal complex, a moderate density of labelling appeared in the rostral septohippocampal nucleus (SHi), just ventral to the DTT (Figure 7B, Figure 8A). The intermediate part of the lateral septum (LSI) displayed scarce labelling, with the labelled somata located next to the medial septal nucleus (MS) (Figure 7B-C). In the rest of the complex, we observed very scarce labelling in the dorsal and ventral part of the lateral septum (LSD, LSV respectively).

The vertical and horizontal limb of the diagonal band (VDB, HDB respectively) and the MS presented a moderate number of labelled somata lining up at the boundary with the LSI (Figure 7C). At the rostral HDB, labelled somata clustered in the lateral edge of the HDB, next to the olfactory tubercle (Tu; Figure 7C). In contrast, more caudally intensely labelled somata were distributed homogeneously in the caudal HDB and adjacent magnocellular preoptic nucleus (MCPO; Figure 7D). Within the basal cerebral hemispheres, at rostral levels a number of darkly stained cells were observed in the territory located between the nucleus accumbens (Acb) and the Tu (not shown). In addition, a group of intensely labelled cells was observed in the semilunar nucleus (SL; Figure 7B, 8A). Finally, the substantia innominata (SI) presented moderate labelling, and the ventral pallidum (VP) and interstitial nucleus of the posterior limb of the anterior commissure (IPAC) showed a few, scattered labelled somata (Figure 7C-E).

Retrograde labelling in the thalamus

After FG injections in the MeA, retrograde labelling was observed in the anterior, midline and posterior-intralaminar-peripeduncular thalamic regions. Within the anterior thalamus the paraventricular thalamic nucleus (PVA) displayed a large number of labelled cell bodies (Figure 7D, E; Fig. 9A), with a very striking heterogeneous distribution (Table 2). In its rostral edge, it presented a very dense labelling with darkly stained cells. At intermediate rostro-caudal levels, the labelling decreased to scarce (Figure 7E-G), and even more caudally, the posterior paraventricular thalamic nucleus (PVP) showed a high density of intensely labelled cells (Fig. 7H, I; 8D).

In addition, a low density of labelled cells could be observed in the mediodorsal nucleus (MD) and medial habenula (MHb). In one injection (M1256), the central medial thalamic nucleus and the lateral habenular nucleus also showed a few labelled cells.

Ventrally, a group of labelled neurons appeared in nucleus reuniens (Re; Fig. 7E-G; Fig. 9D) and the zona incerta (ZI) also showed a few labelled cell bodies (Figure 7F, G).

In the caudal thalamus, dense retrograde labelling appeared in the SPF, and a group of labelled cells appeared near the midline, among the tracts of the pv, apparently connecting the cell groups in the PVP and SPF (Figs. 7I and 8D). Within the SPF, a small group of labelled cell bodies extended caudo-laterally into its parvocellular part (SPFPC; Fig. 7J). Even more caudally, a high density of retrogradely labelled cells was seen in the posterior intralaminar (PIL) and peripeduncular nucleus (PP). Retrogradely labelled cells appeared also in the medial division of the medial geniculate nucleus (MGM) (Figure 7K, Figure 8E) and the suprageniculate nucleus (SG), where labelling was scarcer.

Retrograde labelling in the hypothalamus

In the hypothalamus labelled cells were present from preoptic to mammillary levels, but their density was quite low with two exceptions, the ventromedial hypothalamic nucleus (VMH) and the posterior hypothalamic nucleus (PH).

In the preoptic hypothalamus, sparse labelled neurons were present in the medial preoptic nucleus (MPO) and the medial and lateral preoptic areas (MPA, LPO; Fig. 7D, Table 2). At anterior levels, sparse labelled cell bodies were seen in the anterior hypothalamic area (AH) and paraventricular (Pa). At tuberal levels the VMH showed a moderate number of labelled cells (Figure 7G-H) bilaterally, with clear ipsilateral dominance (Fig. 8B). In addition, sparse labelled cells appeared in the dorsomedial (DM) and arcuate nucleus (Arc), in the tuber cinereum (TC) and in the lateral hypothalamic area (LH; Figs. 7E-I and 8B).

Within the mammillary hypothalamus, labelled cells were present in the PH (Fig. 7H-J), mainly at caudal levels. In addition, retrograde labelling was scarce in the ventral premammillary nucleus (PMV). Finally, the supramammillary nucleus (SuM) displayed a few, sparse retrogradely labelled cells (Figure 7K).

Retrograde labelling in the midbrain and brainstem

Labelled cells were very scarce and scattered in diverse nuclei of the midbrain and brainstem, including the ventral tegmental area (VTA), interpeduncular nucleus (IP),

periaqueductal gray (PAG), rostral linear nucleus of the raphe (RLi) and the dorsal (DR) and median raphe nuclei (MnR) (Table 2). The few retrogradely labelled cells found in the PAG were scattered across its different subdivisions. In addition, the parabrachial nucleus (PB) presented a moderate density of labelled cells, both in its medial and lateral divisions (Figure 7L, Figure 8F).

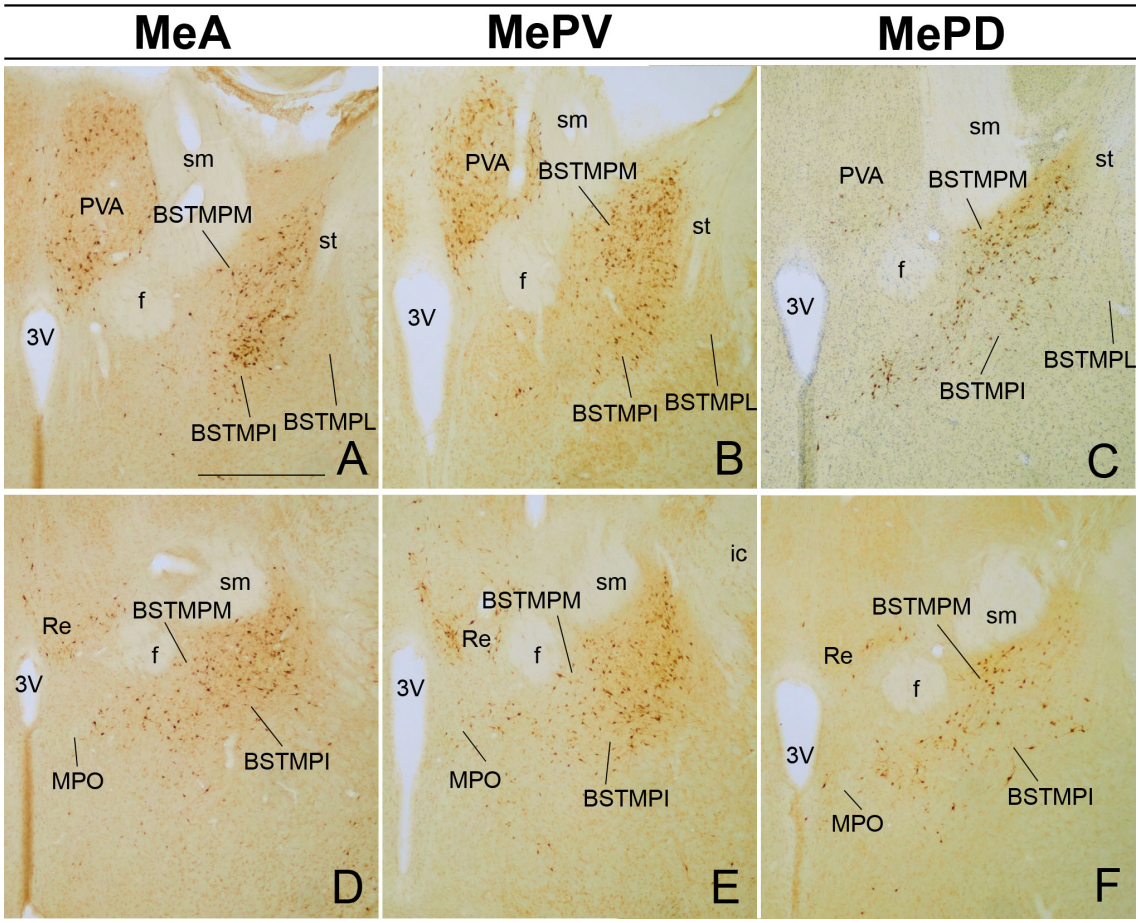

Fig 9 Photomicrographs of frontal sections illustrating the retrograde labelling present in the medial subdivision of the bed nucleus of the stria terminalis (BSTM) after Fluorogold injections in the medial amygdaloid nucleus. (A, D) Retrograde labelling after an injection in the anterior part of the medial amygdala, case M1318, showing the resulting dense labelling in the posterointermediate part of the BSTM (A is rostral, D is caudal). **(B, E)** Retrograde labelling after an injection in the posteroventral part of the medial amygdala, case M1303, illustrating the dense labelling observed in the posterointermediate part of the BSTM and the heterogeneous labelling present by the posteromedial part of the BSTM (B is rostral, E is caudal). **(C, F)** Retrograde labelling after an injection in the posterodorsal part of the medial amygdala, case M1257, illustrating the dense labelling showed by the posteromedial part of the BSTM (C is rostral, F is caudal). Note also the dense labelling in the anterior paraventricular thalamic nucleus in A and B. For abbreviations, see list. Scale bar in (A) valid for (B-F): 500 µm

Contralateral labelling

Although FG injections in the MeA gave rise mainly to ipsilateral retrograde labelling, labelled cells were also observed in the side of the brain contralateral to the injection. In general, these nuclei were the contralateral counterparts of the ipsilateral structures that presented very dense or dense labelling. Thus contralateral labelling was scarce in the amygdaloid PLCo and PMCo, the thalamic SPF, PIL and PP, the VMH in the hypothalamus and the PB in the brainstem. Occasional (very scarce) labelling was also observed in the contralateral LEnt, in the hippocampal formation; the LSI, VDB, and HDB in the septal complex; the SL and SI in the striato-pallidum; numerous structures in the amygdala and BST (MeA, BLA, BMP, APir, BSTMPM, BSTMPI); the PVA, Re, ZI, pv and SPFPC in the thalamus; the MPO, Pa, PH, PMV and Arc in the hypothalamus; and the PAG, AH and DR in the midbrain and brainstem.

3.3.2.2. Retrograde labelling after FG injections into the posteroventral subdivision of the medial amygdaloid nucleus (MePV)

Six injections of FG involved the MePV, three of which were restricted to this subnucleus (cases M1303, M1312 and M1313; Fig. 6D, E and J) and the remaining encompassed also adjoining regions such as the caudal MeA (M1249), the ventral MePD (M1259) and the ACo and PMCo (M1301). The results of non-restricted injections are consistent with the pattern of labelling revealed by restricted cases, which is described below.

Experiment M1303 is illustrated as representative case of retrograde transport of FG from the MePV (Fig. 10). In general, retrograde labelling was present in the same nuclei observed after FG injections in the MeA. Differences pertained to the relative density of labelled cells and their distribution within the nucleus in some centres of the olfactory systems, cortex, septum, striato-pallidum, thalamus and hypothalamus (see Table 2). Therefore, we will focus our description on those differences.

Retrograde labelling in the olfactory systems

As in the case of FG injections in the MeA, very dense labelling was observed throughout the MiA of the AOB (Figures 10A and 11A). In contrast, no labelling appeared in the MOB.

Among the secondary olfactory centres, the observed retrograde labelling was in general less dense than after the injection in the MeA. Thus, the DTT and anterior Pir presented scarce labelling (Figure 10B-D), and only in the caudal part of the Pir (next to the PLCo), we observed a moderate density of retrogradely labelled cells (mainly in layer II, Figure 10H-J). Similar to the Pir, the DEn showed scarce labelling in its rostral part and moderate labelling caudally (Figure 10C-J). Last of all, the VEn showed moderate labelling (Figure 10D-J).

Retrograde labelling in the amygdala

Within the vomeronasal amygdala, as described in the injections in the MeA, the PMCo showed in general a very dense labelling with darkly stained somata (Table 2). The intranuclear distribution of labelled stomata was heterogeneous (although not as conspicuous as in the case of MeA injections), with labelling being dense rostrally and caudally but moderate at intermediate levels (Figs. 10J, K and 11D).

Regarding to the mixed nuclei with vomeronasal predominance (Table 2), the MeA showed also a very dense labelling (Figures 10H and 11C). Within the MeA, the labelling presented a heterogeneous distribution, with moderate and dense labelling observed in the MeAD and MeAV respectively (Figures 10G and 11B). The MePD showed in general a dense labelling (Table 2), with a heterogeneous distribution of labelled somata (Figure 10I, J). Darkly stained somata were aligned along the most medial part of the cellular layer in the limit with the external layer. The inner part of the cellular layer presented moderate labelling (which was denser than that observed in the same location after the MeA injections) (Figure 10I, Figure 7H respectively). In addition, the BAOT presented very dense labelling (Figures 10G and 11B) and the AAV and AAD, showed moderate and scarce labelling respectively (Figure 10E, F).

Within the olfactory amygdala (including the mixed nuclei with olfactory predominance) the retrograde labelling observed was very similar to that obtained following the injection in the MeA (Table 2). Thus, the PLCo (Figure 10I, J) and ACo (figures 10F-I and 11B, C) presented dense labelling, while the APir (Figure 11D) and CxA (figure 10E-H) showed scarce labelling. Finally, in the LOT we observed very scarce labelling with the labelled neurons present in layer I (Figure 10F).

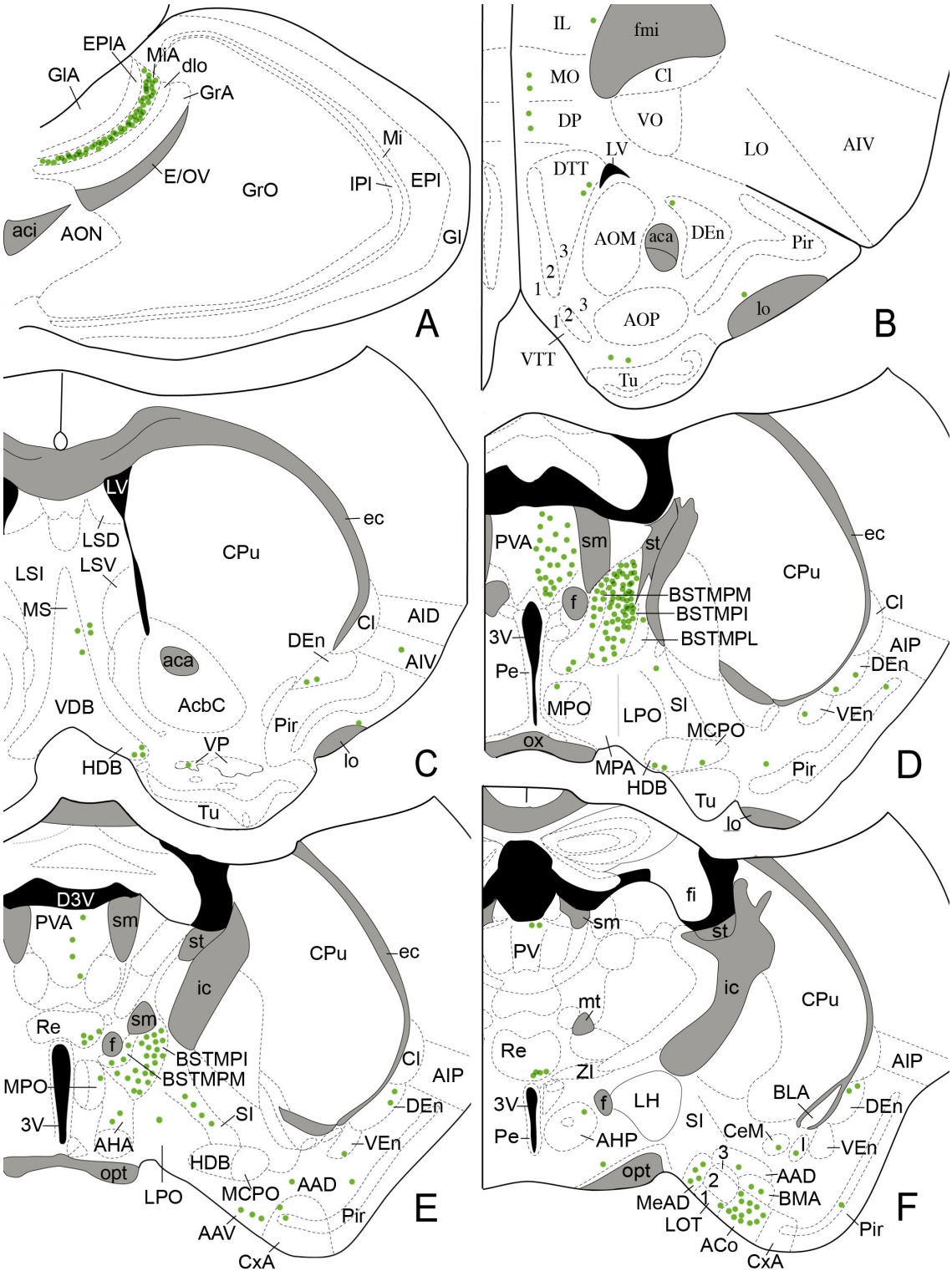
EPIA
MiA
dlo
GlA
GrA
E/OV
GrO
Mi
IPl
EPl
Gl
aci
AON
A
IL
fmi
MO
Cl
DP
VO
LV
LO
AIV
DTT
AOM
aca
DEn
Pir
3
2
1
AOP
lo
VTT
Tu
B
LV
ec
LSD
CPu
LSI
LSV
MS
Cl
AID
DEn
AIV
aca
VDB
AcbC
Pir
VP
HDB
lo
C
Tu
PVA
sm
st
ec
CPu
BSTMPM
f
BSTMPI
Cl
3V
BSTMPL
AIP
DEn
Pe
MPO
LPO
SI
MCPO
VEn
ox
MPA
HDB
Pir
D
Tu
lo
D3V
PVA
sm
st
CPu
ec
ic
Re
sm
f
BSTMPI
BSTMPM
Cl
AIP
MPO
DEn
SI
3V
AHA
VEn
HDB
opt
LPO
MCPO
AAD
Pir
AAV
CxA
E
fi
sm
st
PV
ic
mt
CPu
Re
Zl
AIP
3V
f
LH
BLA
DEn
Pe
AHP
SI
CeM
l
VEn
3
opt
AAD
2
MeAD
1
BMA
LOT
ACo
CxA
Pir
F

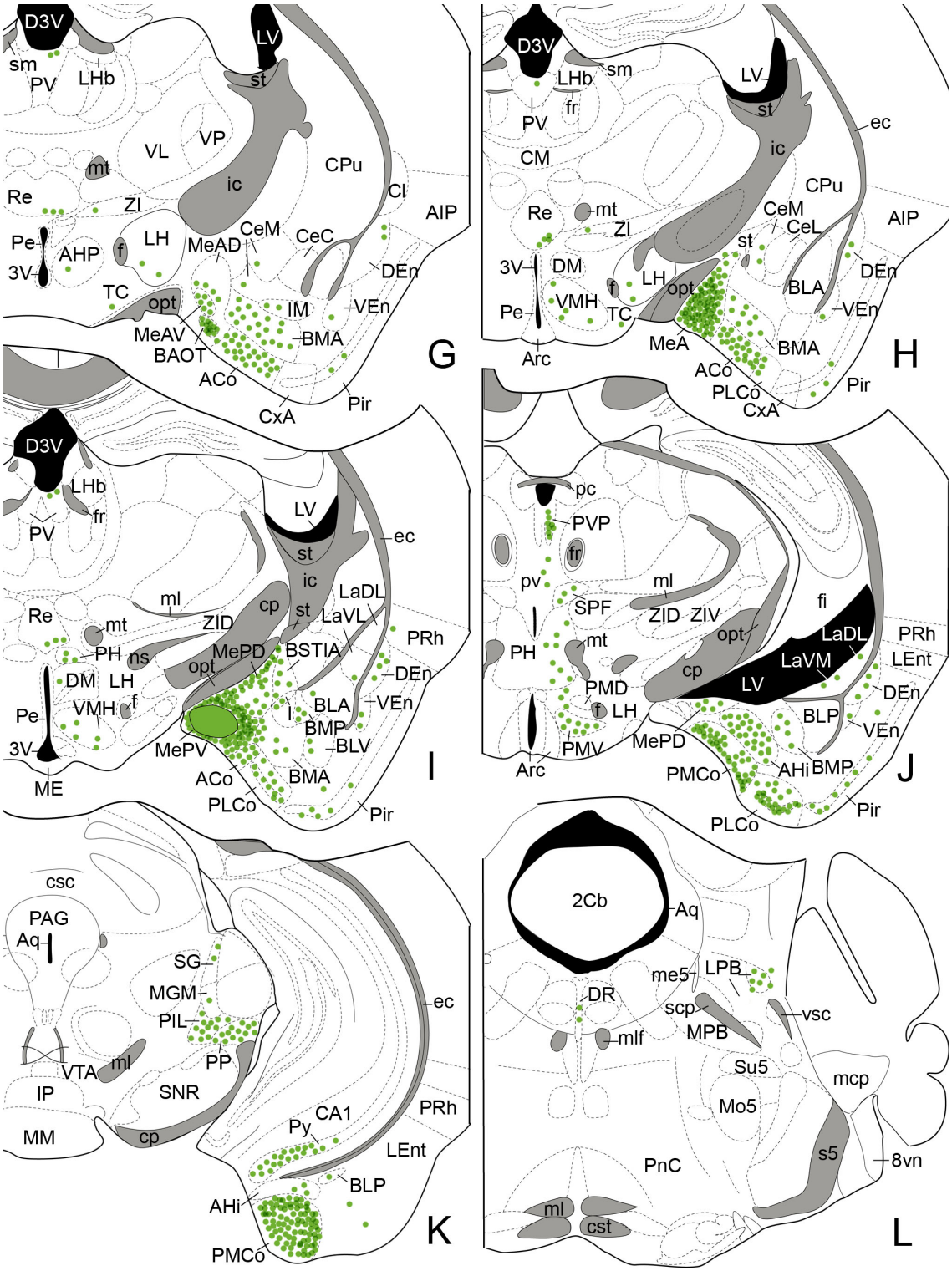

Fig. 10 Summary of the distribution of retrograde labelling following a Fluorogold injection in the posteroventral medial amygdaloid nucleus, plotted onto semi-schematic drawings of parasagittal (A) and frontal (B-L) sections through the mouse brain. The injection site is depicted in panel **(I)**. **A** is rostral, **L** is caudal. The semi-schematic drawings are based on the case 1303, which presented the largest restricted injection. For abbreviations, see list.

Within the basolateral complex (Table 2), the BMA and BMP showed in general a moderate labelling (Table 2) with a heterogeneous distribution. In the BMA the labelling was mainly located in its anterior part (Figure 10F-I), whereas in the BMP retrogradely labelled cells were more frequent in its posterior aspect (Figure 10I-K). Within the lateral amygdaloid nucleus, the LaVM presented scarce labelling and only a few cells were present in the LaDL and LaVL (Fig. 10I, J). Retrograde labelling was also scarce in the basolateral nucleus, where it was mainly observed in the BLP and BLV (Figure 10H-K).

With regard to the AHi, as observed following MeA injections, it showed a moderate amount of labelling (Table 2), present mainly in its rostral part (Figure 10J, K).

Finally, the central amygdala and associated intercalated cell masses showed almost the same pattern of retrograde labelling that we observed following the MeA injections (Table 2), with only a few labelled cells observed mainly in the CeM, the IM and I (Figure 10F-H, Table 2).

Labelling in the bed nucleus of the stria terminalis (BST)

The labelling obtained in the BST followed the same pattern described after the injections in the MeA (Table 2). The densest labelling was present in the posterior aspect, where retrogradely cells were mainly present in the BSTMPI (Figs. 9B, E and 10D, E). In the BSTMPM we observed a moderate density of labelled cells, mainly found in its anterodorsal part (Figs. 9B, E and 10D, E). In addition, very scarce labelling was present in the BSTMA and the BSTLV (Table 2). Finally, the BSTIA showed a moderate amount of retrogradely labelled cells, with darkly stained somata located along its limit with the MePD (Figure 10I).

Retrograde labelling in the cortex and hippocampal formation

In general, the retrograde labelling resulting from the MePV injections was less dense than the one observed in the MeA injections (Table 2). Scarce retrogradely labelled cells were present in the MO and DP, with only a few cells observed in the IL, PrL and AI (Figure 10B-H). Within the hippocampal formation, the CA1 showed moderate labelling, with the labelled cells restricted to its ventral part (Fig. 11D). Some of these labelled cells were darkly stained. By contrast, the LEnt presented scarce labelling (Figure 10J, K).

Labelling in the septum and ventral forebrain

As described for the cortex, the septum and striatum showed less retrograde labelling than that observed after the MeA injections (Table 2). The SHi presented scarce labelling (Table 2), with darkly stained somata mainly clustered dorsal to the SL (as shown in the MeA injections, see figure 8A). The LSI and LSV showed scarce or very scarce labelling respectively (Figure 10C, Table 2), whereas no labelling appeared in the LSD.

In the MS, VDH and HDB/MCPO, the location and distribution of the labelled somata was similar to that previously described for the MeA injections (see description above). The main difference was a relatively scarcer number of labelled cells in the diagonal band (Figure 10C-E).

In the rostral striato-pallidum, as described in the MeA injections, a group of darkly stained somata were located between the Tu and the Acb (see Figure 10B). In addition, the SL presented moderate labelling (Table 2), with some darkly stained cells. More caudally, a few labelled cells were present in the VP (Figure 10C). Finally, the SI showed also moderate labelling (Figure 10D-F).

Retrograde labelling in the thalamus

The PVA, PV, PVP and Re showed the same densities and distribution of retrograde labelling described in the MeA injections (see the description above, Table 2). Briefly, the PVP and PVA showed dense and moderate labelling respectively, with only scarce labelling observed at intermediate levels (PV) between the PVA and the PVP (Figures 9B, E and 10D-J). The Re presented a moderate number of retrogradely labelled cells.

Regarding to the structures of the posterior intralaminar thalamus (SPFPC, PIL, PP and MGM), all showed the same densities of labelling, distribution of labelled somata, and presence of darkly stained somata as described in the MeA injections (see the description above, Table 2). In summary, the PIL and PP showed dense labelling, the SPFPC presented moderate labelling and the MGM showed scarce labelling (Fig. 10J, K).

Finally, the pv, SPF and SG presented also the same distribution of labelled somata than that described in the MeA injections, but with less density of labelling (Table 2, Fig. 10J, K).

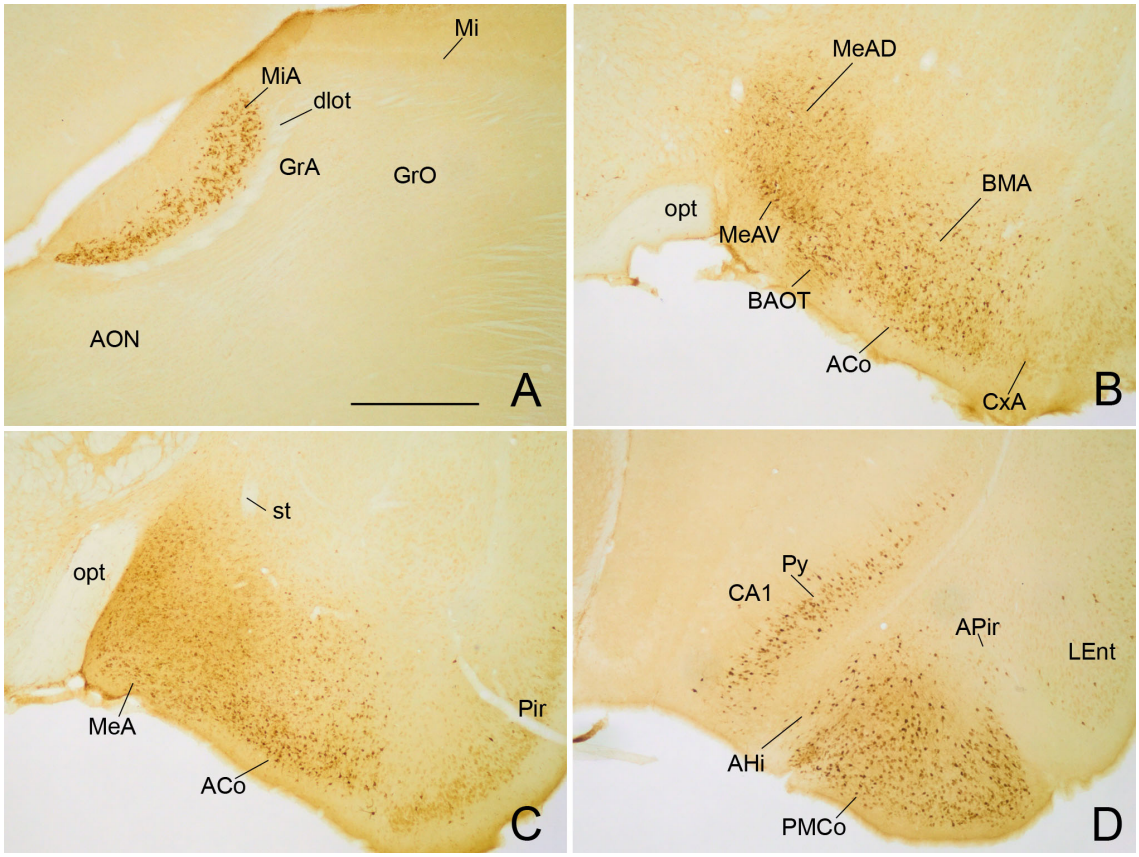

Fig. 11 Photomicrographs of parasagittal (A) and frontal (B-D) sections through the mouse telencephalon, illustrating the retrograde labelling observed in animals receiving a Fluorogold injection in the posteroventral medial amygdaloid nucleus. The images correspond to the retrograde labelling presented in the cases M1313 **(A, D)** and M1303 **(B, C)**. **(A)** Retrogradely labelled mitral cells in the accessory olfactory bulb. **(B)** Numerous labelled cells in the anterodorsal and anteroventral subdivisions of the anterior medial amygdaloid nucleus, as well as in the bed nucleus of the accessory olfactory tract, the anterior cortical amygdaloid nucleus and the basomedial nucleus. **(C)** Very dense retrogradely labelled cells in the anterior medial amygdaloid nucleus, just rostral to the injection site. **(D)** Retrogradely labelled cells in the posteromedial cortical amygdaloid nucleus and in the ventral hippocampus. For abbreviations, see list. Scale bar in A (valid for B–D): 500 µm.

Retrograde labelling in the hypothalamus

The VMH, MPO, AH, LH and DM presented the same densities of retrograde labelling (Table 2) and distribution of labelled somata previously described for the MeA injections (see description above). Briefly, the VMH showed moderate labelling. In the

MPO, AH and LH we observed scarce labelling, and only very few cells appeared in the DM (Fig. 10D-J).

The most relevant difference with the retrograde labelling observed after the injection in the MeA is the dense labelling with darkly stained somata present in the PMV of the mammillary hypothalamus (Figure 10J, Table 2). We also observed minor differences in the PH, SuM and TC. In the case of the PH, the labelling was moderate (as in the MeA injections) but labelled cells were strikingly clustered ventrally to the pv and dorsally to the PMD (Fig. 10I, J). In the cases of the SuM and the TC, both showed scarce labelling (Table 1 and Figure 10G, H).

Retrograde labelling in the midbrain and brainstem

The PB showed a moderate density of labelled cells with the somata mainly located between its rostral part and the beginning of the fourth ventricle (Figure 10L). In addition, the DR presented a low number of retrogradely labelled cells (Figure 10L) and only very scarce labelling was present in the PAG and the MnR (Table 2).

Contralateral labelling

As described in the injection in the MeA, the retrograde labelling resulting from the MePV injections was mostly ipsilateral, although some structures showed bilateral labelling. We observed moderate labelling in the contralateral PMCo, PIL and PP, and scarce labelling in the VMH and PB. In addition, we observed very scarce labelling in several amygdaloid structures (MeA, MePV, AVV, ACo and BMA), in some BST subnuclei (BSTMPM and BSTMPI), in the hippocampal CA1, in the septum and ventral forebrain (LSI, MS, HDB, VDB, SL and SI), in the thalamus (PVA, PV, PVP, pv, Re, ZI, SPF and SPFPC), in the hypothalamus (MPO, LH, Arc and PH) and finally in the PAG and Mn of the midbrain and brainstem.

3.2.2.3 Retrograde labelling after FG injections into the posterodorsal division of the medial amygdaloid nucleus (MePD)

We obtained six injections in the MePD; three restricted and three non-restricted. Figure 6G, H shows the location and extension of the restricted injections (cases M1209, M1257 and M1320). All these injections affected the cellular layer of the caudal half of the MePD. Figure 1K illustrates the location of the FG injection in case M1257, which

served to illustrate the observed retrograde labelling throughout the brain (Figure 12). The non-restricted injections affected adjoining structures, such as the MePV (case M1307), the MeA (case 1308) or the BMA (case M1307), but were useful to corroborate the observed labelling.

The three restricted injections gave rise to a similar pattern of retrograde labelling, described below and summarize in Table 2. In general, a smaller number of neural structures presented labelling and they showed less density of labelled cells compared with the MeA and MePV injections. Differences were mainly observed in the AOB and some centres of the amygdala, BST and hypothalamus (see Table 2). We will focus our description on those differences.

Retrograde labelling in the olfactory systems

In contrast to the results obtained following the injections in the MeA and MePV, the retrograde labelling observed in the AOB was strikingly heterogeneous, being much denser in the rostral than in the caudal MiA (Figs. 12A and 13A). Regarding to the MOB, in two injections (cases M1257 and M1209), the Mi presented very scarce labelling, with lightly stained somata observed in the lateral and medial aspects of the MOB (Table 2).

In the secondary olfactory centres, including the DTT, Pir and endopiriform nucleus, the distribution of retrograde labelling was similar to that observed after the injections in the MePV (Figure 12B-H), although a lesser amount of retrogradely labelled cells was observed (Table 2).

Retrograde labelling in the amygdala

In the vomeronasal amygdala, the injections in the MePD resulted only in a moderate amount of retrogradely labelled cells in the PMCo. This contrasts with the result obtained after MeA and MePV injections, in which the PMCo presented very dense labelling. The intranuclear distribution of the retrograde labelling follows the same pattern described following the injections in the MeA and MePV, that is, dense in its rostral and caudal parts (Figure 12G, I and 13C), and moderate at intermediate levels (Figure 12H).

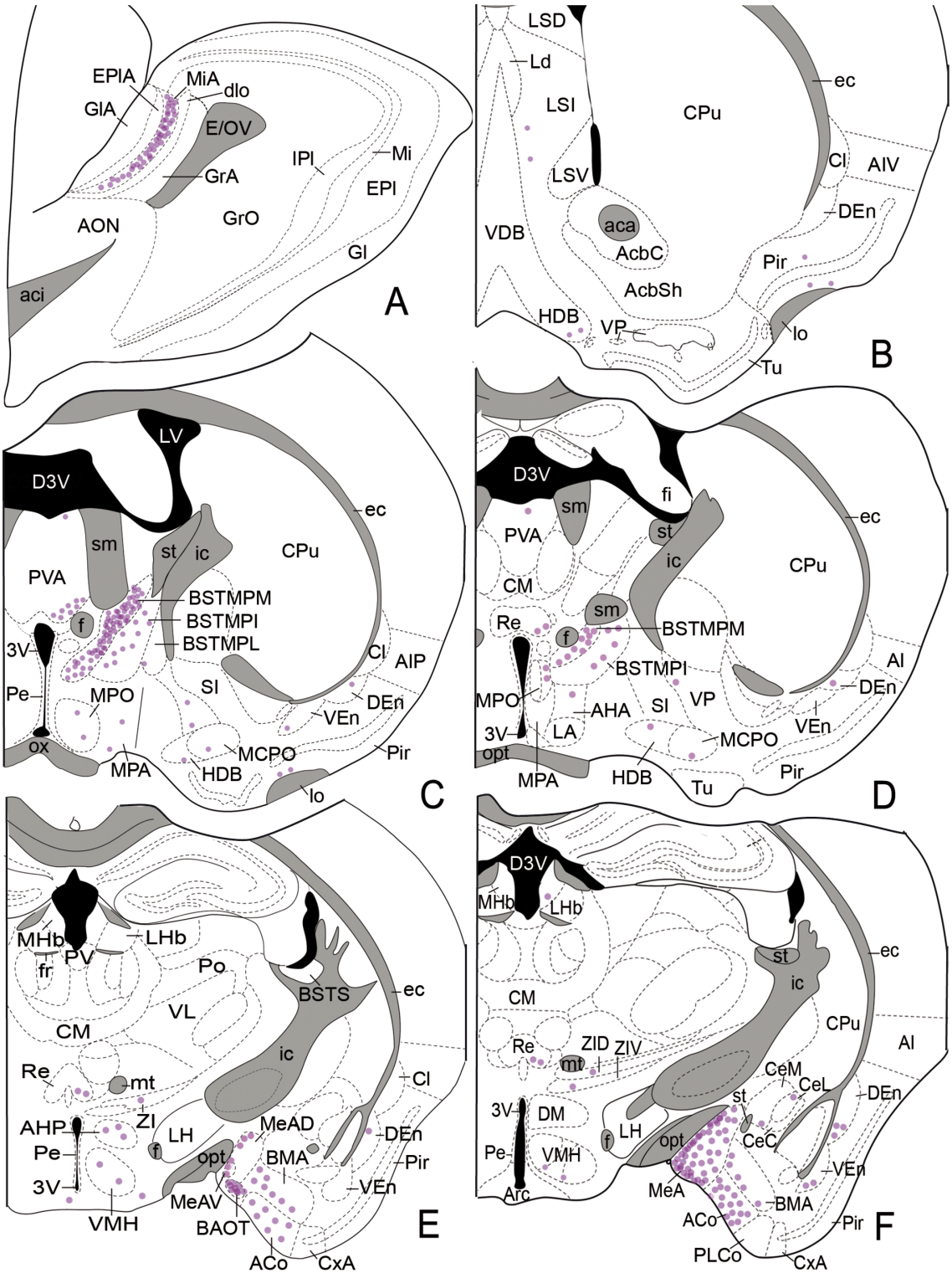
EPIA
MiA
dlo
GlA
E/OV
IPl
Mi
GrA
EPl
AON
GrO
Gl
aci
A
LSD
Ld
ec
LSI
CPu
Cl
AIV
LSV
DEn
VDB
aca
AcbC
Pir
AcbSh
HDB
VP
lo
Tu
B
LV
D3V
ec
sm
st
ic
CPu
PVA
BSTMPM
f
BSTMPI
BSTMPL
3V
Cl
AIP
Pe
MPO
SI
DEn
VEn
ox
MPA
MCPO
HDB
Pir
lo
C
D3V
fi
sm
ec
PVA
st
ic
CPu
CM
Re
sm
f
BSTMPM
BSTMPI
Al
MPO
AHA
SI
VP
DEn
3V
LA
MCPO
VEn
opt
MPA
HDB
Tu
Pir
D
MHb
LHb
PV
fr
Po
BSTS
ec
VL
CM
ic
Re
mt
Cl
ZI
AHP
LH
MeAD
DEn
Pe
f
opt
BMA
Pir
3V
MeAV
VEn
VMH
BAOT
ACo
CxA
E
D3V
MHb
LHb
st
ec
ic
CM
CPu
Al
Re
ZID
ZIV
mt
CeM
CeL
DEn
3V
DM
st
LH
CeC
Pe
VMH
opt
VEn
Arc
MeA
BMA
ACo
Pir
PLCo
CxA
F

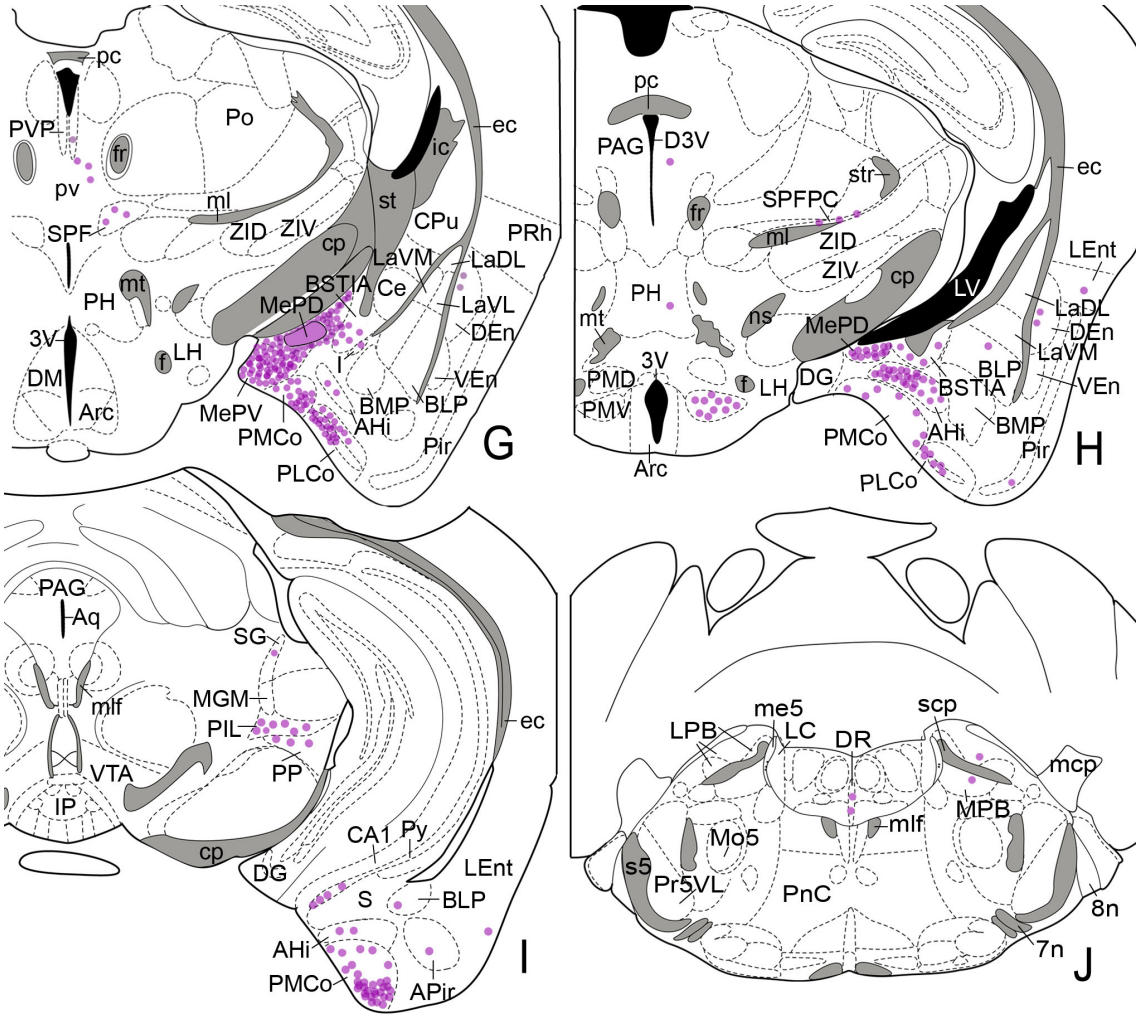

Fig. 12 Semi-schematic drawings of parasagittal (A) and frontal (B-J) sections through the mouse brain showing the distribution of retrogradely labelled somata following a Fluorogold injection in the posterodorsal medial amygdaloid nucleus. The injection site is depicted in panel **(G)**. **A** is rostral, **J** is caudal. The semi-schematic drawings are based on case M1257, which presented the largest restricted injection. For abbreviations, see list.

Within the mixed chemosensory nuclei with vomeronasal predominance (Table 2), the MeA showed very dense labelling, with labelled cells located mainly at the caudal MeA (Figure 12F). Noteworthy, in contrast to the results obtained following injection in the MeA and MePV, at rostral levels the MeAD and MeAV subnuclei showed only moderate and very scarce labelling, respectively (Fig. 12E). More caudally, the MePV presented very dense labelling (Fig. 12G). The BAOT presented dense labelling (Figure 12E), with darkly stained cells. Finally, the AAV and AAD showed very few labelled cells, in contrast with the moderate labelling observed after MeA and MePV injections (Table 1).

The structures composing the olfactory amygdala, including the mixed nuclei with olfactory predominance, showed less density of labelling following the injections in the MePD than after the injections in the MeA and MePV (Table 2). The densest labelling was observed in the ACo, mainly present in the caudal aspect of the nucleus (Figure 12E, F). The PLCo presented moderate labelling, with darkly stained cells located mainly in the medial part of the layer II (Figs. 12G, H and 13B). In addition, the APir (Fig. 12I) and the LOT presented only a few labelled cells. Noteworthy, the CxA was devoid of labelled somata, in sharp contrast to what we observed in the case of MeA and MePV injections (Table 1, Figure 12E, F).

Compared with the MeA and MePV injections, the basolateral complex was almost devoid of labelled cells with the exception of the BMA, which showed a moderate density a labelling (Figure 12E, F). Finally, within the deep amygdaloid nuclei, the AHi presented, in general, a denser labelling than that observed following injection in the MeA and MePV, with retrogradely labelled cells located mainly in its rostral and medial aspect (Figure 12G-H, Figure 13C).

Finishing with the description of the amygdala, within the central amygdala the CeM showed a low number of retrogradely labelled cells (as observed after injections in the MeA and MePD, Table 2), while the I and IM presented very scarce labelling (Figure 12E, G).

Labelling in the BST

Within the BST complex, unlike the MeA and MePV injections, only the BSTMPM, the BSTMPI and the BSTIA presented retrograde labelling (Table 2). In addition, the density of labelled cells in the BSTMPM and BSTMPI differed from the observed density of labelled cells after the MeA and MePV (Table 2). Figure 9C, F illustrates the labelling observed in the BSTMPM and BSTMPI. The BSTMPM presented very dense labelling, with more labelled neurons present in its dorsal part (Fig. 9C and 12C). In contrast, the BSTMPI presented moderate labelling (Figure 12C, D). Finally, the BSTIA showed a moderate number of retrogradely labelled cells (Figure 12G, H).

Retrograde labelling in the cortex and hippocampal formation

The retrograde labelling in neocortical structures was very scarce following the injections in the MePD (and scarcer if compared with the results of injections in the

MeA and MePD), with a few cells present in the MO, IL, DP, Cl and PRh (Table 2). Within the hippocampal formation, similar to the findings after injections in the MeA and MePD, the CA1 showed moderate labelling, with the labelled cells restricted to its ventral part (Fig. 12I), and a low number of labelled cells were observed in the LEnt (Fig. 12I).

Labelling in the septum and ventral forebrain

The distribution of the labelled somata within these areas was similar to what we observed in the MeA and MePD injections. In the lateral septum, the LSI showed scarce labelling, and only a few labelled cells appeared in the LSV and SHi (Figure 12B, Table 2). The MS and HDB/MCPO showed scarce labelling while the VDB presented very scarce labelling (Figure 12B-D). Within the striato-pallidum, the SL and SI displayed scarce labelling.

Retrograde labelling in the thalamus

The injections in the MePD gave rise to a smaller number of retrogradely labelled cells in the anterior midline thalamus, but the location and distribution of labelled cells follow a similar pattern to that described following the injections in the MeA and MePV (Table 2, Figs 12C-G and 9C). In the posterior intralaminar thalamic complex the distribution and density of the observed labelling in the SPFPC, PIL and MGM was very similar to that described following the MeA and MePV injections (Fig. 12G-I). In contrast, the PP and SG presented less labelled cells (Table 1).

Retrograde labelling in the hypothalamus

Retrograde labelling in the hypothalamus following the MePD injections differed from the one observed after the tracer injections in the MeA and MePD mainly in the PMV, the MPO and the VMH (Table 2). Within the preoptic hypothalamus, the MPO showed moderate labelling (only scarce labelling was obtained after the injections in the MeA and MePV), with darkly stained cells mainly located next to the BSTMPM (Figure 12C, D, Table 2). Within the tuberal hypothalamus, the VMH presented scarce labelling (Figure 12E, F), compared to the moderate labelling showed after the MeA and MePV injections (Table 2). Within the mammillary hypothalamus, the PMV showed very dense labelling (Figs. 12H and 13D), compared with the few labelled cells found after the MeA injections. Finally, in the anterior hypothalamus, and the rest of structures of

the tuberal and mammillary hypothalamus, the observed labelling was very similar to that described after the injection in the MeA and MePV (Table 2).

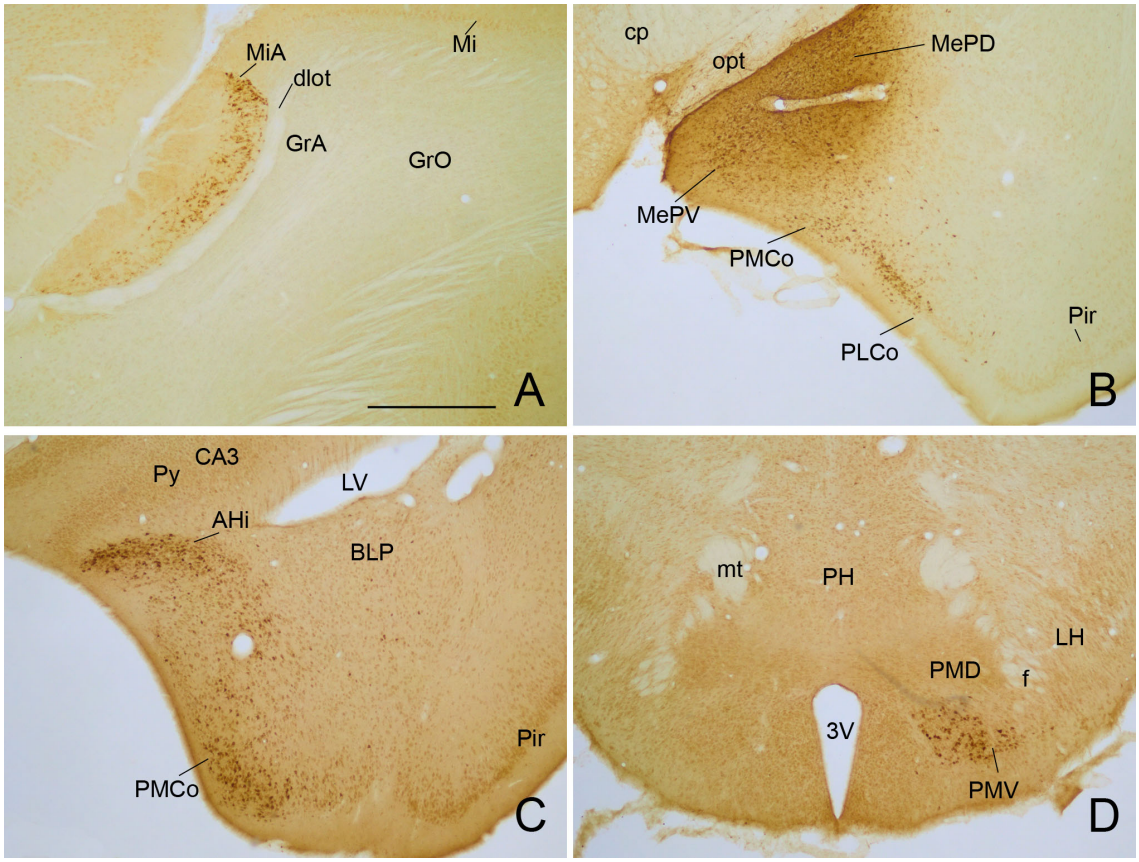

Fig. 13 Photomicrographs of parasagittal (A) and frontal (B-D) sections through the mouse forebrain, illustrating the retrograde labelling present in animals receiving a Fluorogold injection in the posterodorsal medial amygdaloid nucleus (MePD). The images correspond to the retrograde labelling presented in the cases M1257 **(A, B)** and M1302 **(C, D)**. **(A)** Retrogradely labelled mitral cells in the accessory olfactory bulb, mainly present in its anterior part. **(B)** Numerous labelled cells in the posteroventral medial amygdaloid subnucleus, as well as in the posterolateral cortical amygdaloid nucleus. Note that only scarce labelling is present at this level in the posteromedial cortical amygdaloid nucleus. **(C)** Dense retrograde labelling in the lateral aspect of the posteromedial cortical amygdaloid nucleus and in the medial part of the amygdalo-hippocampal area. **(D)** Retrogradely labelled cells in the ventral premammillary nucleus of the hypothalamus. For abbreviations, see list. Scale bar in A (valid for B–D): 500 µm

Retrograde labelling in the midbrain and brainstem

The retrograde labelling obtained was virtually identical to that observed following the injections in the MePV (Figure 12H-J, Table 2), with the PB being the only exception. It showed scarce labelling and the labelled cells located mainly in its medial and lateral divisions (Figure 12J).

Contralateral labelling

As described before in the MeA and MePV injections, the retrograde labelling found after FG injection in the MePD was mainly ipsilateral but a few labelled neurons were present in the contralateral hemisphere. Within the contralateral amygdala, the PMCo and MePV presented scarce labelling with darkly stained somata, and a few labelled cells were also present in the MeA, MePV and PLCo. In the BST, the BSTMPM and BSTMPI presented very scarce labelling. Within the septum and ventral forebrain, the MS, HBD and SL showed a very low number of labelled cells. Regarding to the thalamus, the SPF displayed scarce labelling, while the PVA, Re, SPFPC, PP and PIL presented only occasional labelling. Finally, within the hypothalamus, brainstem and midbrain the Arc, VMH, LH, TC, PMV, PH, PAG and PB showed a few scattered labelled cells.

3.2.3 Discussion

The results presented in this work describe for the first time, using restricted injections of retrograde tracers, the pattern of afferent projections to the main subdivisions of the Me in female mice. The results obtained confirm the general pattern of afferents to the Me (as a whole) inferred from a number of anterograde tracing studies in other rodents, mainly male rats and hamsters (see Pitkanen 2000). This indicates that, in spite of the interspecies and intersexual differences in sociosexual behaviours in which the Me is likely to be involved, the connectivity of the Me is common. In addition, the analysis of the centripetal connections to the three subnuclei the medial amygdala reveals that, although a small number of differences in the inputs to the anterior, posteroventral and posterodorsal subdivisions of the Me exists, a common pattern of inputs predominate. The MePD is the subnucleus that shows more

important differences in connectivity compared to the MeA and MePV, with these two subnuclei being more similar (see discussion below). The projections to all three medial amygdaloid subnuclei are mainly ipsilateral, although some of the afferent inputs are bilateral with ipsilateral predominance.

Projections to the medial amygdaloid nucleus from the olfactory system

Our results confirm and extend previous works that demonstrated that the Me receives convergent projections arising from the AOB and the MOB (Pro-Sistiaga et al. 2007; Kang et al. 2009; Cadiz-Moretti et al. 2013,). The AOB provides massive inputs to the three subnuclei of the Me. These projections are a direct source of pheromonal information to the Me (Zufall and Leinders-Zufall 2007). In addition, our results reveal that the MePD is dominated by inputs from the anterior AOB, whereas the remaining divisions of the Me show similar afferents from both AOB divisions. Similar results have been reported in rats (Mohedano-Moriano et al. 2007). In addition, the work of Mohedano-Moriano et al. (2007) also showed that the AOB efferent to the BSTMPM is originated by the rostral part of the AOB. The preferential projection from the anterior AOB to the MePD was not found in previous tracing studies in mice (retrograde: Salazar and Brannan, 2001; anterograde: von Campenhausen and Mori 2000). However, Salazar and Brennan (2000) injected retrograde tracers only in the MeA and MePV, and therefore could not observe the differential retrograde labelling in the AOB. In the case of the injections of anterograde tracers in the rostral and caudal AOB divisions, it is difficult to detect a difference in the density of the anterograde labelling. However, a careful examination of the terminal fields in the MePD shown in the figure 4 of von Campenhausen and Mori (2000) suggests that the injections in the rostral AOB gave rise to a denser anterograde labelling in the MePD layer I.

Therefore, the anterior part of the AOB projects more strongly to the MePD and the BSTMPM, two structures strongly interconnected (present results, Pardo-Bellver et al. 2012). The rostral part of the AOB receives inputs from vomeronasal sensory neurons expressing the V1 type of receptors (V1R), which are activated by small, volatile molecules with pheromonal activity (Leinders-Zufall et al. 2000; Fortes-Marco et al. 2013). In contrast, the posterior AOB receives inputs from vomeronasal sensory neurons expressing the V2 type of receptors, which are activated by nonvolatile proteinaceous compounds of high molecular weight (Krieger et al. 1999; Fortes-Marco

et al, 2013). Volatiles detected by V1R induce neuroendocrine effects (e.g. oestrous induction, puberty acceleration or delay; see Halpern and Martínez-Marcos 2003) and therefore the MePD and BSTMPM may be particularly involved in mediating the effects of these volatile pheromones.

Regarding to the MOB, our results of retrograde tracing confirm that it sends moderate projections to the MeA and very weak projections to the MePD (Kang et al. 2009; Cadiz-Moretti et al. 2013).

Among the structures receiving direct projections from both the AOB and MOB, the strongest degree of convergence is found in the MeA. Thus, on anatomical grounds, the MeA is the most important place of integration of vomeronasal and olfactory information within the amygdaloid complex (Petrulis 2013). In this regard, an unanswered question is the nature of the olfactory information relayed to the Me. An interesting possibility is that only mitral cells receiving information from sensory neurons with specialist receptors, such as those expressing TRPM5 (Thompson et al. 2012) innervate the Me. By this pathway, information about semiochemicals detected by the MOB may be integrated in the Me with the vomeronasal information relayed by the AOB. In agreement with this view, it has been shown that mitral cells of the MOB projecting to the Me are activated by male urinary volatiles in female mice, but not by female urinary volatiles or by predator odours (Kang et al. 2009). Moreover, olfactory sensory cells expressing a particular receptor, OR37C, innervate mitral cells that project specifically to the MePD (Bader et al. 2012). The sensory cells expressing receptors of the OR37 family respond to the presence of long-chain fatty aldehydes (Bautze et al. 2012), some of which are present in anal gland secretions (Bautze et al. 2014). These data reinforce the idea that the Me receives an olfactory input carrying information about specific semiochemicals.

Within the olfactory system, the olfactory cortex sends more projections to the MeA compared to the MePV, while it sends only very light projections to the MePD, in agreement with McDonald (1998). Regarding to the input from the Pir, the Me received stronger projections arising from the posterior Pir compared to the anterior Pir, corroborating previous descriptions (Christensen and Frederickson 1998).

Haberly (2001) suggested that the Pir functions more as an associative cortex than a primary sensory region. The posterior Pir presents more bidirectional connections with

the amygdala than the anterior Pir (Haberly 2001). In addition, electrophysiological data revealed that, while the anterior Pir process sensory information of the odorants, the posterior Pir shows associative encoding characteristics (Calu et al., 2006). Thus, the posterior Pir may act as an associative cortex that sends, mainly to the MeA and to a less extent to the MePV, highly processed olfactory information that includes the behavioural significance of the odorant.

Intramygdaloid projections to the medial amygdaloid nucleus.

In agreement with our previous anterograde study (Pardo-Bellver et al. 2012), the injections of retrograde tracers in the different Me subnuclei confirmed the existence of a dense and intricate set of intranuclear connections. Previous anatomical and functional data obtained in hamsters (Meredith and Westerry 2004; Maras and Petrulis 2010a,b,c) and mice (Choi et al. 2005; Samuelson and Meredith 2009a,b) have suggested that the MeA would act as a filter for the chemosensory information received from the bulbs. From the MeA, conspecific-related information would be sent through the MePD and predator-related information through the MePV. Our results show that the interconnections between the MePD and MePV allow the activity in each one of these subnuclei to influence the other. In addition, both the MePV and the MePD project back to the MeA (as shown previously in rats, Canteras et al. 1995), and therefore the information flow through the Me is, by no means, unidirectional.

The Me shows also an important set of intraamygdaloid inputs, originated mainly in other nuclei of the chemosensory amygdala (Gutiérrez-Castellanos et al. 2010). As shown by previous anterograde (rat: Canteras et al. 1995; mice: Gutiérrez-Castellanos et al. 2014), and retrograde (hamster: Coolen and Wood 1998) tracing studies, the PMCo gives rise to an important projection to all three Me subnuclei, allowing strong intraamygdaloid processing of vomeronasal information. The Me is composed to a large extent by neurons originated in subpallial territories (Bupesh et al. 2011), whereas the PMCo is a cortical structure (Gutiérrez-Castellanos et al. 2014). The projection from the PMCo to the Me can therefore be interpreted as a cortico-subcortical pathway within the vomeronasal system. This view is supported by retrograde tracing experiments with sodium selenide, revealing that the projection from the PMCo to the Me is originated by zinc-positive (putative glutamatergic) cells (Christensen and Frederickson 1998). Like in other circuits of the cerebral hemispheres, the cortical component, the PMCo, is

mainly involved in intratelencephalic pathways (Gutiérrez-Castellanos et al. 2014), while the subcortical element (the Me) gives rise to the major extratelencephalic outputs (Canteras et al. 1995; Pardo-Bellver et al. 2012). Our results also indicate that the projection from the PMCo to the MePD is apparently less dense than to the other Me subnuclei (thus confirming previous anterograde tracing data, Gutiérrez-Castellanos et al. 2014) and arises preferentially from a specific portion of this nucleus, suggesting the possibility of a topographical organization of this cortico-subcortical pathway within the vomeronasal system. This possibility, however, needs experimental confirmation.

The Me also receives projections from the rest of amygdaloid structures receiving a predominant input from the AOB, namely the BAOT and AA. In the latter case, however, it is noteworthy that the projection from the AA innervates mainly the anterior and posteroventral Me subnuclei. Although there is little information available on the connections and function of the AA (Martínez-García et al. 2012), this finding suggests that it is more related to the MeA and MePV than to the MePD, which in turn is the Me subnucleus more strongly involved in reproductive-related functions (Simerly 2002).

In contrast with the strong inputs to the Me originated in the vomeronasal amygdala, the olfactory amygdaloid nuclei are heterogeneous regarding their projections to the Me. The PLCo and CoA give rise to important projections to the Me, whereas the CxA, APir and LOT originate only a light projection to the Me. The inputs from the CxA, APir and LOT target mainly the MeA and MePV, as exemplified by the projection from the APir (see Table 2). Therefore, on anatomical grounds, the MePD is less influenced by the olfactory information processed in the amygdaloid nuclei. Similar results regarding the projections from the olfactory amygdala to the Me were observed in rats and hamsters (Coolen and Wood 1998; Pitkänen 2000; Majak and Pitkänen 2003).

The deep structures of the amygdala, namely the basolateral complex and the central nucleus, originate only minor projections to the Me, with the exception of the basomedial nucleus, which has an important interconnections with the MeA (present results; Petrovich et al. 1996; Pardo-Bellver et al. 2012). The MePV receives also a moderate projection from the basomedial nucleus, whereas the MePD shows only very minor afferents from the basolateral amygdaloid complex. In contrast, the MePD receives an important projection from the AHi, in agreement with previous anterograde data (Canteras et al. 1992a). This is consistent with the interpretation that the AHi is

strongly related to the vomeronasal system (see Swanson and Petrovich 1998; Martinez-García et al, 2012). Regarding the central amygdala, its medial subdivision originates a very light projection to the Me. This afferent reciprocates a much denser projection from the Me to the medial Ce (Pardo-Bellver et al. 2012). We hypothesize that this connection may play a role in the fear behaviour elicited by predator-derived chemicals. In fact, recent findings show that the Me is critically involved in the acquisition (and expression) of olfactory conditioned fear (Cousens et al. 2012). In addition, lesions of the basolateral complex (encompassing the lateral nucleus and neighbouring structures) also abolish olfactory fear conditioning (Cahill and McGaugh 1990; Cousens and Otto 1998). Since both the Me and the basolateral complex play a key role in olfactory fear conditioning, the direct interconnections between the Me and the basomedial nucleus (present results, Canteras et al. 1995, Petrovich et al. 1996; Pardo-Bellver et al. 2012) may provide the link allowing the information related to the odour-shock association to be integrated in both structures.

Afferent projections to the medial amygdaloid nucleus from the bed nucleus of the stria terminalis.

The BST is one the main targets of the efferent projections of the Me (Gomez and Newman 1992; Canteras et al. 1995; Coolen and Wood 1998; Dong et al. 2001; Pardo-Bellver et al. 2012). By contrast, the present experiments show that the projections from the BST back to the Me are not so important, with the exception of the posteromedial subdivisions of the BST. Only the BSTMPI and the BSTMPM (and the BSTIA) give rise to substantial projections to the Me subnuclei. These projections are topographically organized: the BSTMPI projects preferentially to the MeA and MePV, whereas the BSTMPM innervates preferentially the MePD. The reciprocal projection between the BSTMPM and the MePD reinforces the view that these nuclei are part of the network of sexually dimorphic nuclei (Guillamon and Segovia 1997; Gu et al. 2003) enriched in receptors for sexual steroids (Simerly et al. 1990; Mitra et al. 2003) that control socio-sexual behaviours (Newman 1999; Swann et al. 2009). The reciprocal projection between the BSTMPI and the MeA is consistent with the mixed projections of both structures to the defensive and reproductive behavioural control columns of the hypothalamus (Canteras et al. 1995; Pardo-Bellver et al. 2012; Swanson 2000). The MePV, as in other cases, is similar in this respect to the MeA. The compartment-specific interconnections between the Me and posteromedial subdivisions of the BST

suggest the existence of two subsystems within the medial extended amygdala. On the one hand, the MePD-BSTMPM is strongly dominated by a vomeronasal input (reaching both nuclei) mainly arising from V1R-expressing sensory neurons (see above: "Projections to the Me from the olfactory system"). This subsystem of the medial extended amygdala shows a clear sexual dimorphism attaining the size and cell number (Morris et al. 2008; Tsukahara et al. 2011). On the other hand, the MeA is interconnected mainly with the BSTMPI, where sexual dimorphism is less apparent, but affects at least a population of vasopressinergic cells (Rood et al. 2013; Otero-Garcia et al. 2014). This subsystem received mixed olfactory and vomeronasal inputs (reaching only the MeA). Finally, the MePV shows intermediate features, as it is interconnected with both BSTMPM and BSTMPI.

Afferent projections to the medial amygdaloid nucleus from cortical areas and the hippocampus

Within the entire cortex, the prefrontal cortex was almost the only cortical area that presented projections to the Me. The prefrontal cortex sends more inputs to the MeA than to the MePV and MePD, with the last two nuclei receiving very light inputs.

Among the different subdivisions of the prefrontal cortex, the AI was the region that presented more projections to the MeA, showing moderate retrograde labelling. The existence of this projection has been previously shown with anterograde tracing experiments in rats (McDonald et al. 1996, 1998; Shi and Cassell 1998). The projections from the AI to the MeA may be involved in the relay of multimodal sensory information (McDonald 1998; Shi and Cassell 1998). The projection to the Me is also originated by the posterior AI (not part of the prefrontal cortex), which probably relays somatosensory information that may play a role in the relay of footshock information (unconditioned stimulus) in fear conditioning paradigms (Shi and Davis 1999). An additional prefrontal projection to the Me arises from the IL (present results in mice; Hurley et al. 1991 and McDonald et al. 1996, 1998, in rats). The IL projection to the amygdala is involved in the extinction of fear conditioning (Sierra-Mercado et al. 2011), and therefore the projection of the IL to the Me may play a similar role in the case of olfactory fear conditioning, which depends on the Me (Cousens et al. 2012).

Regarding to the hippocampal formation, we found that CA1, ventral subiculum and LEnt send more projections to the MeA than to the MePV, with the MePD apparently

receiving the lightest projection. Previous works described a similar pattern of projections in the rat, using both retrograde (Christensen and Frederickson 1998) and anterograde tracer experiments (Canteras and Swanson 1992; McDonald 1998; Kishi et al. 2006; Cenquizca and Swanson 2007). These projections are reciprocal, since the Me also projects to the ventral CA1, subiculum and LEnt (Canteras et al., 1995; Pardo-Bellver et al. 2012). Although there are no functional data indicating a possible role of the ventral CA1 projections to the Me, it seems that the ventral hippocampus is specifically involved in defense/fear-related behaviour (Kjelstrup et al. 2002), probably in relation with the processing of the contextual stimuli (Maren and Fanselow 1995, Zhang et al 2001). This subregion of the ventral CA1 is also connected with the PMCo and projects to the AOB (de la Rosa-Prieto et al. 2009). We hypothesized that the anatomical interconnections described between the vomeronasal system and the ventral hippocampus allow pheromonal and spatial information to be integrated, and consequently modulate the behavioural response to chemicals signals as a function of the spatial context (e.g., own versus alien territory).

Afferent projections to the medial amygdaloid nucleus from the basal telencephalon

Within the septum and striatum, the medial septum, diagonal band/MCPO, SL and SI presented the most important inputs to the Me (showing a moderate to scarce projection).

Previous works have described that the MCPO (Nitecka 1981) and HDB (Ottersen 1980) send projections to the Me, although these works did not differentiated between the subdivisions of the Me. Our results confirm and extend these findings. Similar to the inputs described for the cortex, the MeA receives the strongest projection, the MePD the weakest, and the MePV is intermediate between those two.

The MS, diagonal band and MCPO are classified as the medial group of the septal region (Risold 2004). This region has important connections with the ventral (temporal) hippocampal field, entorhinal and prefrontal cortex (Risold 2004), areas that send, as described in the present work, projections to the Me (predominantly to the MeA). The MS may have a role in maintaining the arousal level required for sexual activity (Gulia et al., 2008), and consequently its input to the Me may influence the activity of this nucleus in this context.

Projections to the medial amygdaloid nucleus from the hypothalamus

Our results show that the Me receives relatively minor projections arising from hypothalamic nuclei, with four exceptions: the PMV, VMH, PH and MPO. The PMV sends massive projections to the MePV and MePD. The VMH and PH send moderate projections to the MeA and MePV, and finally the MPO sends moderate projections to the MePD.

Within the entire hypothalamus, only the PMV projects massively to the Me. This nucleus shows strong projections to the MePD and MePV, while it presents only light projections to the MeA. The important projection arising from the PMV to the MePD is consistent with previous works in male rats (Ottersen 1980; Canteras et al. 1992b). Canteras et al. (1992b) described also a moderate projection to the rostral part of the MeA, which we observed as scarce in our preparations, probably as a result of the small size of our injections. In contrast to our results, Canteras et al. (1992b) found no projection from the PMV to the MePV in male rats. Possible explanations of this discrepancy may be either interspecific differences or sexual dimorphism, since we used female mice our experiments. Further studies are needed to clarify these inconsistencies.

The PMV displays strong bidirectional connections with the MePD and MePV (present findings, Canteras et al. 1995; Pardo-Bellver et al. 2012), and with sexually dimorphic areas related to reproductive and aggressive behaviours, as well as to neuroendocrine zones of the hypothalamus (Canteras et al. 1992b). It is part of a hypothalamic circuit involved in the control of reproductive behaviour (Swanson 2000), and in fact it is strongly influenced by gonadal steroid hormones (Canteras et al. 1992b). The PMV shows high levels of c-fos expression in male mice exposed to female soiled bedding (Yokosuka et al. 1999), but also in female rats during maternal aggression experiments (Motta et al. 2013). Furthermore, in male hamsters it is activated by both mating and agonistic interactions (Kollack-Walker and Newman 1995). Therefore, as suggested by Yokosuka et al (1999), this nucleus may play an important role in the control of the motivation of copulatory and/or aggressive behaviour. Thus, the PMV, by means of its massive feedback input to the MePV and MePD may be modulating the chemosensory processing in these subdivisions of the Me, probably in relation with the behavioural response (reproductive or aggressive) that the animal is executing.

Regarding the afferents from the preoptic hypothalamus, consistent with our results a projection from the MPO to the Me was described previously in rats (Ottersen 1980). We extend this finding showing that the MPO projects mainly to the MePD, and to a lesser extent also to the MeA and MePV. Since the MPO is part of the reproductive-related hypothalamic circuit (Swanson 2000), this finding further supports the hypothesis that the MePD is more related with sexual behaviour.

The VMH and PH send moderate projections to the MeA and MePV and scarce projections to the MePD. Previous works have reported that the VMH projects more densely to the rostral part of the MeA compared to the other Me subnuclei, and described that these projections to the Me originate mainly from the central and the dorsomedial parts of the VMH (Ottersen 1980; Canteras et al. 1994). Our results in female mice partially contrast with these data in male rats, since we found that the MeA and MePV receive more projections from the VMH than the MePD, and found no differences in the origin of these projections according to the VMH subdivisions. The ventrolateral division of the VMH has been proposed to be part of the reproductive behavioural control column of the hypothalamus, whereas its dorsomedial division would be part of the defensive circuit (Swanson 2000; Choi et al. 2005). However, recent electrophysiological data and optogenetic activation experiments have revealed that within the ventrolateral VMH there are neuronal populations involved in mating and conspecific aggression (Lin et al. 2011; Falkner et al. 2014). Therefore, without further characterization of the properties of the retrogradely labelled cells in the VMH, it is not possible to known whether the feedback projection they provide to the Me is related to sexual or aggressive behaviours.

Previous works have reported projections arising from the PH to the medial amygdala (Nitecka 1981; Vertes et al. 1995), which in turn projects (although lightly) to the PH (Pardo-Bellver et al. 2012). The PH projects to a number of subcortical and cortical "limbic-related" structures, and it has been suggested to be involved in various components of emotional behaviour, including emotional learning (Vertes et al. 1995). In this regard, it integrates cardiorespiratory and motor responses and controls the theta rhythm of the hippocampus (Vertes et al. 1995).

Finally, with regard to the minor hypothalamic afferents to the Me, previous works in the rat have reported, consistent with our results, light projections arising from the AH

(Risold et al. 1994), DM (Thompson et al. 1996), Arc (Ottersen 1980; Krieger et al. 1979) and LH (Nitecka 1981; Ottersen 1980; Veening 1978) to the Me. A minor discrepancy with the present results is the presence of a moderate projection from the TC to the Me (Nitecka 1981; Canteras et al. 1994), which we observed to be scarce.

Projections from the thalamus and brainstem to the medial nucleus of the amygdala

The thalamic afferents to the Me arise mainly from the midline and posterior intralaminar nuclei. These afferents are common to the three Me subnuclei, although the projection to the MePD tends to be somewhat lighter than that of the MeA and MePV (Table 2). The midline thalamic nuclei that project to the Me are the paraventricular and reuniens, both of which also receive projections from the Me (Canteras et al. 1995; Pardo-Bellver et al. 2012). The afferent projection from the paraventricular thalamic nucleus to the Me has been previously described in rats (Li and Kirouac 2008; Vertes and Hoover 2008). This thalamic nucleus is related to arousal and attention processes, and therefore its input to the Me may modulate the attention towards the chemical signals processed in the Me.

The afferent projections from the posterior intralaminar thalamic complex (encompassing the SG, MGM, PIN, SPF, PIL and PP) to the Me are very similar to those described from the same structures to the central and lateral nuclei of the amygdala (Turner and Henkerham 1991). These projections have been shown to relay auditory (LeDoux et al. 1990a), somatosensory (LeDoux et al. 1987; Bordi and LeDoux 1994; Lanuza et al. 2008) and visual (Doron and LeDoux 1999; Linke et al. 1999) information, and play a key role in the acquisition of fear conditioning (LeDoux et al. 1990b). It is not known whether the same neurons of the posterior intralaminar thalamic complex project to both the Me and the central and lateral amygdaloid nuclei. In any case, it is likely that this thalamic projection sends (at least) somatosensory information to the Me, given that it is necessary in the acquisition of olfactory fear conditioning (Cousens et al. 2012) and shows increased expression of c-Fos following the delivery of footshock (Pezzone et al. 1992; Rosen et al., 1998).

A very different kind of somatosensory information that has been shown to activate the medial amygdala is that derived from vaginocervical stimulation (Erskine 1993; Pfaus et al. 1993, 1996; Polston and Erskine 1995, Tetel et al, 1993). The somatosensory genital information may reach the Me through the thalamic SPF (Veening and Coolen

1998). The convergence of genital somatosensory information with chemosensory information (about odorants and pheromones) would take place in the Me, thus allowing the association of chemical cues with the reinforcing mating experience. This kind of olfactory-genitosensory learning in the Me may be the reason that explains why sexually experienced animals with lesions of the vomeronasal organ show very small deficits in sexual behaviour (Meredith 1986).

Finally, within the brainstem the main afferent projection to the Me is originated by the parabrachial nucleus. This nucleus may relay viscероceptive (from its medial aspect) and nociceptive information (from its lateral aspect) (Fulwiler and Saper 1984; Bourgeais et al. 2001; Lanuza et al. 2004). We found retrogradely labelled neurons both in the medial and lateral parabrachial nucleus, mainly following tracer injections in the MeA. This afferents may relay sensory information relevant to associate chemical stimuli with aversive learning (such as olfactory fear conditioning).

The medial amygdala connections and its role in defensive and sociosexual behaviours

The results of the present study show that the three subdivisions of the Me receive a similar pattern of afferent projections, with some quantitative differences in the density of the neural inputs from particular structures. Previous works studying the efferent projections of the Me have emphasized these differences, and moreover functional data relate the MePD with reproductive-related behaviours and the MePV with defensive behaviours. However, both for the afferents (present results) and for the efferents (Canteras et al. 1995; Pardo-Bellver et al. 2012), minor connections are observed between the MePD and hypothalamic nuclei related with defensive behaviour, such as the anterior hypothalamic area and the dorsomedial VMH. In the same vein, moderate connections are present between the MePV and the hypothalamic reproductive-related nuclei, such as the MPO, the ventrolateral part of the VMH and the PMV. Therefore, on anatomical grounds, the segregation between these two systems is not clear. Instead, the differences between the connectivity of the MePD and MePV are only a matter of relative density, with basically the same pattern of connections shared by both subnuclei. Regarding the anterior part of the Me, it is very similar to the MePV, i.e., it shows relevant connections with hypothalamic nuclei related to reproductive and defensive behaviours.

In agreement with the anatomical data showing that the MeA and MePV are interconnected with circuits related with both sexual and defensive behaviours, male mice exposed to female urine show an increase c-Fos expression in all subdivisions of the Me (Samuelsen and Meredith 2009a,b), and the same result was obtained in female mice exposed to male-soiled bedding (Halem et al. 1999; Moncho-Bogani et al. 2005). In addition, odours from heterospecifics (including predators and non-predators) were observed to induce c-Fos expression in the MeA (Meredith and Westberry 2004; Samuelsen and Meredith 2009a,b). A specific c-fos induction in the MePV was found in rats (Dielenberg et al. 2001) and mice (Choi et al. 2005) exposed to cat odours, although, as detailed above, the MePV also respond to conspecifics of the same and opposite sex (Meredith and Westberry 2005; Samuelsen and Meredith 2009a,b). A recent multisite extracellular recording study in mice in the MePD and MePV found that, although neurons responding to conspecific stimuli were more often located dorsally in the posterior Me, and neurons responding to predator urinary stimuli were more often located ventrally, there were also individual cells distributed throughout the posterior Me responding to conspecific and defensive stimuli (Bergan et al. 2014). In summary, the chemical cues described to activate the MeA and MePV (in addition to sexually related odours and odours from same sex conspecifics), include odours from ill conspecifics (Arakawa et al. 2010), and from predators (Takahashi, 2014). Consistent with these functional data, the MeA and MePV have been suggested to play a general role in the categorization of the chemical cues detected (mainly) by the vomeronasal organ and acting as a filter to convey appropriate chemosensory information to the MePD or other downstream targets (Meredith and Westberry 2004; Samuelsen and Meredith 2009a,b; Maras and Petrulis 2010a,b,c). In contrast, the MePD, according to both anatomical and functional data, has been proposed to be specifically involved in the control of sexual behaviour (Swann et al. 2009). However, in rats the MePD is also activated following aggressive encounters between males (Veening et al. 2005), and thus it may play a role also in agonistic interactions. Finally, we want to note that the Me (as a whole) is involved in olfactory fear conditioning, as well as in learning to fear the context where the predator odours were presented (Takahashi et al. 2007).

In summary, the Me is involved in the unconditioned responses elicited by social and sexual cues, as well as predator-derived chemicals, and also in learning to associate olfactory cues with aversive (and maybe appetitive) experiences.

3.2.4 Reference

Arakawa H, Arakawa K, Deak T (2010) Oxytocin and vasopressin in the medial amygdala differentially modulate approach and avoidance behaviour toward illness-related social odour. Neuroscience 171:1141-1151.

Bader A, Breer H, Strotmann J (2012) Untypical connectivity from olfactory sensory neurons expressing OR37 into higher brain centres visualized by genetic tracing. Histochem Cell Biol 137:615-628.

Bautze V, Schwack W, Breer H, Strotmann J (2014) Identification of a natural source for the OR37B ligand. Chem Senses 39:27-38.

Bautze V, Bar R, Fissler B, Trapp M, Schmidt D, Beifuss U, Bufe B, Zufall F, Breer H, Strotmann J (2012) Mammalian-specific OR37 receptors are differentially activated by distinct odorous fatty aldehydes. Chem Senses 37:479-493.

Bergan JF, Ben-Shaul Y, Dulac C (2014) Sex-specific processing of social cues in the medial amygdala. Elife 3:e02743. doi: 10.7554/eLife.02743.

Bordi F, LeDoux JE (1994) Response properties of single units in areas of rat auditory thalamus that project to the amygdala. II. Cells receiving convergent auditory and somatosensory inputs and cells antidromically activated by amygdala stimulation. Exp Brain Res 98:275-286.

Bourgeais L, Gauriau C, Bernard JF (2001) Projections from the nociceptive area of the central nucleus of the amygdala to the forebrain: a PHA-L study in the rat. Eur J Neurosci 14:229-255.

Bupesh M, Legaz I, Abellan A, Medina L (2011) Multiple telencephalic and extratelencephalic embryonic domains contribute neurons to the medial extended amygdala. J Comp Neurol 519:1505-1525.

Cadiz-Moretti B, Martinez-Garcia F., Lanuza E (2013) Neural substrate to associate odorants and pheromones: convergence of projections from the main and accessory olfactory bulbs in mice. In: East ML, Dehnhard M (eds) Chemical Signals in Vertebrates 12. Springer Science, New York, pp 3-16.

Cahill L, McGaugh JL (1990) Amygdaloid complex lesions differentially affect retention of tasks using appetitive and aversive reinforcement. Behav Neurosci 104:532-543.

Calu DJ, Roesch MR, Stalnaker TA, Schoenbaum G (2007) Associative encoding in posterior piriform cortex during odor discrimination and reversal learning. Cereb Cortex 17:1342-1349.

Canteras NS, Swanson LW (1992) Projections of the ventral subiculum to the amygdala, septum, and hypothalamus: a PHAL anterograde tract-tracing study in the rat. J Comp Neurol 324:180-194.

Canteras NS, Simerly RB, Swanson LW (1992a) Connections of the posterior nucleus of the amygdala. J Comp Neurol 324:143-179.

Canteras NS, Simerly RB, Swanson LW (1992b) Projections of the ventral premammillary nucleus. J Comp Neurol 324:195-212.

Canteras NS, Simerly RB, Swanson LW (1994) Organization of projections from the ventromedial nucleus of the hypothalamus: a *Phaseolus vulgaris*-leucoagglutinin study in the rat. J Comp Neurol 348:41-79.

Canteras NS, Simerly RB, Swanson LW (1995) Organization of projections from the medial nucleus of the amygdala: a PHAL study in the rat. J Comp Neurol 360:213-245.

Cenquizca LA, Swanson LW (2007) Spatial organization of direct hippocampal field CA1 axonal projections to the rest of the cerebral cortex. Brain Res Rev 56:1-26.

Chamero P, Marton TF, Logan DW, Flanagan K, Cruz JR, Saghatelian A, Cravatt BF, Stowers L (2007) Identification of protein pheromones that promote aggressive behaviour. Nature 450:899-902.

Choi GB, Dong HW, Murphy AJ, Valenzuela DM, Yancopoulos GD, Swanson LW, Anderson DJ (2005) Lhx6 delineates a pathway mediating innate reproductive behaviors from the amygdala to the hypothalamus. Neuron 46:647-660.

Christensen MK, Frederickson CJ (1998) Zinc-containing afferent projections to the rat corticomedial amygdaloid complex: a retrograde tracing study. J Comp Neurol 400:375-390.

Coolen LM, Wood RI (1998) Bidirectional connections of the medial amygdaloid nucleus in the Syrian hamster brain: simultaneous anterograde and retrograde tract tracing. J Comp Neurol 399:189-209.

Cousens G, Otto T (1998) Both pre- and posttraining excitotoxic lesions of the basolateral amygdala abolish the expression of olfactory and contextual fear conditioning. Behav Neurosci 112:1092-1103.

Cousens GA, Kearns A, Laterza F, Tundidor J (2012) Excitotoxic lesions of the medial amygdala attenuate olfactory fear-potentiated startle and conditioned freezing behavior. Behav Brain Res 229:427-432.

de la Rosa-Prieto C, Ubeda-Banon I, Mohedano-Moriano A, Pro-Sistiaga P, Saiz-Sanchez D, Insausti R, Martinez-Marcos A (2009) Subicular and CA1 hippocampal projections to the accessory olfactory bulb. Hippocampus 19:124-129.

Dielenberg RA, Hunt GE, McGregor IS (2001) "When a rat smells a cat": the distribution of Fos immunoreactivity in rat brain following exposure to a predatory odor. Neuroscience 104:1085-1097.

Dong HW, Petrovich GD, Swanson LW (2001) Topography of projections from amygdala to bed nuclei of the stria terminalis. Brain Res Rev 38:192-246.

Doron NN, LeDoux JE (1999) Organization of projections to the lateral amygdala from auditory and visual areas of the thalamus in the rat. J Comp Neurol 412:383-409.

Erskine MS (1993) Mating-induced increases in FOS protein in preoptic area and medial amygdala of cycling female rats. Brain Res Bull 32:447-451.

Falkner AL, Dollar P, Perona P, Anderson DJ, Lin D (2014) Decoding ventromedial hypothalamic neural activity during male mouse aggression. J Neurosci 34:5971-5984.

Fortes-Marco L, Lanuza E, Martinez-Garcia F (2013) Of pheromones and kairomones: what receptors mediate innate emotional responses? Anat Rec (Hoboken) 296:1346-1363.

Fulwiler CE, Saper CB (1984) Subnuclear organization of the efferent connections of the parabrachial nucleus in the rat. Brain Res 319:229-259.

Gomez DM, Newman SW (1992) Differential projections of the anterior and posterior regions of the medial amygdaloid nucleus in the Syrian hamster. J Comp Neurol 317:195-218.

Goodson JL (2005) The vertebrate social behavior network: evolutionary themes and variations. Horm Behav 48:11-22.

Gu G, Cornea A, Simerly RB (2003) Sexual differentiation of projections from the principal nucleus of the bed nuclei of the stria terminalis. J Comp Neurol 460:542-562.

Guillamon A, Segovia S (1997) Sex differences in the vomeronasal system. Brain Res Bull 44:377-382.

Gulia KK, Jodo E, Kawauchi A, Miki T, Kayama Y, Mallick HN, Koyama Y (2008) The septal area, site for the central regulation of penile erection during waking and rapid eye movement sleep in rats: a stimulation study. Neuroscience 156:1064-1073.

Gutiérrez-Castellanos N, Martínez-Marcos A, Martínez-García F, Lanuza E (2010) Chemosensory function of the amygdala. Vitam Horm 83:165-196.

Gutiérrez-Castellanos N, Pardo-Bellver C, Martínez-García F, Lanuza E (2014) The vomeronasal cortex - afferent and efferent projections of the posteromedial cortical nucleus of the amygdala in mice. Eur J Neurosci 39:141-158.

Haberly LB (2001) Parallel-distributed processing in olfactory cortex: new insights from morphological and physiological analysis of neuronal circuitry. Chem Senses 26:551-576.

Halem HA, Cherry JA, Baum MJ (1999) Vomeronasal neuroepithelium and forebrain Fos responses to male pheromones in male and female mice. J Neurobiol 39:249-263.

Halpern M, Martinez-Marcos A (2003) Structure and function of the vomeronasal system: an update. Prog Neurobiol 70:245-318.

Hurley KM, Herbert H, Moga MM, Saper CB (1991) Efferent projections of the infralimbic cortex of the rat. J Comp Neurol 308:249-276.

Isogai Y, Si S, Pont-Lezica L, Tan T, Kapoor V, Murthy VN, Dulac C (2011) Molecular organization of vomeronasal chemoreception. Nature 478:241-245.

Kang N, Baum MJ, Cherry JA (2009) A direct main olfactory bulb projection to the 'vomeronasal' amygdala in female mice selectively responds to volatile pheromones from males. Eur J Neurosci 29:624-634.

Kang N, Baum MJ, Cherry JA (2011) Different profiles of main and accessory olfactory bulb mitral/tufted cell projections revealed in mice using an anterograde tracer and a whole-mount, flattened cortex preparation. Chem Senses 36:251-260.

Kishi T, Tsumori T, Yokota S, Yasui Y (2006) Topographical projection from the hippocampal formation to the amygdala: a combined anterograde and retrograde tracing study in the rat. J Comp Neurol 496:349-368.

Kjelstrup KG, Tuvnes FA, Steffenach HA, Murison R, Moser EI, Moser MB (2002) Reduced fear expression after lesions of the ventral hippocampus. Proc Natl Acad Sci U S A 99:10825-10830.

Kollack-Walker S, Newman SW (1995) Mating and agonistic behavior produce different patterns of fos immunolabeling in the male Syrian hamster brain. Neurosci 66:721-736.

Krieger J, Schmitt A, Lobel D, Gudermann T, Schultz G, Breer H, Boekhoff I (1999) Selective activation of G protein subtypes in the vomeronasal organ upon stimulation with urine-derived compounds. J Biol Chem 274:4655-4662.

Krieger MS, Conrad LC, Pfaff DW (1979) An autoradiographic study of the efferent connections of the ventromedial nucleus of the hypothalamus. J Comp Neurol 183:785-815.

Lanuza E, Nader K, LeDoux JE (2004) Unconditioned stimulus pathways to the amygdala: effects of posterior thalamic and cortical lesions on fear conditioning. Neuroscience 125:305-315.

Lanuza E, Moncho-Bogani J, LeDoux JE (2008) Unconditioned stimulus pathways to the amygdala: effects of lesions of the posterior intralaminar thalamus on foot-shock-induced c-Fos expression in the subdivisions of the lateral amygdala. Neuroscience 155:959-968.

LeDoux JE, Farb C, Ruggiero DA (1990a) Topographic organization of neurons in the acoustic thalamus that project to the amygdala. J Neurosci 10:1043-1054.

LeDoux JE, Cicchetti P, Xagoraris A, Romanski LM (1990b) The lateral amygdaloid nucleus: sensory interface of the amygdala in fear conditioning. J Neurosci 10:1062-1069.

LeDoux JE, Ruggiero DA, Forest R, Stornetta R, Reis DJ (1987) Topographic organization of convergent projections to the thalamus from the inferior colliculus and spinal cord in the rat. J Comp Neurol 264:123-146.

Lehman MN, Winans SS, Powers JB (1980) Medial nucleus of the amygdala mediates chemosensory control of male hamster sexual behavior. Science 210:557-560.

Leinders-Zufall T, Lane AP, Puche AC, Ma W, Novotny MV, Shipley MT, Zufall F (2000) Ultrasensitive pheromone detection by mammalian vomeronasal neurons. Nature 405:792-796.

Li S, Kirouac GJ (2008) Projections from the paraventricular nucleus of the thalamus to the forebrain, with special emphasis on the extended amygdala. J Comp Neurol 506:263-287.

Lin D, Boyle MP, Dollar P, Lee H, Lein ES, Perona P, Anderson DJ (2011) Functional identification of an aggression locus in the mouse hypothalamus. Nature 470:221-226.

Linke R, De Lima AD, Schwegler H, Pape HC (1999) Direct synaptic connections of axons from superior colliculus with identified thalamo-amygdaloid projection neurons in the rat: possible substrates of a subcortical visual pathway to the amygdala. J Comp Neurol 403:158-170.

Majak K, Pitkanen A (2003) Projections from the periamygdaloid cortex to the amygdaloid complex, the hippocampal formation, and the parahippocampal region: a PHA-L study in the rat. Hippocampus 13:922-942.

Maras PM, Petrulis A (2010a) Anatomical connections between the anterior and posterodorsal sub-regions of the medial amygdala: integration of odor and hormone signals. Neuroscience 170:610-622.

Maras PM, Petrulis A (2010b) The anterior medial amygdala transmits sexual odor information to the posterior medial amygdala and related forebrain nuclei. Eur J Neurosci 32:469-482.

Maras PM, Petrulis A (2010c) Lesions that functionally disconnect the anterior and posterodorsal sub-regions of the medial amygdala eliminate opposite-sex odor preference in male Syrian hamsters (*Mesocricetus auratus*). Neuroscience 165:1052-1062.

Maren S, Fanselow MS (1995) Synaptic plasticity in the basolateral amygdala induced by hippocampal formation stimulation in vivo. J Neurosci 15:7548-7564.

Martínez-García F, Novejarque A, Gutiérrez-Castellanos N, Lanuza E (2012) Piriform cortex and amígdala. In: Watson C, Paxinos G, Puelles L (eds) The Mouse Nervous System. Academic Press, San Diego, pp 140-172.

McDonald AJ (1998) Cortical pathways to the mammalian amygdala. Prog Neurobiol 55:257-332.

McDonald AJ, Mascagni F, Guo L (1996) Projections of the medial and lateral prefrontal cortices to the amygdala: a *Phaseolus vulgaris* leucoagglutinin study in the rat. Neuroscience 71:55-75.

Meredith M (1986) Vomeronasal organ removal before sexual experience impairs male hamster mating behavior. Physiol Behav 36:737-743.

Meredith M, Westberry JM (2004) Distinctive responses in the medial amygdala to same-species and different-species pheromones. J Neurosci 24:5719-5725.

Mitra SW, Hoskin E, Yudkovitz J, Pear L, Wilkinson HA, Hayashi S, Pfaff DW, Ogawa S, Rohrer SP, Schaeffer JM, McEwen BS, Alves SE (2003) Immunolocalization of estrogen receptor beta in the mouse brain: comparison with estrogen receptor alpha. Endocrinology 144:2055-2067.

Mohedano-Moriano A, Pro-Sistiaga P, Ubeda-Banon I, Crespo C, Insausti R, Martinez-Marcos A (2007) Segregated pathways to the vomeronasal amygdala: differential projections from the anterior and posterior divisions of the accessory olfactory bulb. Eur J Neurosci 25:2065-2080.

Moncho-Bogani J, Martinez-Garcia F, Novejarque A, Lanuza E (2005) Attraction to sexual pheromones and associated odorants in female mice involves activation of the reward system and basolateral amygdala. Eur J Neurosci 21:2186-2198.

Morris JA, Jordan CL, King ZA, Northcutt KV, Breedlove SM (2008) Sexual dimorphism and steroid responsiveness of the posterodorsal medial amygdala in adult mice. Brain Res 1190:115-121.

Motta SC, Guimaraes CC, Furigo IC, Sukikara MH, Baldo MV, Lonstein JS, Canteras NS (2013) Ventral premammillary nucleus as a critical sensory relay to the maternal aggression network. Proc Natl Acad Sci U S A 110:14438-14443.

Newman SW (1999) The medial extended amygdala in male reproductive behavior. A node in the mammalian social behavior network. Ann N Y Acad Sci 877:242-257.

Nitecka L (1981) Connections of the hypothalamus and preoptic area with nuclei of the amygdaloid body in the rat; HRP retrograde transport study. Acta Neurobiol Exp 41:53-67.

Nodari F, Hsu FF, Fu X, Holekamp TF, Kao LF, Turk J, Holy TE (2008) Sulfated steroids as natural ligands of mouse pheromone-sensing neurons. J Neurosci 28:6407-6418.

Otero-Garcia M, Martin-Sanchez A, Fortes-Marco L, Martínez-Ricós J, Agustin-Pavón C, Lanuza E, Martínez-García F (2014) Extending the socio-sexual brain: arginine-vasopressin immunoreactive circuits in the telencephalon of mice. Brain Struct Funct 219:1055-1081.

Ottersen OP (1980) Afferent connections of the amygdaloid complex of the rat and cat. II. Afferents from the hypothalamus and the basal telencephalon. J Comp Neurol 194:267-289.

Ottersen OP, Ben-Ari Y (1979) Afferent connections of the amygdaloid complex of the rat and cat. I. Projections from the thalamus. J Comp Neurol 187:401-424.

Papes F, Logan DW, Stowers L (2010) The vomeronasal organ mediates interspecies defensive behaviors through detection of protein pheromone homologs. Cell 141:692-703.

Pardo-Bellver C, Cadiz-Moretti B, Novejarque A, Martinez-Garcia F, Lanuza E (2012) Differential efferent projections of the anterior, posteroventral, and posterodorsal subdivisions of the medial amygdala in mice. Front Neuroanat 6:33.

Paxinos G, Franklin KBJ (2001) The mouse brain in stereotaxic coordinates. Academic Press, San Diego.

Petrovich GD, Risold PY, Swanson LW (1996) Organization of projections from the basomedial nucleus of the amygdala: A PHAL study in the rat. J Comp Neurol 374:387-420.

Petrulis A (2013) Chemosignals, hormones and mammalian reproduction. Horm Behav 63:723-741.

Pezzone MA, Lee W-, Hoffman GE, Rabin BS (1992) Induction of c-Fos immunoreactivity in the rat forebrain by conditioned and unconditioned aversive stimuli. Brain Res 597:41-50.

Pfaus JG, Marcangione C, Smith WJ, Manitt C, Abillamaa H (1996) Differential induction of Fos in the female rat brain following different amounts of vaginocervical stimulation: modulation by steroid hormones. Brain Res 741:314-330.

Pfaus JG, Kleopoulos SP, Mobbs CV, Gibbs RB, Pfaff DW (1993) Sexual stimulation activates c-fos within estrogen-concentrating regions of the female rat forebrain. Brain Res 624:253-267.

Pitkanen A (2000) Connectivity of the rat amygdaloid complex. In: Aggleton J (ed) The Amygdala. A functional analysis, 2nd edn. Oxford University Press, Oxford, pp 31-115.

Polston EK, Erskine MS (1995) Patterns of induction of the immediate-early genes c-fos and egr-1 in the female rat brain following differential amounts of mating stimulation. Neuroendocrinology 62:370-384.

Pro-Sistiaga P, Mohedano-Moriano A, Ubeda-Banon I, Del Mar Arroyo-Jimenez M, Marcos P, Artacho-Perula E, Crespo C, Insausti R, Martinez-Marcos A (2007) Convergence of olfactory and vomeronasal projections in the rat basal telencephalon. J Comp Neurol 504:346-362.

Risold PY (2004) The septal region. In: Paxinos G (ed) The Rat Nervous System (3rd edn). Academic Press, San Diego, pp 605-632.

Risold PY, Canteras NS, Swanson LW (1994) Organization of projections from the anterior hypothalamic nucleus: a *Phaseolus vulgaris*-leucoagglutinin study in the rat. J Comp Neurol 348:1-40.

Riviere S, Challet L, Fluegge D, Spehr M, Rodriguez I (2009) Formyl peptide receptor-like proteins are a novel family of vomeronasal chemosensors. Nature 459:574-577.

Rood BD, Stott RT, You S, Smith CJ, Woodbury ME, De Vries GJ (2013) Site of origin of and sex differences in the vasopressin innervation of the mouse (*Mus musculus*) brain. J Comp Neurol 521:2321-2358.

Rosen JB, Fanselow MS, Young SL, Sitcoske M, Maren S (1998) Immediate-early gene expression in the amygdala following footshock stress and contextual fear conditioning. Brain Res 796:132-142.

Samuelsen CL, Meredith M (2009a) Categorization of biologically relevant chemical signals in the medial amygdala. Brain Res 1263:33-42.

Samuelsen CL, Meredith M (2009b) The vomeronasal organ is required for the male mouse medial amygdala response to chemical-communication signals, as assessed by immediate early gene expression. Neuroscience 164:1468-1476.

Scalia F, Winans SS (1975) The differential projections of the olfactory bulb and accessory olfactory bulb in mammals. J Comp Neurol 161:31-55.

Shi C, Davis M (1999) Pain pathways involved in fear conditioning measured with fear-potentiated startle: lesion studies. J Neurosci 19:420-430.

Shi CJ, Cassell MD (1998) Cortical, thalamic, and amygdaloid connections of the anterior and posterior insular cortices. J Comp Neurol 399:440-468.

Sierra-Mercado D, Padilla-Coreano N, Quirk GJ (2011) Dissociable roles of prelimbic and infralimbic cortices, ventral hippocampus, and basolateral amygdala in the expression and extinction of conditioned fear. Neuropsychopharmacology 36:529-538.

Simerly RB, Chang C, Muramatsu M, Swanson LW (1990) Distribution of androgen and estrogen receptor mRNA-containing cells in the rat brain: an in situ hybridization study. J Comp Neurol 294:76-95.

Swann J, Fabre-Nys C, Barton R (2009) Hormonal and pheromonal modulation of the extended amygdala: Implications for social behavior. In: Pfaff DW, Arnold AP, Fahrbach SE, Etgen AM, Rubin RT (eds) Hormones, Brain and Behavior, 2nd edn. Academic Press, San Diego, pp 441-474.

Swanson LW (2000) Cerebral hemisphere regulation of motivated behavior. Brain Res 886:113-164.

Swanson LW, Petrovich GD (1998) What is the amygdala? Trends Neurosci 21:323-331.

Takahashi LK (2014) Olfactory systems and neural circuits that modulate predator odor fear. Front Behav Neurosci 8:72.

Takahashi LK, Hubbard DT, Lee I, Dar Y, Sipes SM (2007) Predator odor-induced conditioned fear involves the basolateral and medial amygdala. Behav Neurosci 121:100-110.

Tetel MJ, Getzinger MJ, Blaustein JD (1993) Fos expression in the rat brain following vaginal-cervical stimulation by mating and manual probing. J Neuroendocrinol 5:397-404.

Thompson JA, Salcedo E, Restrepo D, Finger TE (2012) Second-order input to the medial amygdala from olfactory sensory neurons expressing the transduction channel TRPM5. J Comp Neurol 520:1819-1830.

Thompson RH, Canteras NS, Swanson LW (1996) Organization of projections from the dorsomedial nucleus of the hypothalamus: a PHA-L study in the rat. J Comp Neurol 376:143-173.

Tirindelli R, Dibattista M, Pifferi S, Menini A (2009) From pheromones to behavior. Physiol Rev 89:921-956.

Tsukahara S, Tsuda MC, Kurihara R, Kato Y, Kuroda Y, Nakata M, Xiao K, Nagata K, Toda K, Ogawa S (2011) Effects of aromatase or estrogen receptor gene deletion on

masculinization of the principal nucleus of the bed nucleus of the stria terminalis of mice. Neuroendocrinology 94(2):137-147.

Turner BH, Herkenham M (1991) Thalamoamygdaloid projections in the rat: a test of the amygdala's role in sensory processing. J Comp Neurol 313:295-325.

Usunoff KG, Schmitt O, Itzev DE, Haas SJ, Lazarov NE, Rolfs A, Wree A (2009) Efferent projections of the anterior and posterodorsal regions of the medial nucleus of the amygdala in the mouse. Cells Tissues Organs 190:256-285.

Veening JG (1978) Subcortical afferents of the amygdaloid complex in the rat: an HRP study. Neurosci Lett 8:197-202.

Veening JG, Coolen LM (1998) Neural activation following sexual behavior in the male and female rat brain. Behav Brain Res 92:181-193.

Vertes RP, Hoover WB (2008) Projections of the paraventricular and paratenial nuclei of the dorsal midline thalamus in the rat. J Comp Neurol 508:212-237.

Vertes RP, Crane AM, Colom LV, Bland BH (1995) Ascending projections of the posterior nucleus of the hypothalamus: PHA-L analysis in the rat. J Comp Neurol 359:90-116.

Yokosuka M, Matsuoka M, Ohtani-Kaneko R, Iigo M, Hara M, Hirata K, Ichikawa M (1999) Female-soiled bedding induced fos immunoreactivity in the ventral part of the premammillary nucleus (PMv) of the male mouse. Physiol Behav 68:257-261.

Zhang WN, Bast T, Feldon J (2001) The ventral hippocampus and fear conditioning in rats: different anterograde amnesias of fear after infusion of N-methyl-D-aspartate or its noncompetitive antagonist MK-801 into the ventral hippocampus. Behav Brain Res 126:159-174.

Zufall F, Leinders-Zufall T (2007) Mammalian pheromone sensing. Curr Opin Neurobiol 17:483-489.

3.3 Chapter 3

Afferent connections to the anterior cortical amygdala and the cortex-amygdala transition zone in mice

3.3.1 Introduction

The amygdaloid complex is an important structure controlling social, sexual and maternal behaviours in rodents. It has been proposed to be a key structure in associative emotional learning, as it has been demonstrated for olfactory fear conditioning, where neutral or conditioned stimuli, such as odours, are associated with unconditioned aversive stimuli, such as foot-shock (Cousen and Otto, 1998). In addition to its role in this kind of aversive learning, the amygdala may also play an important role in appetitive learning. In these learning the unconditioned appetitive stimuli (e.g. pheromones) can be associated with other neutral olfactory stimuli, since the amygdala received strong direct projections arising from the main and accessory olfactory bulbs.

The main olfactory bulb (MOB) receives projection from the main olfactory epithelium which is activated by volatile stimuli, while the accessory olfactory bulb (AOB), received projections from the vomeronasal organ, which is mainly activated by non-volatile molecules (Krieger et al. 1990), although a number of volatile vomeronasal stimuli have also been described (Leinders-Zufall et al. 2000). Some of these non-volatile molecules are detected by the vomeronasal system and act as innate attractive chemical cues (sexual pheromones, Martínez-Ricos et al. 2008). It has been showed that naïve female mice only displayed sexual attraction to male-derived volatile odours after they have experienced both, non-volatile and volatile stimuli derived from males (see Martinez-García et al. 2009). Thus, this indicates that female mice display a learned attraction for male volatiles after they associated them with the non-volatile male derived chemicals, namely sexual pheromones. Since the MOB (that is activated by odours) and the AOB (that is activated by pheromones) project to the amygdaloid complex, this is a highly probable place where this appetitive associative learning can take place.

The projections arising from the MOB and AOB converge in some corticomedial amygdaloid nuclei, such as the medial amygdaloid nucleus (Me), the anterior cortical amygdala (ACo) and the cortex-amygdala transition zone (CxA) (Pro-Sistiaga et al., 2007; Kang et al. 2009; Cadiz-Moretti et al. 2013). Therefore, these nuclei are possible candidates where the pheromonal and olfactory stimuli can be associated to generate a learned sexual attraction for male volatiles (Cadiz-Moretti et al. 2013).

Within these nuclei, the Me has been by far the most studied, since it was early reported as an amygdaloid area receiving convergent projections from the MOB and AOB (Scalia and Winans, 1975) and in addition, the lesion of the Me was shown to mediate the chemosensory control of sexual behaviours (Lehman and Winans, 1980). Regarding to the other nuclei receiving convergent projections, there are no studies focused in the CxA and very few in the ACo. However, it is possible that these nuclei also play a role in associative emotional learning and/or, other types of socio-sexual behaviours, due to its connections with the olfactory and vomeronasal systems.

To our knowledge, previous studies that described the afferent connections to the ACo and CxA presented some limitations. On one hand, detailed descriptions of the afferent connections of the ACo were based on non-restricted injections that extended to the BMA (Ottersen and Ben-Ari, 1979; Ottersen, 1980; 1982). On the other hand, recent studies that showed retrograde tracer injections restricted to the CxA (in rat, Pro-Sistiaga et al. 2007) or ACo (in mice, Kang et al. 2009), were used to corroborate the afferent projections arising from the AOB and MOB, and lacked a detailed description of the resulting labelling. Regarding to functional studies, it has been reported in female mice that the ACo exhibit Fos immunoreactive cells induced by the exposure to male urinary odours, indicating that ACo neurons are activated by these volatiles (Martel and Baum, 2009; Brock et al. 2012). Majkutewicz et al. (2010) showed that ACo, in addition with other mesolimbic structures, displayed an increased Fos expression after electrical stimulation of the ventral tegmental area (VTA). These authors suggested that ACo might play a role in eating and exploratory behaviours by means of processing the reinforcing properties of olfactory stimuli.

The aim of this work is to describe the afferent connections to the ACo and CxA, which are currently unknown. With this description, we want to highlight the possible importance of these structures in the processing of convergent vomeronasal and olfactory information, as well as to clarify what other inputs influence the processing of chemosensory information in these brain areas.

3.3.2 Results

For the description of the results, we followed the cytoarchitecture and nomenclature by Paxinos and Franklin (2004). The divisions of the bed nucleus of the stria terminalis are

the same considered in Chapter 2. To make easier the description of the intraamygdaloid afferents, the amygdaloid complex was divided following the architecture proposed by Martínez-García et al. (2012) and the functional divisions of the chemosensory amygdala proposed by Gutierrez-Castellanos et al. (2010): olfactory and vomeronasal nuclei, receiving inputs only from the MOB or AOB, respectively; and mixed nuclei, receiving inputs from both bulbs, with either olfactory or vomeronasal predominance (see Table 3).

As explained in Chapter 2, the extent and boundaries of the injection sites were delineated with fluorescence microscopy (Fig. 15). In addition, retrograde labelling in structures adjoining the injection sites were analysed in fluorescence material.

In this section the distribution and relative density of retrogradely labelled cells are described for the CxA and ACo injections. In addition, an injection located in the rostral Pir was obtained and is used as a control for the CxA injections.

3.3.2.1 Description of the cytoarchitecture of the CxA and ACo.

To determine the boundaries, extension and cytoarchitectonic organization of the CxA and ACo, we worked with two parallel series of the brain of an animal, one stained with the Nissl technique and the other processed with the acetyl cholinestarase (AChase) histochemistry (Fig. 14).

The CxA displayed a moderate reactivity to the AChase histochemistry, with a clear boundary with the ACo and a more diffuse boundary with the piriform cortex (Pir), which showed a low AChase reactivity (Fig 14A, B, C, D). The rostral edge of the CxA accordingly with the AChasa staining, lies between the anterior amygdala and the rostral Pir and dorsal to the lateral olfactory tract (*lo*; not shown). More caudally, the CxA lies between the ACo and the Pir. The intensity of the AChasa reactivity gradually diminish until it presented a light reactivity similar to that of the Pir, so the caudal edge it is not clear distinguishable. According to the intensity of the AChase staining, we considered as the caudal edge of the CxA the level illustrated in the Fig 14D. The CxA shows the trilaminar organization typical of paleocortical structures, forming a continuum with the Pir (Fig 14A', B', C', D').

The ACo presented a negative AChase reactivity, with clear boundaries with the CxA and nucleus of the lateral olfactory tract (LOT) in its rostral part (14A, B, C) and

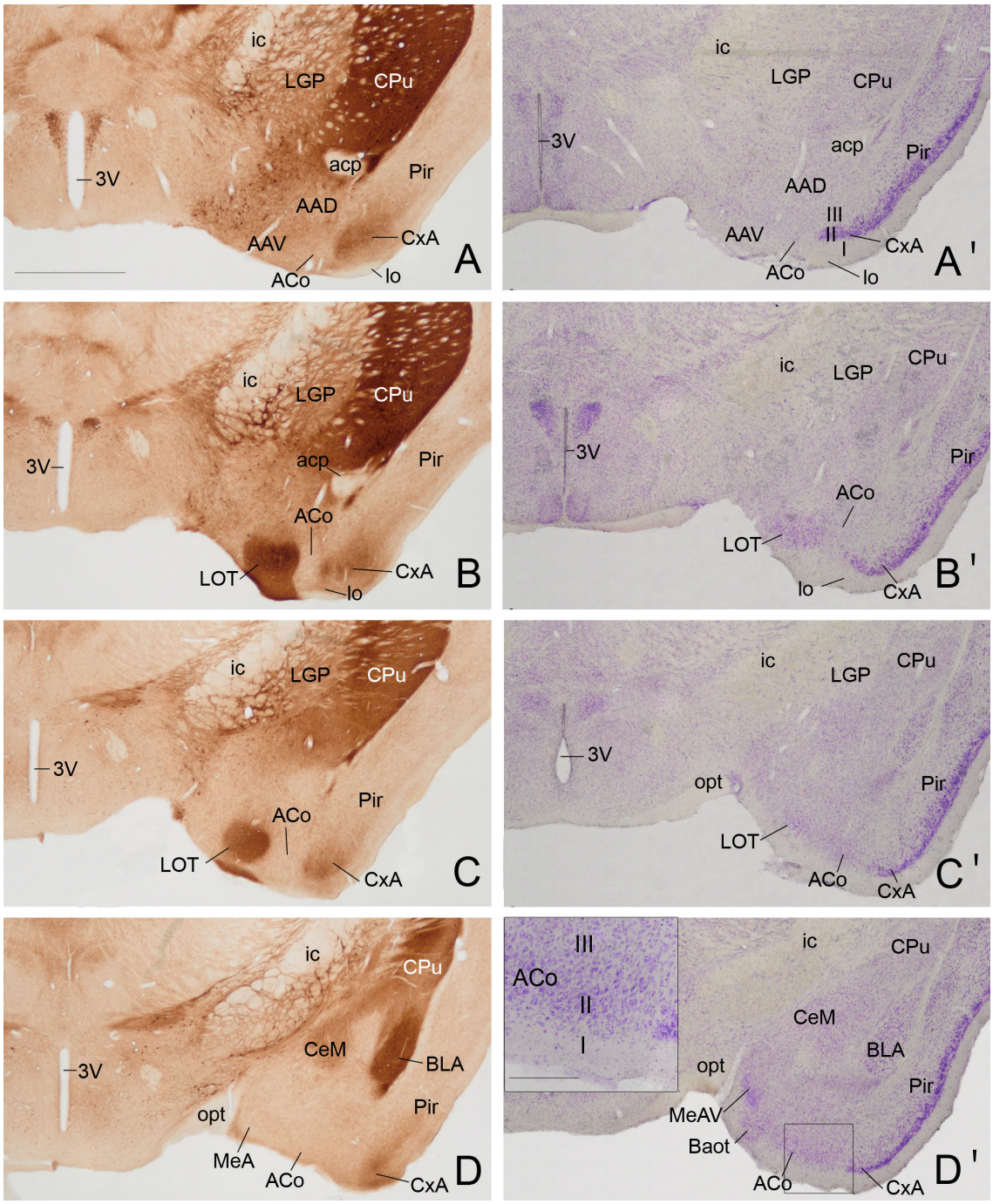

Fig 14. Photomicrographs of the acetyl-cholinesterase (AChasa) histochemistry and Nissl staining in parallel series of a mouse brain (A-D'). AChasa reactivity at different antero-posterior levels of the amygdaloid complex **(A, B, D, E)** and Nissl staining of its parallel series **(A', B', C', D')**. Note the differences in AChasa reactivity between the cortex-amygdala transition zone and anterior cortical amygdala **(A-D)** and the differences in their laminar definition **(A'- D'). (D')** Inset of the ACo showing its loosely laminar organization. Scale bar in A, valid for **A-D** and **A'- D'**: 1mm. Scale bar in D' inset: 100 µm

caudally with no clear boundary with the anterior subdivision of the Me (MeA) (Fig 14D). It showed a trilaminar organization, although much less clear than that of the CxA (Fig 14A', B', C', D'). Superficially, an outer molecular layer, layer I, was present (Fig 1D', inset). Deep to layer I, layer II presented a dense population of cell bodies loosely organized compared to the layer II of CxA (Fig 14D', inset). Finally, an inner layer III, which showed more sparse cell bodies than layer II (Fig 14D', inset), can be recognized.

Table 3. Semiquantitative rating of the density of the retrograde labelling resulting after tracer injections in rostral and caudal parts of the cortex-amygdala transition zone and in the anterior cortical amygdaloid nucleus.

++++ very dense; +++ dense; ++ moderate; + scarce; - very scarce; 0 not found.

		CxA	caudal CxA	ACo
OLFACTORY SYSTEM				
Accessory Olfactory Bulb	MiA	+	+	++
Main Olfactory Bulb	Mi	++++	++++	++++
Olfactory Cortex	DTT/VTT	+/0	++/++	++/+
	AOL	0	0	+
	AOM	0	+	-
	AOP	-	+	+
	rostral Pir	++	+++	++
	caudal Pir	+	++++	+++
	DEn/VEn	++/+	++/++	+++/++
AMYGDALA AND BST				
Vomeronasal	PMCo	-	+	+++
Olfactory	PLCo	+	+++	+++

		CxA	caudal CxA	ACo
	APir	0	+	++
Vomeronasal predominance	MeA	+	++	++
	MeAV/MeAD	+/+	+/+	++/++
	MePV	-	++	++
	MePD	0	-	++
	BAOT	++	-	++++
	AAV/AAD	+/+	++	++/++
Olfactory predominance	ACo	++	++	injection
	CxA	injection	injection	+++
	LOT	+	+	+++
Central	CeC	0	0	0
	CeL	0	0	-
	CeM	-	+	+
	I	0	0	-
	IM	0	0	-
Basolateral complex	BLA	0	+	-
	BLP	0	0	+
	BLV	0	+	+
	BMA	-	++	++
	BMP	0	+++	++
	LaDL/LaVM/LaVL	0	+++	+/0/0
Amygdalohippocampal transition area	AHi	0	-	+
BSTL	BSTLP	0	0	-
	BSTLV	0	0	-

		CxA	caudal CxA	ACo
BSTM	BSTMA	0	0	-
	BSTMV	0	0	-
	BSTMPM	0	0	+
	BSTMPI	0	-	++
	BSTMPL	0	-	+
	BSTIA	0	0	++
CORTEX AND HIPPOCAMPAL FORMATION				
	AID/AIV	0	-/+	+/+++
	AIP	-	+	++
	PrL	0	+	+
	CI	0	-	-
	MO	0	+	+
	LO	0	-	0
	IL	0	0	-
	DP	0	0	-
	PRh	0	+	+
	Ect	0	+	+
Hippocampal formation	LEnt	+	++	++
	CA1	0	+	+
	S	0	0	+
	CA3	0	-	+
SEPTUM/STRIATUM				
Lateral septal complex	LSI	0	0	-
	LSD	0	0	0

		CxA	caudal CxA	ACo
	LSV	0	0	0
	SHi	-	+	+++
Medial septum/Diagonal band	MS	0	0	+
	HDB/MCPO	++	++	++
	VDB	+	+	+
Striato-pallidum	VP	+	+	+
	SL	+	++	-
	SI	-	+	+
	IPAC	-	+	-
THALAMUS				
	PVA/PV	0	0	+/-
	PVP	0	0	++
	Re	0	+	+
	CM	0	-	0
	IMD	0	-	0
	Rh	0	-	0
	MD	0	0	0
	MHb	0	0	0
	ZI	0	-	-
	pv	0	+	++
	SPF	0	+	++
	SPFPC	0	-	+++
	PIL	0	0	+++
	SG	0	0	-
	PP	0	0	+

		CxA	caudal CxA	ACo
	MGM	0	0	+
HYPOTHALAMUS				
Preoptic	MPA	0	0	-
	MPO	0	0	-
	LPO	0	0	0
	RCh	0	-	0
Anterior	AH	0	0	-
	Pa	0	0	0
Tuberal	VMH	0	+	+
	DM	0	-	0
	LH	0	-	+
	Arc	0	0	0
	TC	0	-	-
Mammilary	PMD/PMV	0	0/-	-/-
	SuM	0	0	-
	PH	0	0	++
BRAINSTEM AND MIDBRAIN				
	PAG	0	-	+
	RPC	0	0	0
	SNC	0	0	0
	SNR	0	0	0
	VTA	++	+	+
	RLi	-	0	-
	DR	+	++	+
	IP	0	+	0
	PB	0	-	++

		CxA	caudal CxA	ACo
	LC	0	-	+
	PnO	0	0	-

3.3.2.2 Retrograde labelling after FG injections into the cortex-amygdala transition zone (CxA)

Four restricted injections were obtained in the CxA (Fig 15A-C, I), two of which involved the most ventral part of its layer I and probably the *lo* (1311 and 1329). The other two (1324 and 1331) were centred in cell-dense layer II. Also, in three of these injections (1329, 1324, 1311), a small deposit of the tracer could be observed along the micropipette track involving the ventral endopiriform nucleus (VEn), the interstitial nucleus of the posterior limb of the anterior commissure (IPAC) and the caudate-putamen (CPu; Fig 2B). In addition, five more injections were centred in the CxA, three of them extended to the Pir and the other two to the ACo. The pattern of labelling was similar in all the restricted injections (case 1324 is illustrated in Fig 16) and the labelling in the non-restricted injections was consistent with the pattern observed.

Since the size of the tracer injections had to be small to avoid affecting the adjoining Pir, in general, the retrogradely labelled cell bodies presented a few granules of DAB precipitate in the perinuclear cytoplasm, and the density of labelling was scarce along the brain. The olfactory system presented the highest density of labelled cells. In addition, some nuclei showed a moderate number of labelled somata in other brain structures, such as the bed nucleus of the accessory olfactory tract (BAOT) and ACo in the amygdala, the nucleus of the horizontal limb of the diagonal band (HDB) and magnocellular preoptic nucleus (MCPO) in the septum and the VTA in the brainstem.

Retrograde labelling in the olfactory system

Injections of FG into the CxA gave rise to a very dense labelling throughout the mitral cell layer of the main olfactory bulb (Mi) (Table 3). The somata were darkly stained and in some cases, the labelling extended to the proximal dendritic tree (Fig 16A and Fig 17A). Few labelled cells were also observed in the external and internal plexiform layers (EPl and IPl) of the MOB. In the injections of FG located in the layer II of the

CxA (cases 1324 and 1331), the mitral cell layer of the AOB (MiA) presented scarce labelling (Table 3, Fig 16A and Fig 17B), whereas in the injections located in the layer I and extending into the *lo* (cases 1311 and 1329), the MiA presented a dense labelling (not illustrated).

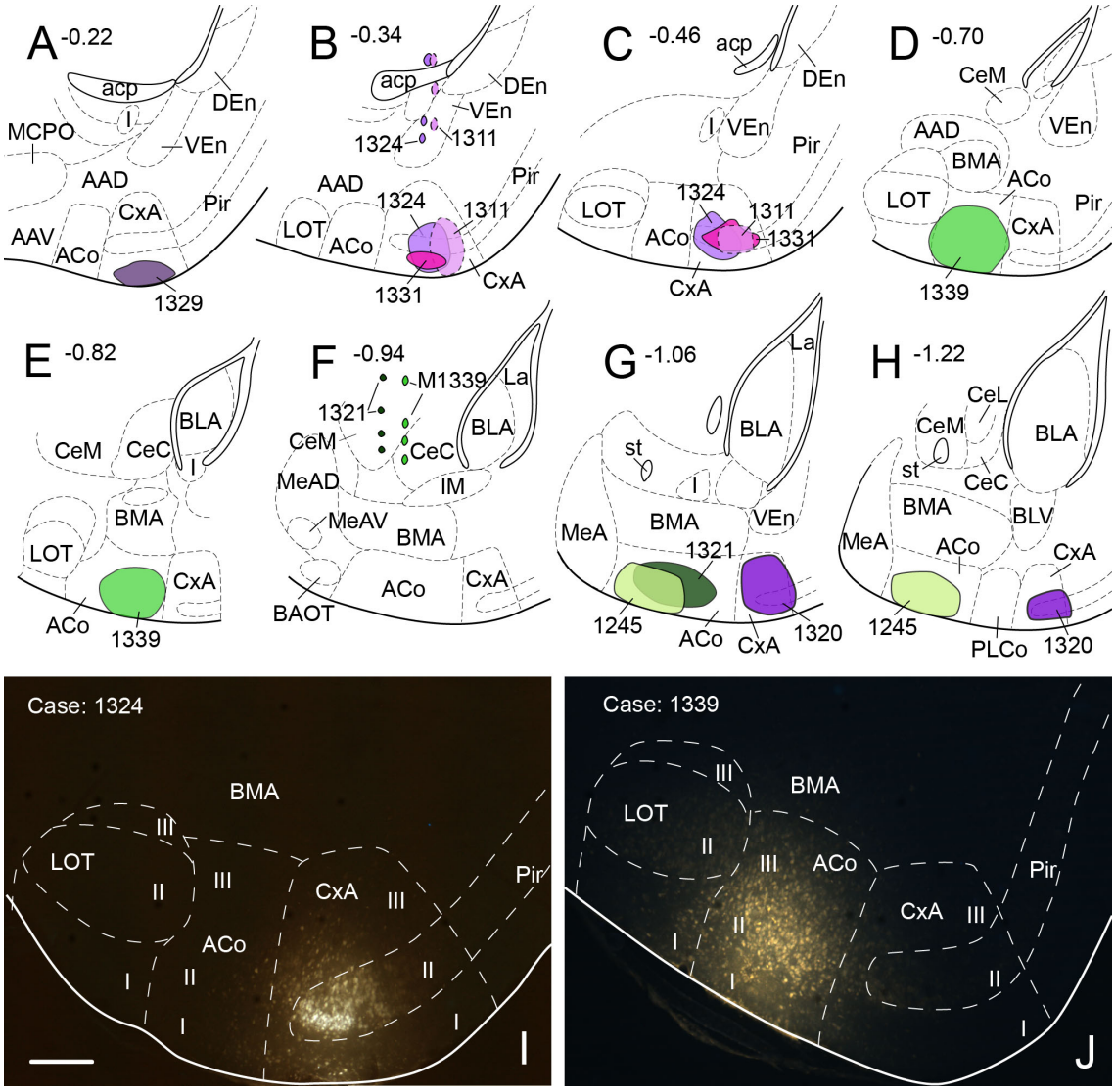

Fig. 15 Injection sites in the cortex-amygdala transition zone and anterior cortical amygdala in mice. (A–J) Schematic drawings representing the extent of the tracer injections in the cortex-amygdala transition zone (CxA) and anterior cortical amygdala (ACo). The injections in the rostral CxA are represented in panels **A-C**; the injection in the caudal CxA are shown in panels **G, H** and the ACo injections are represented in panels **D, E and G, H**. Single injections are identified with the animal code. Panels **B** and **F** depict the tracer deposits along the micropippete track after the injections 1324 and 1311 **(B)** and 1339 and 1321 **(F)**. **(I, J)** Fluorescent photomicrographs through the amygdala showing representative injections sites of Fluorogold. **(I)** Injection site in rostral CxA, case 1324. **(J)** Injection site in ACo, case 1339. Scale bar in I, valid for J = 200 µm

Within the olfactory cortex, the Pir showed a heterogeneous labelling with its rostral part presenting a moderate density of labelled cells and its caudal part showing scarce or very scarce labelling (Table 3, Fig 16B-E). In the rostral part of the Pir, the labelled somata were mainly located in the external part of the layer II and presented a few granules inside each cell body (Fig 17C). Some darkly stained somata were also present in the layer IA next to the *lo* and in the layer III. The dorsal endopiriform nuclei (DEn) and the VEn presented also a heterogeneous labelling, with their rostral parts showing more labelled somata than their caudal parts (Table 3, Fig 16B-E). The DEn showed some darkly stained somata. Finally, the dorsal tenia tecta (DTT) and the posterior part of the anterior olfactory nucleus (AOP) showed only a few retrogradely labelled cells (Table 3).

Retrograde labelling in the amygdala

Within the nuclei with olfactory predominance (Table 3), the ACo presented in general a moderate density of labelled cells (table 3), with its rostral part showing more labelling than its caudal aspect (Fig 16C, D and Fig 17D, E). The LOT showed scarce labelling, with the labelled somata mainly located in the layer II (Fig 16C). Within the nuclei with vomeronasal predominance (Table 3), the BAOT presented a moderate density of labelling (Fig 16D and Fig 17D), although in the injections located superficially (likely affecting the *lo*) more numerous labelled cells were observed. The dorsal and ventral part of the anterior amygdaloid area (AAD and AAV, respectively) and the MeA showed a scarce number of labelled cells and the posteroventral subdivision of the medial amygdala (MePV) showed very scarce labelling (Table 3, Fig 16C-E, Fig 17D). Within the olfactory nuclei (Table 3), the posterolateral cortical amygdaloid nucleus (PLCo) showed a heterogeneous labelling. The labelled cells were mainly located in its rostral part, in layer I and II (Fig 16E and Fig 17E), while the caudal part of the PLCo was almost devoid of labelling. To finish with the chemosensory amygdala, the posteromedial cortical amygdaloid nucleus (PMCo) showed very scarce labelling (not showed). In the rest of the amygdaloid complex, only the medial division of the central amygdaloid nucleus (CeM) and the anterior part of the basomedial amygdaloid nucleus (BMA) showed very scarce labelling (Table 3, Fig 16D, E).

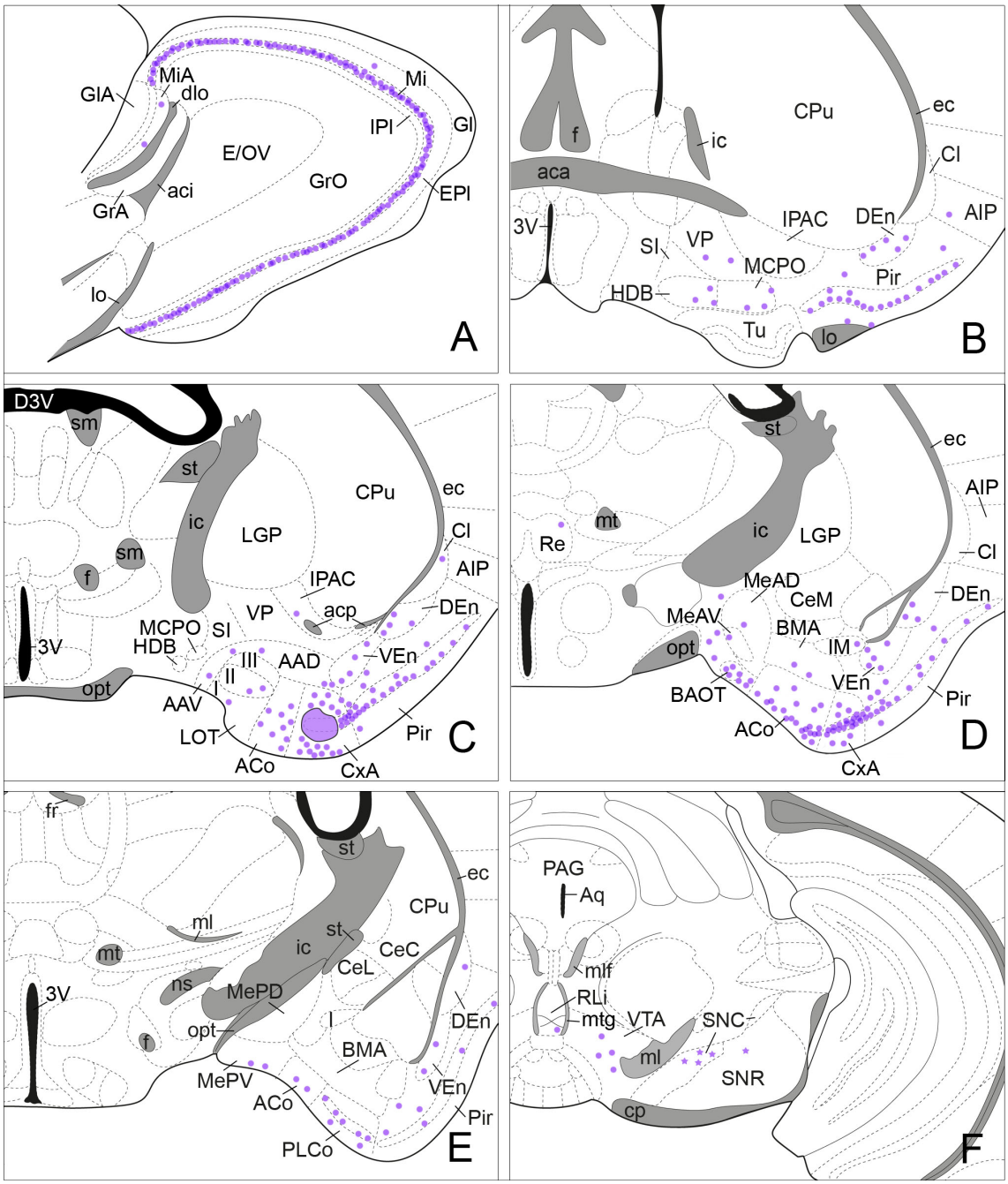

Fig. 16 Semi-schematic drawings of parasagittal (A) and frontal (B-F) sections through the mouse brain showing the distribution of retrogradely labelled somata following a Fluorogold tracer injection in the cortex-amygdala transition zone. The injection site is depicted in panel **(C)**. The semi-schematic drawings are based on the case 1324, which presented the largest restricted injection located in layer II. **B** is rostral, **F** is caudal. For abbreviations, see list.

Retrograde labelling in the Cortex including the Hippocampal formation

Within the cortex, only the lateral entorhinal cortex (LEnt) and the posterior part of the agranular insular cortex (AIP) presented some labelled somata (Table 3, Fig 16B, C). In

the two superficial injections, very scarce labelling was also observed in the ventral part of the agranular insular cortex (AIV; not shown, Table 3).

Retrograde labelling in the Septum and Striatum

Within the diagonal band, the HDB and MCPO presented a moderate density of labelling. In the rostral part of the HDB, the labelled somata were located in its limit with the olfactory tubercle (Tu), while more caudally, when it is adjoining the MCPO, the labelling was homogeneously distributed (Fig 16B, C). In addition, the ventral horizontal diagonal band (VDB) showed scarce labelling (Table 3). Within the striato-pallidum, the ventral pallidium (VP) and semilunar nucleus (SL) showed scarce labelled cells (Table 3, Fig 16B, C) and the *substantia innominata* (SI) and the IPAC presented very scarce labelling (Table 3, Fig 16B, C). Finally, the septohypothalamic nucleus (SHi) also presented very scarce labelling (Table 3).

Retrograde labelling in the midbrain and brainstem

Within the midbrain, the ventral tegmental area (VTA) presented a moderate number of labelled somata (Table 3, Fig 16F and Fig 17F). In addition, in the brainstem, the dorsal raphe (DR) and the rostral linear nucleus of the raphe (RLi) showed scarce and very scarce labelling respectively (Table 3). The three injections that presented a deposit of the tracer along the micropipette track affecting the CPu, showed labelled cells in the *substantia nigra*, which were present both in its *pars compacta* and *pars reticulata* (Table 3, Fig 16F). Remarkably, the injection without this leaking in the CPu did not show labelled cells in these structures.

Contralateral labelling

Although the FG injections gave rise mainly to ipsilateral retrograde labelling, very few labelled cells (with very few granules of DAB precipitate) were also observed in the contralateral Pir and LOT.

3.3.2.3 Retrograde labelling after a FG injection in the caudal edge of the CxA

One restricted injection of FG was obtained in the caudal edge of the CxA, centred in layer II (Fig 15G, H). Although its location was considered to be part of the caudal CxA taking into account the AChase histochemistry (Fig 14D), the retrograde labelling

yielded by this injection differed from the labelling pattern observed in the more rostral injections of CxA. This injection was also larger than the rostral ones. Taking into account the different sizes between the rostral and caudal injections, the following description is based mainly on the differences in the pattern of projections and in some important differences in density (Table 3).

Regarding to the olfactory system, the labelling observed in the Pir was homogenously distributed throughout the external and internal parts of its layer II. This destribution contrast with the external labelling presented in the layer II of the Pir in the rostral injections of the CxA. Also, not only the AOP presented labelled cells, but in addition, the medial part of the anterior olfactory nucleus (AOM) presented a scarce amount of labelling (Table 3). Remarkable, this injection presented scarce labelling in the MiA, similar to the injections that were located in the layer II of the rostral CxA (Table 3, Fig 15B, C and G, H).

Regarding to the amygdala, within the chemosensory amygdala, the PLCo presented a dense labelling (Table 3) and the PMCo showed a heterogeneous labelling ranging from very scarce in its anterior part to a moderate density of labelled cells in its caudal part (not shown). In the basolateral complex (Table 3), the caudal CxA injection gave rise to an important labelling in some nuclei in contrast to the almost un-existing labelling showed by the rostral CxA injections. The lateral amygdaloid nucleus (La) showed dense labelling mainly located in its ventral part. The anterior and posterior part of the basomedial amygdaloid nucleus (BMA and BMP, respectively) presented a moderate density of labelled cells and the anterior and ventral parts of the basolateral amygdaloid nucleus (BLA and BLV, respectively) showed scarce labelling (Table 3). Within the extended amygdala, the posterointermediate and posterolateral parts, of the medial division of the bed nucleus of the stria terminalis (BSTMPI and BSTMPL, respectively) presented a very scarce amount of labelled cells (Table 3).

Regarding to the cortex, this injection gave rise to scarce or very scarce labelling in some parts of the frontal cortex such as, the dorsal part of the AI (AID) and AIV, the prelimbic cortex (PrL), the medial and lateral orbital cortex (MO and LO, respectively) and in more caudal cortical areas such as the perirhinal cortex (PRh), the ectorhinal cortex (Ect) and in the pyramidal cell layer CA1 and CA3 of the hippocampal formation (Table 3).

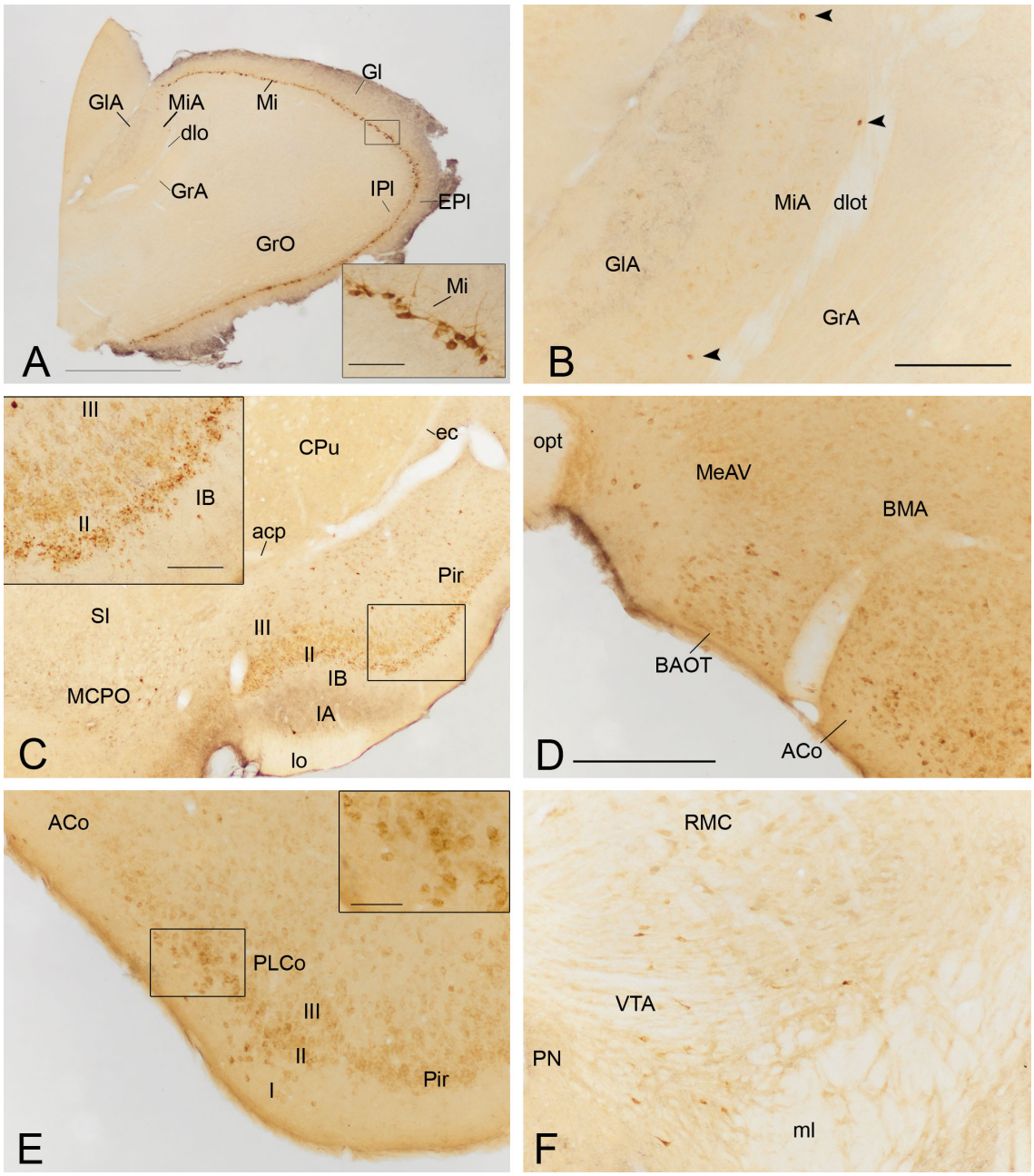

Fig. 17 Photomicrographs of frontal sections illustrating the retrograde labelling through the mouse telencephalon of animals receiving a Fluorogold injection in the cortex-amygdala transition zone. The images correspond to the retrograde labelling presented in the cases 1324 **(A, B, D, E)**, 1331 **(C)** and 1311 **(F)**. **(A)** Retrograde labelling in the main olfactory bulb (MOB). The inset in **(A)** depicts the darkly stained somata of mitral cells, which in some cases also show the proximal dendrites labelled. **(B)** A few retrogradely labelled neurons in the accessory olfactory bulb. The arrowheads indicate retrogradely labelled cells in the mitral cell layer. **(C)** Labelling in the rostral part of the piriform cortex (Pir) and magnocelluar preoptic nucleus. The inset illustrates the labelled cells in layer II of the Pir, mainly located in its external part. **(D)** Moderate amount of retrogradely labelled cells in the bed nucleus of the accessory olfactory tract (BAOT) and anterior cortical amygdaloid nucleus (ACo). **(E)** Retrogradely labelled neurons in the posterolateral cortical amygdaloid nucleus (PLCo). The inset shows the labelling mainly located in the layer I and II of the PLCo. **(F)**

Retrograde labelling in the ventral tegmental area (VTA). For abbreviations, see list. Scale bar in A, 1mm. Scale bar in B, valid for C: 500 μm. Scale bar in inset in A and C: 100 μm. Scale bar in D, valid for (E, F): 250 μm. Scale bar in inset in E: 50 μm

In contrast to the injections in the rostral CxA, which did not give rise to thalamic or hypothalamic labelling, this injection in the caudal CxA resulted in scarce or very scarce labelling in some thalamic nuclei including the reuniens thalamic nucleus (Re), the central medial thalamic nucleus (CM), the intermediodorsal thalamic nucleus (IMD), the rhomboid thalamic nucleus (Rh), the zona incerta (ZI), the periventricular fiber system (pv), the subparafascicular thalamic nucleus (SPF) and parvicellular part of the SPF (SPFPC) (Table 3). In addition, in the hypothalamus scarce labelling was observed in the ventromedial hypothalamic nucleus (VMH) and very scarce labelling in the retrochiasmatic area (RCh), the dorsomedial hypothalamic nucleus (DM), the lateral hypothalamic area (LH), the *tuber cinereum* area (TC) and the ventral part of the premammillary nucleus (PMV) (Table 3).

Lastly, in the midbrain and brainstem, in addition to the labelled cells presented by the VTA and DR, scarce labelling was observed in the interpeduncular nucleus (IP), the periaqueductal grey (PAG), the locus coeruleus (LC) and the parabrachial nucleus (PB), which were not labelled after the CxA injections (Table 3).

3.3.2.4 Control injections

Two restricted injections were obtained in the ventral Pir, rostral to the CxA injections. In one injection, the FG tracer was used and it was centred in layer III, involving also layer II, in the other, BDA tracer was used and it was centred in layer I involving the lo. Both injections were of similar sizes to those described for the rostral CxA.

In general the labelling observed after the Pir injections presented a similar pattern of labelling to the one described for the CxA injections, with some differences in the density of labelling in a few structures. In summary, the most important differences were observed in the amygdala, brainstem and midbrain, and are described in more detail below. In contrast, the olfactory system, the cortex, hippocampal formation, septum and striatum presented a similar pattern of labelling distribution with some

differences relative to the density of the labelled cells in some centres. Finally, similar to the CxA injections, the hypothalamus and thalamus did not show labelled cells.

Regarding the most important differences with the injections in the rostral CxA, within the nuclei of the amygdala with olfactory predominance, the LOT showed a moderate density of labelled cells, with a higher amount of darkly stained somata and an important contralateral labelling. The ACo presented very scarce labelling. Within the nuclei with vomeronasal predominance, the MeA presented very scarce labelling and the posterodorsal subdivision of the Me (MePD), MePV and BAOT did not showed labelled cells. In the basolateral complex, the BLA and BMP showed a few labelled cells. And finally within the brainstem and midbrain, the DR presented a moderate number of labelled cells and the VTA showed a few number of labelled cells.

With regard to minor differences with the CxA injections, within the olfactory system, in the olfactory bulbs the MiA was completely devoid of labelled cells. The Pir showed a dense labelling, with the labelled cells mainly located in the inner part of the layer II, contrasting with the external location of the labelled cells in the CxA injections. The Pir also showed an important contralateral labelling. Also, a moderate density of labelling was observed in the ventral tenia tecta (VTT; mainly located in the layer II and III) and AOM, which also presented contralateral labelling. Finally, within the prefrontal cortex, very scarce labelling was observed in the MO and LO.

3.3.2.5 Retrograde labelling after FG injections into the anterior cortical amygdaloid nucleus (ACo)

Five injections were aimed at the ACo, three of which were restricted to this nucleus (Fig 15D-H). Two of the restricted injections involved the superficial layer I (cases 1339 and 1245) and one was mainly located in layer II (case 1321). In two of the three injections, a small deposit of tracer could be observed along the micropippete track in the CPu, the lateral globus pallidus and the central amygdaloid nucleus (Ce; cases 1321 and 1339, Fig 15F). Additionally, two more injections were centred in ACo, but extended to CxA. The pattern of labelling was similar in all the restricted injections (case 1339 is illustrated in Fig 18) and the labelling in the non-restricted injections was consistent with the pattern observed.

In general, the ACo injections gave rise to a high density of retrograde labelling in the olfactory system, the chemosensory amygdala and the posterior intralaminar thalamus. In addition, the central and basolateral complex of the amygdala, several nuclei of the BST complex, some cortical areas including the hippocampal formation, the septum and striatum, and several hypothalamic, mesencephalic and brainstem nuclei presented retrograde labelling in a degree from moderate to very scarce.

Retrograde labelling in the olfactory system

After the retrograde injections in the ACo, a very dense labelling was observed throughout the Mi with darkly stained somata (Table 3, Fig 18A and Fig 19A). Moreover, few labelled cells were present in the IPl, EPl and glomerular layer of the MOB. The AOB also showed retrograde labelling in the MiA and few labelled cells in its glomerular layer (Table 3, Fig 18A and 19A). Similar to the retrograde labelling observed in the CxA injections, the density of labelling in the MiA depended on which layer of the ACo was centred the injection. The superficial injections (cases 1245 and 1339) gave rise to a dense labelling in the MiA, while the deep injection (case 1321) gave rise to a scarce labelling.

Regarding the olfactory cortex, some areas showed a remarkably retrograde labelling. The Pir presented a heterogeneous pattern of labelling (Fig 18B-F), presenting in its rostral part a moderate number of labelled cells (Table 3). These labelled somata were mainly located in the inner part of layer II (Fig 18B) contrasting with the external location of the retrograde labelling observed after the CxA injections (Fig 16B, D and Fig 17C). In layer I, few labelled cells were located surrounding the *lo*. In the intermediate levels, the labelling was dense and the labelled cells distributed homogeneously between the layers II and III and finally, in its caudal part, the density of labelling was moderate (Fig 18C-F and 19C, D). Noteworthy, in the most rostral injection (case 1339), the density of labelling along the Pir was higher than the other two injections. The DEn also presented a heterogeneous labelling, showing more labelled somata in its rostral part than in its caudal part, while the VEn showed a moderate number of labelled cells along its extension (Table 3, Fig 18B-F and Fig 19C, D). Both nuclei presented darkly stained somata. The DTT presented a moderate number of labelled somata mainly located in its layer III (Table 3, Fig 19B) and the VTT showed scarce labelling with the labelled somata mainly located in layer II (Table

3, not shown). Finally, the lateral part of the anterior olfactory nucleus (AOL), the AOP and AOM presented a few labelled somata (Table 3, Fig 19B).

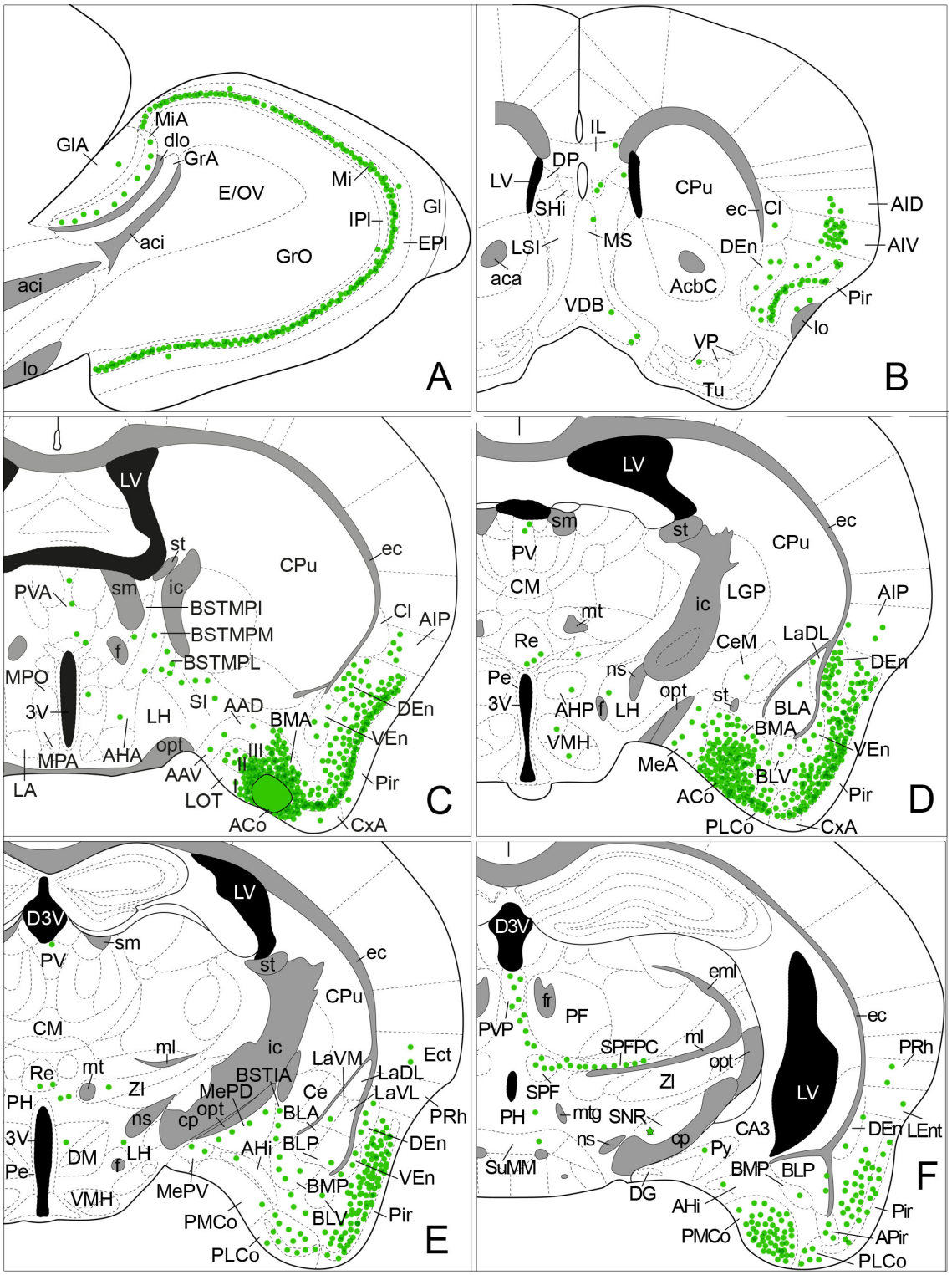

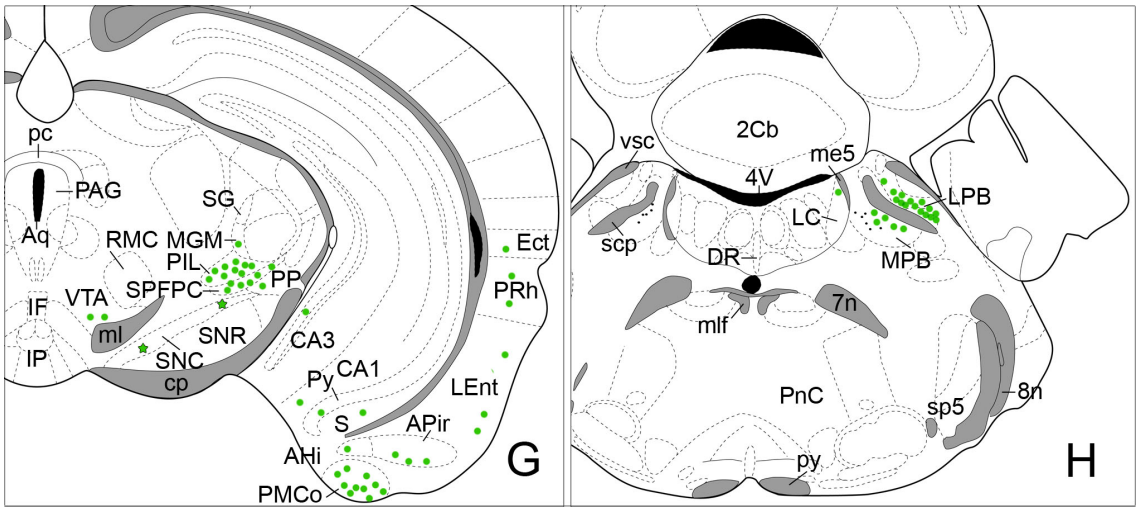

Fig. 18 Summary of the distribution of retrograde labelling following a Fluorogold injection in the anterior cortical amygdaloid nucleus, plotted onto semi-schematic drawings of parasagittal (A) and frontal (B-H) sections through the mouse brain. The injection site is depicted in panel **(C)**. **B** is rostral, **H** is caudal. The semi-schematic drawings are based on the case 1339, which presented the largest restricted injection. For abbreviations, see list.

Retrograde labelling in the amygdala

Within the amygdaloid complex, the chemosensory amygdala presented the densest population of retrograde labelled cells. In addition, within the deep nuclei, the Ce, basolateral and the amygdalohippocampal area (AHi) showed retrograde labelling, contrasting with the almost absence of labelled cells in these nuclei after the CxA injections.

In the olfactory amygdala (Table 3), the injections gave rise to a heterogeneous labelling in the PLCo, with the labelled somata distributed along all its layers but more densely located in its layer II. This nucleus showed more labelled cells in its rostral part than in its caudal part (Fig 18D-F and Fig 19C, D). The amygdalopiriform transition area (APir) presented a moderate number of labelled cells (Table 3, Fig 18F, G and Fig 19D).

With regard to the nuclei with olfactory predominance (Table 3), the CxA and LOT showed dense labelling (Table 3). In the CxA, all the layers presented labelled cells but layer II presented a higher number of them, while in the LOT the labelled cells were almost strictly located in its layer II (Fig 18C-D).

In the vomeronasal amygdala (Table 3), the injections gave rise to a heterogeneous labelling in the PMCo, with the labelled somata located in its cellular layer (Fig 18E-G). Its rostral part was almost depleted of retrograde labelling (Fig 18E and 19C), while its caudal part showed a dense number of labelled somata (Fig 18F, G and 19D).

Regarding to the nuclei with vomeronasal predominance, the BAOT showed a very dense labelling after the superficial injections (Table 3, not shown), while in the deep injection it showed a moderate to dense labelling (not shown). The AAV, AAD and the three subdivisions of the Me presented a moderate number of labelled cells (Table 3, Fig 18C-E and Fig 19C). In the Me, the labelled cells were mainly located in its cellular layer. In addition, the posterodorsal subdivision of the Me (MePD) presented a conspicuous heterogeneity in the labelling distribution, with the labelled somata mainly aligned along the limit of its cellular and external layer (Fig 19C).

Within the deep amygdala, in the basolateral complex, the BMA and BMP presented a moderate density of labelled cells (Table 3, Fig 18C-F and Fig 19C, D), with the BMA showing more labelled cells in its rostral (Fig 18C, D) than in its caudal part (not shown). The posterior part of the basolateral amygdaloid nucleus (BLP) and BLV presented scarce labelling and the BLA showed very scarce number of labelled cells (Table 3, Fig 18D-F and Fig 19C, D). Within the lateral amygdaloid nucleus, only the dorsolateral part of the La (LaDL) showed labelling, with a scarce number of labelled somata (Table 3, Fig 18D, E). Regarding to the Ce, it showed in general few labelled cells (Table 3, Fig 18D, E). As a final point, the AHi presented also scarce labelling (Table 3, Fig 18E-G and Fig 19D).

Retrograde labelling in the bed nucleus of the stria terminalis (BST)

In general, the BSTMPI and the intraamygdaliod division of the BST (BSTIA) presented the strongest labelling among the entire BST complex, while the rest of the complex presented scarce cells. In two of the three injections, the BSTMPI showed a moderate number of labelled somata and the posteromedial part of the medial division of the BST (BSTMPM) and BSTMPL showed scarce labelling (Table 3, Fig 18C). The remaining division of the BST complex that showed labelling were the ventral and anterior parts of the medial division (BTSMV and BTSMA, respectively), the ventral and posterior parts of the lateral division (BTSLV and BTSLP, respectively), which

presented very scarce labelled cells (Table 3). Finally, the BSTIA, showed a moderate density of labelling (Fig 18E, Fig 19C).

Retrograde labelling in the Cortex including the Hippocampal formation

In the neocortex, only the AI showed and important amount of labelling, while few labelled cells were observed in the prefrontal and the perirhinal regions. Thus, within the cortex, the PrL, MO, dorsal peduncular cortex (DP), infralimbic cortex (IL), claustrum (Cl), PRh and Ect display scarce or very scarce labelling (Table 3, Fig 18B-G). Regarding to the AI, it displayed a striking heterogeneous labelling. The AIV presented dense labelling, while the AID showed scarce labelling with the labelled cells mainly located in layer V in both parts (Table 3, Fig 18B). The posterior part of the AI (AIP) displayed a moderate density of labelling (Table 3, Fig 18C, D).

Within the hippocampal formation, the LEnt presented a moderate density of labelling (Table 3, Fig 18F, G) and the CA3, CA1 and subiculum (S) showed scarce labelled somata located in their ventral parts (Table 3, 18G). The observed labelled somata in the CA1 and CA3 were located in the Py.

Retrograde labelling in the Septum and Striatum

In general, the injections in ACo gave rise to scarce labelling in the septum and striatum, with exception of the SHi in the septum and the HDB/MCPO in the striatum. The SHi presented dense labelling and darkly stained somata just ventral to the DTT (Table 3, not shown), while caudally it presented few labelled cells (Fig 18B).

Within the diagonal band, the HDB and MCPO showed a moderate density of labelling with some darkly stained somata, while the VDB presented a scarce number of labelled cells (Table 3, not shown). In the VDB and rostral part of the HDB, the retrograde labelling was mainly present in their limits with the Tu. Finally, few labelled somata were observed in the medial septal nucleus (MS) lining up at the boundary with the intermediate part of the lateral septal nucleus (Table 3, Fig 18B).

Within the striato-pallidum, the SL, VP and IPAC also showed a few, scattered labelled somata (Table 3, Fig 18B, C). In addition, the SI presented scarce labelling with labelled cells mainly located between the BSTMPL and the anterior amygdaloid nucleus

(Fig 18C). To finish with the description of straitum, at its rostral level, darkly stained cells were observed in the territory located between the AOP and the Tu (Fig 19B).

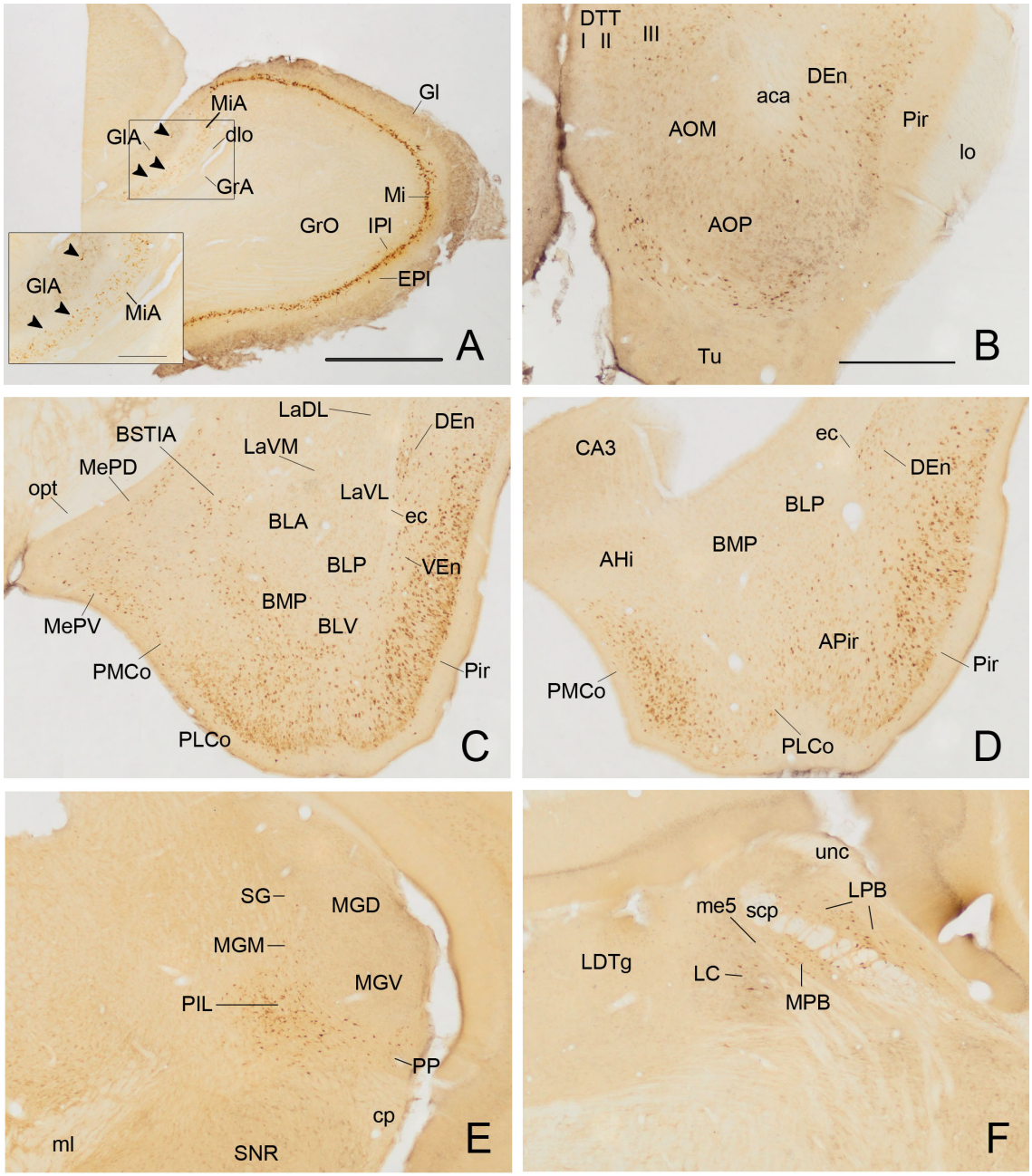

Fig. 19 Photomicrographs of parasagittal (A) and frontal (B-F) sections through the mouse telencephalon, illustrating the retrograde labelling observed in animals receiving a Fluorogold injection in the anterior cortical amygdaloid nucleus. The images correspond to the retrograde labelling presented in the cases 1339 **(A-D)** and 1245 **(E, F)**. **(A)** Retrogradely labelled mitral cells in the main olfactory bulb. Inset in A shows retrograde labelling in the mitral and glomerular cell layer (see arrowheads) of the accessory olfactory bulb. **(B)** Retrograde labelling present in the territory between the posterior part of the anterior olfactory nucleus and the olfactory tubercle. **(C)** Numerous labelled cells in the caudal piriform cortex and dorsal part of the endopiriform nucleus within the olfactory system. In the amygdala, dense labelling is

present in the posterolateral cortical amygdaloid nucleus, and a moderate density of labelled cells is shown by the posteroventral and posterodorsal subdivision of the medial amygdaloid nucleus (MePV and MePD, respectively), the intraamygdaloid division of the bed nucleus of the stria terminalis and the posterior part of the basomedial amygdaloid nucleus. Note the heterogeneous distribution of the retrograde labelling in the MePD, with the labelled cells mainly located in the external part its cellular layer. At this level, the posteromedial cortical amygdaloid nucleus is almost devoid of labelling. **(D)** Dense retrograde labelling in the caudal part of the posteromedial cortical amygdaloid nucleus and moderate density of retrogradely labelled cells in the amygdalopiriform transition area. Within the olfactory cortex, dense labelling is present in the posterior part of the piriform cortex. **(E)** Important labelling in the posterior intralaminar thalamic region. (**F**) Retrogradely labelled cells in the medial and lateral parabrachial nucleus and the locus coeruleus. For abbreviations, see list. Scale bar in A: 1 mm. Scale bar in inset en A: 250 μm. Scale bar in B (valid for B–F): 500 μm.

Retrograde labelling in the Thalamus

After the FG injections, retrograde labelling was observed in the paraventricular and the posterior intralaminar thalamic regions. The anterior paraventricular thalamic nucleus (PVA) showed a striking heterogeneous labelling. In its rostral edge, it presented a moderate density of labelled cells lining up in its medial and ventral aspects (Fig 18C). In its intermediate levels and more caudally it showed very scarce labelling, with the labelled somata located in its most dorsal aspect (Table 3, Fig 18D, E). Finally, in the posterior part of the paraventricular thalamic nucleus (PVP), the labelling density increases to moderate (Table 3, Fig 18F). In addition, the Re and ZI showed few labelled cells (Table 3, Fig 18D-F)

In the caudal thalamus, a moderate density of labelling was observed next to the midline along the pv, lining up between the PVP and the SPF, which also presented a moderate density of labelling (Table 3, Fig 18F). Laterally, within the posterior intralaminar thalamic complex, the SPFPC showed dense labelling, which was also observed in the posterior intralaminar thalamic nucleus (PIL; Table 3, Fig 18F, G and Fig 19E). In addition, the peripeduncular nucleus (PP) and medial part of the medial geniculate nucleus (MGM) presented a scarce number of labelled cells and the suprageniculate thalamic nucleus (SG) very scarce labelling (Table 3, Fig 18G and Fig 19E).

Retrograde labelling in the Hypothalamus

In general, the hypothalamus displayed only sparse and scattered retrograde labelling. Thus, in the preoptic and anterior hypothalamus, the medial preoptic area (MPA), the medial preoptic nucleus (MPO) and the anterior hypothalamic area (AH) presented very scarce number of labelled cells (Table 3, Fig 18C, D). Within the tuberal hypothalamus, the VMH and LH present scarce labelling and the TC very scarce labelled cells (Table 3, Fig 18D, E). Finally, at mammillary levels, the posterior hypothalamic area (PH) presented a moderate density of labelling along its extension (Table 3, Fig 18E, F) and the PMV, the dorsal part of the premammillary nucleus (PMD) and supramammillary nucleus (SuM) showed very scarce labelling (Table 3, Fig 18F).

Retrograde labelling in the Midbrain and Brainstem

To finish with the description of the observed retrograde labelling, the midbrain and brainstem showed few labelled cells, with the exception of the PB in the brainstem, which presented a moderate density of labelling in its medial and lateral divisions (Table 3, Fig 18H and Fig 19F).

In the remaining nuclei of the midbrain and brainstem, the PAG, VTA, DR and LC showed scarce labelling (Table 1, Fig 18G, H) and the RLi and the oral part of the pontine reticular nucleus (PnO) very scarce labelled cells (Table 3, not shown). In addition, in the cases where tracer deposits appeared along the micropipette tract in the CPu, labelled cells were observed in the *sustantia nigra* (Fig 18F, G; shown with star forms).

Contralateral retrograde labelling

Although the observed retrograde labelling was mostly ipsilateral to the FG injections, a few labelled cells were also present in some contralateral nuclei. In the olfactory system, the rostral Pir presented moderate labelling located in its layer II and few sparse labelled somata in its caudal part. The DTT showed very scarce number of labelled cells in its layer III. Within the amygdala, the PLCo showed scarce labelling and the PMCo and BMA very scarce labelled somata. In the hippocampal formation, the LEnt displayed a few labelled cells. The diagonal band and SI showed very scarce labelling. Within the thalamus, the SPF, SPFPC and PP presented scarce labelling and the PIL, PVA, PVP, pv, Re and ZI showed very scarce labelled cells. The hypothalamus

displayed a few labelled cells in the VMH, LH and PH. Finally, scarce number of labelled cells was also observed in the PAG, VTA, CLi and PB.

3.3.3 Discussion

To our knowledge, this is the first study focused on the description of the afferent connections of the CxA and ACo. The data available in the literature correspond to studies aiming to characterize the connections of other structures that project to the CxA and/or ACo. In addition, in some cases tracer injections were performed in the ACo, but the injection sites were not restricted to this structure (Ottersen, 1980; 1982). The majority of the reported injections of retrograde tracers in the CxA and ACo were done in rat (Ottersen 1982; Pro-Sistiaga et al. 2007) with only one report available in mouse (Kang et al. 2009).

Our results show that CxA and ACo present partially different patterns of connections with brain structures. The CxA shows a relatively restricted set of afferent connections, as it receives mainly projections from the olfactory system and basal forebrain, with minor afferents from the amygdala. The ACo shares this set of afferents but, in addition, presents important projections arising from the chemosensory amygdala and the midline and posterior intralaminar thalamus. Moreover, the ACo also presents moderate projections from some nuclei of the deep (multimodal) amygdala, the BST and cortical structures including the hippocampal formation. Finally, minor connections to the ACo arise from the hypothalamus, brainstem and midbrain.

The set of afferents presented by the CxA is similar to that of the rostral Pir (see Control injections in Results) while the afferent projections showed by the ACo resemble more those presented by the medial amygdaloid nucleus (chapter 2). The ACo is highly connected not only with several chemosensory nuclei of the amygdala, but also with the multimodal amygdaloid nuclei and the midline and posterior intralaminar thalamic complex. This suggests that the ACo is involved in the processing of chemosensory as well as multimodal information, probably in relation to its emotional meaning, while the CxA is more exclusively related with the processing of chemosensory (mainly olfactory) information.

Another interesting result found in this study is that the rostral part of the CxA shows a different pattern of connections from its caudal part. As described above, the rostral CxA is mainly connected to the olfactory system and basal forebrain, with minor connections with the amygdala, while the caudal CxA, in addition to share these connections, presents a denser input arising from the chemosensory and deep nuclei of the amygdala. Besides these afferents, the caudal CxA also shows minor connections with the cortex including the hippocampal formation, thalamus, hypothalamus, brainstem and midbrain. So, it seems that, while the rostral CxA presents connections more similar to the rostral Pir, the caudal CxA is in an intermediate position resembling in some aspects the connections to the ACo and in others, to the caudal Pir. To our knowledge, there are no studies reporting the afferent connections to the posterior Pir with retrograde tracing. However, a review of the literature describing afferent projections to the Pir reveals that it receives afferents from the amygdala (Luksin and Price, 1983; Shammah-Lagnado and Santiago 1999; Pardo-Bellver et al. 2012; Gutierrez-Castellanos et al. 2014), the hypothalamus (Canteras et al. 1994), the thalamus (Vertes and Hoover, 2008) and brainstem (Saper and Loewy, 1980).

The results are discussed following the sections of Table 3, comparing at the same time the retrograde labelling found for the CxA and ACo.

Technical considerations and discussion on the nomenclature

In the present study, the afferent connections to the CxA were described by using restricted injections that necessarily had to be of a reduced size, to avoid affecting the neighbouring Pir. The small size of these injections may result in reduced (or even unobserved) labelling in brain areas that send minor projections to the CxA, or in an underestimation of the relative density of the projections from some of the nuclei.

In addition, it is important to note that the majority of previous anatomical works did not differentiate between the Pir and the CxA, describing the observed labelling in the latter as the medioventral part of the Pir (e.g., Haberly and Price, 1978). After studying their descriptions and illustrations, we assigned the observed labelling in the medioventral part of the Pir to what we considered the

CxA according to the AChasa labelling (Fig 14) and the atlas of Paxinos and Franklin (2001).

Regarding the ACo limits, we follow the description of the atlas of Paxinos and Franklin (2001), which coincides to a great extent with the boundaries described by Petrovich et al (1996).

Olfactory system

Our results confirm that the CxA and ACo received convergent projections arising from the main and accessory olfactory bulbs, corroborating previous works done with anterograde and retrograde tracers (Pro-Sistiaga et al. 2007, Kang et al., 2009, Cadiz-Moretti et al. 2013). The MOB is the main sensory input to the CxA and ACo, sending stronger projections to these nuclei than the AOB, which sends minor projections. The afferents from the MOB and AOB are originated throughout all of their mitral cell layer, lacking a topographic organization. These results are consistent with previous reports in rat and mice (in rats: Mohedano-Moriano et al. 2007; Pro-Sistiaga et al. 2007; in mice: Kang et al. 2009), although one work described that the projection to the ACo and PLCo originates mainly in the dorsal olfactory bulb (Miyamichi et al. 2011). In contrast to this lack of topographic organization, the projection from the MOB to the Me apparently arises mainly from its ventral aspect (Kang et al. 2009). In addition, differential projections arise from the rostral versus the caudal part of the AOB to some vomeronasal amygdaloid nuclei, such as the BST, AAD, BAOT and MeAV (Mohedano-Moriano et al. 2007) and MePD (Chapter 2). Regarding to the MOB, Kang et al (2009) reported that the mitral cells located in the ventral MOB projecting to the Me were activated by opposite sex odours and not by same sex odours or predator odours. This suggests that only a fraction of MOB output conveys information to the 'vomeronasal' amygdala. These results raise the question of which type of olfactory and vomeronasal information reaches the CxA and ACo. According to the well-known role of the amygdala in processing emotional information (Martínez-García et al. 2012), it would be expected that projections arising from the olfactory bulbs to these nuclei send chemosensory information related to conspecifics or predators. However, a previous study found that Fos expression in the ACo was induced equally by a novel odour and by cat odour (Dielenberg et al. 2001). Regarding the

conspecific odours, the exposure to volatiles derived from male-soiled bedding induced Fos expression in the ACo in female mice (Moncho-Bogani et al. 2005). Notably, the Fos induction in the ACo was observed equally when the male volatiles were attractive (because of previous chemosensory experience of the females) and when the male volatiles induced no attraction (in inexperienced females). Taken together, the results of these studies (Dielenberg et al. 2001; Moncho-Bogani et al. 2005) suggest that general odorants, and not only emotionally-labelled chemical cues, apparently activate the ACo. The activation by general odorants may allow the ACo to be involved in the association of olfactory cues with other stimuli. However, further studies are needed to test this hypothesis.

Differences in density of retrograde labelling were observed in the AOB depending on which layers were affected by the injections in the CxA and ACo. The superficial injections mainly centred in layer I of both nuclei displayed more labelling in the AOB than those injections that were centred in layer II. The fibres arising from the AOB projecting to CxA and ACo mainly innervate layer I, with only some fibres coursing inward to innervate deep layers (in rat, Pro-Sistiaga et al. 2007; in mouse, Cadiz-Moretti et al. 2013). The fibres in layer I were described as thick and varicose, suggesting the possibility that they also made *in passant* synapses in the distal portions of the dendrites of the CxA and ACo neurons (Pro-Sistiaga et al. 2007; Cadiz-Moretti et al. 2013). Therefore, the differences in the observed retrograde labelling in the AOB could be explained by the uptaking of the tracer by these superficial fibres in the superficial injections. However, we cannot discard the possibility of the uptaking of the tracer by fibres damaged in the *lo* by the micropipette tip.

In addition, we wandered whether the possible damage to the *lo* may cause differences in the density of retrograde labelling in the nuclei that send feedback projections to the AOB (BST, BAOT, MeA, PMCo and ventral CA1) or to the MOB (LOT, ACo, PLCo, PMCo and Pir) (Shipley et al. 1984: Mohedano-Moriano et al. 2012). However, when the density of retrograde labelling in these structures was compared between superficial and deep injections, no important differences were observed. Moreover, we studied the route of the centrifugal fibres to the olfactory

bulbs to discard their possible contamination. Based on the available literature, the centrifugal fibres arising from the BSTMP (Dong and Swanson, 2004), PMCo (Gutierrez-Castellanos et al. 2014), MeA (Pardo-Bellver et al. 2012), LOT (Santiago and Shammh-Lagnado, 2004) and caudal Pir (Luksin and Price, 1983) do not course throughout the *lo,* so it is unlikely that the retrograde labelling observed in these nuclei was due to the uptake of damaged fibres in this tract.

Our findings showed that the CxA and ACo received substantial projections arising from the olfactory cortex. Previous studies have also shown that the olfactory cortex sends more projections to the ACo than to the CxA in agreement with our results (with the CxA been described as the medioventral aspect of the Pir; Luksin and Price, 1983; McDonald 1998; Behan and Haberly, 1999).

An interesting finding of the present study was the differential location shown by the retrograde labelling in the layer II of the rostral Pir in the ACo and CxA injections. Following ACo injections, the retrogradely labelled somata were mainly located in the layer IIb, while after the CxA injections the retrograde labelling was mainly located in the layer IIa. The layer IIb presents pyramidal neurons with one apical dendrite and a well developed basal dendrite, and send caudally directed projections (Haberly and Price, 1978) that, according to the present results, innervate also the ACo. Regarding to the layer IIa, it is mainly composed by neurons with three or less apical dendrites and a short (or inexistent) basal dendrite (Haberly and Price, 1978). Since the apical dendrites of these neurons are located in layer I, their input is probably dominated by the axons originated by the MOB. This is consistent with the view of the CxA as an area devoted to the processing of olfactory information.

Additionally, the ACo received more projections from the caudal than from the rostral Pir, a hodological feature also showed by the Me (Chapter 2). By contrast, the CxA received more projections from the rostral than from the caudal Pir. One of the important characteristics of the Pir connectivity is that it presents more connections with olfactory structured adjacent to the injections site than to distant ones (Haberly and Price, 1978). In agreement with this observation, the posterior Pir presents more bidirectional connections with the amygdala than the anterior Pir (Haberly 2001; Majak et al. 2004). In addition, electrophysiological data

revealed that, while the anterior Pir process sensory information of the odorants, the posterior Pir shows associative encoding characteristics (Calu et al. 2007). Thus, the posterior Pir may act as an associative cortex that sends to the ACo highly processed olfactory information that includes the behavioural significance of the odorant, while the anterior Pir send information related to the features of the odorant to the CxA.

Projection from the amygdaloid complex and BST

The amygdaloid complex displayed a strong set of intrinsic connections between its chemosensory nuclei. This suggests that this circuitry includes well developed feed forward and feedback connections allowing it to perform complex integrative processing of the vomeronasal and olfactory information. Regarding to this, our results showed that the ACo shares this highly interconnected feature, while the CxA showed minor interconnections within the amygdala.

The ACo receives its strongest projections from the chemosensory amygdala. Our results showed that it receives important projections from the olfactory amygdaloid nuclei, such as the PLCo, CxA and LOT. On the available literature, the efferent projections of the LOT (Santiago and Shammah-Lagnado, 2004) and PLCo (Majak and Pitkanen, 2003, named PAC by these authors) have been reported with restricted injections of anterograde tracers. These authors described light projections arising from the LOT and parts of the PLCo to the ACo. The differences between the reported densities of these projections in our study and the previous ones, may be due to the small size of the injections of anterograde tracers, although further studies are needed to corroborate these differences.

The CxA received minor projections arising from the olfactory amygdala, with the ACo sending moderate projections and the PLCo and LOT scarce projections. In agreement with our findings, Santiago and Shammah-Lagnado (2004), illustrated fibres in the CxA (described in the text as the anteromedial Pir) following their injections in LOT.

Regarding to the vomeronasal amygdala, the ACo received important projections arising from the PMCo and BAOT and moderate projections from the Me and AA. In contrast, the CxA received light projections from the PMCO, Me and AA, and

moderate from the BAOT. Similar results were obtained with anterograde injections in the PMCo (Canteras et al. 1992; Gutiérrez-Castellanos et al. 2014) and Me (Canteras et al. 1995; Pardo-Bellver et al. 2012), with minor differences regarding to the density of the anterograde labelling observed in ACo and CxA.

Noteworthy, the PMCo showed a heterogeneous projection to the ACo throughout its antero-caudal extension, with its intermediate part displaying the densest projections. This heterogeneous projection was also observed in the different subdivisions of the Me (Chapter 2). However, previous studies (Kemppainen et al. 2002; Gutiérrez-Castellanos et al. 2014) did not describe differential projections arising from different antero-posterior levels of the PMCo to the rest of the amygdala. It seems that retrograde tracers are better tools to highlight possible heterogenic projections originated by different regions of a nucleus. This heterogeneity in the connections of the PMCo with some amygdaloid nuclei suggests that this nucleus possesses antero-caudal and medio-lateral subdivisions that may send differential information about pheromones to the corticomedial nuclei. Further studies are needed to test this hypothesis.

In summary, the CxA shows light afferences from most of the olfactory and vomeronasal structures, while in turn, the ACo is importantly innervated by both (the olfactory and vomeronasal nuclei). Therefore, although ACo receives a predominant olfactory input from the MOB, its afferences from the secondary centres within the chemosensory amygdala allow further integration of olfactory and vomeronasal information. In this regard, the ACo reminds the connectivity of the medial amygdala.

Regarding the deep amygdaloid nuclei, CxA did not receive projections from these structures. In contrast, the ACo received moderate projections from the basomedial complex and minor projections arising from the basolateral, lateral and central amygdaloid nuclei, as well as from the AHi (Table 3). These results are consistent with previous findings (for the AHi, Kemppainen et al. 2002; for the La, Pitkanen et al. 1995, for the BLA and BLP, Savander et al. 1995). With regard to the basomedial complex, consistent with our results Petrovich et al. (1996) described a dense projection from the anterior BM to ACo, while the posterior BM originated

only a sparse input. Savander et al (1996) found similar results (see their figures 3 and 5), although they described the BM projections to the ACo as light in general.

In summary, the rostral CxA does not receive projections from the associative nuclei of the amygdala (lateral, basolateral, basomedial), suggesting that it is not influenced by the emotional information processed in these structures (Ledoux, 2000). In contrast, the ACo receives moderate projections from the basomedial nucleus, and therefore is probably involved in the processing of emotional information.

Concerning to the BTS complex, it did not project to the CxA, whereas the ACo received projections mainly arising from the BSTMPI and the BSTIA and minor projections from the rest of the nuclei of the complex. These findings are in agreement with previous studies reported in rats (Dong and Swanson, 2004; 2006a; 2006b). This pattern of projections reinforces the view that the CxA is mainly related with the process of olfactory information, whereas the ACo receives projections from the network of sexually dimorphic, steroid-sensitive structures (Me, posterior BST) involved in the control of sociosexual behaviours (Newman, 1999).

Projections from the cortex and hippocampal formation

Our results showed that cortical structures (leaving apart the olfactory cortex), send minor projections to the ACo, with the exception of some prefrontal regions and the AI. In contrast, cortical structures did not project to the CxA. Within the hippocampal formation, the LEnt gave rise to moderate projections to both the CxA and ACo (Table 3).

The dense projections arising from the agranular insular cortex to the ACo have been previously described in rats with anterograde (McDonald et al. 1996; Shi and Cassell, 1998) and retrograde tracers (Ottersen 1982). Our studies showed that this description also applies to mice, and showed that the AIV gave rise to a dense projection to the ACo, while the AID and AIP send minor projections (Table 3).

The AI appears to be a multimodal sensory convergence zone. It receives convergent projections from the gustatory and viscerosensory areas of the

dysgranular and granular insular cortex and the olfactory Pir (Shi and Cassell, 1998). In addition, it is connected with the gustatory thalamic nucleus. It has been suggested that the AI is a multimodal cortical area serving mucosal senses (Krushel and Van der Kooy, 1988). Therefore, the projections arising from the AIV and the AIP may be modulating olfactory information processing in the ACo, putting the odour in a gustatory and viscerosensory context. In addition, the input from the parabrachial nucleus to the ACo (see below) may contribute to the modulation by gustatory/viscerosensory information.

Besides the afferent projections from the AI, the ACo receives minor projections arising from the prefrontal cortex (the IL, DP and PrL). These afferents were previously reported by anterograde studies in rats (Hurley et al. 1991; Takagishi & Chiba, 1991; McDonald et al. 1996; Shi and Cassell, 1998). More caudally, the PRh and Ect also showed light projections to ACo, which in the case of the PRh were previously reported (McDonald 1998).

Regarding to the hippocampal formation, previous works have reported that the LEnt send projections to the ACo (Luskin and Price, 1983; McDonald and Mascagni, 1997). Our results confirm and extend this finding showing that the LEnt sent more projections to the ACo than to the CxA. The LEnt has been considered part of the olfactory cortex (Luksin and Price, 1983), since it receives direct projections from the MOB. The afferent to the ACo is probably part of the connectivity with other structures of the olfactory system. The LEnt has recently been shown to modulate the activity in the Pir and, from a functional point of view, to be involved in fine odour discrimination (Chapuis et al. 2013). The projection to the ACo may be similarly involved in modulating the activity in the olfactory amygdala and probably affecting the currently unknown behavioural responses depending on this structure.

The ventral part of the hippocampus (CA1, CA3 and subiculum) also sends light projections to the ACo. The same area of the ventral hippocampus has been shown to project to the Me (see Chapter 2) and to the PMCo (Gutiérrez-Castellanos et al. 2014). Therefore, on anatomical grounds the ventral hippocampus is well positioned to influence neural processing in the chemosensory amygdala. However, the functional meaning of this influence is currently unknown. Since the

hippocampus process spatial/contextual information (Maren and Fanselow, 1995), these projections may be providing the amygdala with contextual information about the chemical stimuli.

Projections from the Septum and Striatum

The results presented in this work, together with hodological data available in the literature, indicate that the basal forebrain gives rise to a common input to the corticomedial amygdaloid nuclei. Previous works have reported basal forebrain afferences to the Me (see Chapter 2), the LOT (Grove, 1988) and the PMCo (Gutiérrez-Castellanos et al. 2014) similar to those directed to the CxA and ACo described in this work. The projections arising from the diagonal band and SI were previously reported with non-restricted retrograde injections located in the ACo (Ottersen, 1980).

The basal forebrain is composed by cholinergic, GABAergic and peptide-containing neurons (Semba, 2000). It is widely accepted that the AChasa-positive nuclei of the amygdala present this reactivity because of its afferent connections from cholinergic neurons arising from the basal forebrain, which are mainly located in the MS, VDB, HDB, VP, MCPO and SI (Semba, 2000). In this regard, it is noteworthy that, although ACo and CxA received similar amount of projections from the basal forebrain, only CxA showed a positive reaction to the AChasa, while the ACo displayed a negative reactivity. Taking into account the similar projection pattern observed from the basal forebrain to both nuclei and their differences in the AChasa reactivity, it is likely that the CxA and ACo receive a differential input from cholinergic and non-cholinergic subpopulations of neurons located in the basal forebrain.

On the one hand, it is probable that the CxA receives an important amount of projection from cholinergic neurons, since it presented a moderate reactivity to the AChasa histochemistry. The studies related to the possible role of the cholinergic system of the basal forebrain have been mainly focused on the basolateral amygdala (within the amygdaloid complex) and on the Pir within the paleocortical structures. The basaloteral nucleus and the Pir receive their cholinergic innervations from MS, VDB, HDB, VP, MCPO and SI (Kimura et al. 1982;

Woolf et al. 1984; Heckers et al. 1994). Woolf et al. (1984) suggested that the cholinergic system is mainly implicated in modulating the responses of other inputs. The cholinergic afferents received by the basolateral amygdala in rats, are involved in modulating learning and memory processes related to emotional paradigms (Vezdarjanova and McGaugh, 1999; McIntyre et al. 1998) and the reduction of anxiety (Pidoplichko et al. 2013). In the case of the Pir, the cholinergic input modulates odour discrimination learning by means of its synapses with intra-cortical association fibres (Cahpuis and Wilson, 2013). In the light of these results, and taking into account that the CxA seems to be more connected with olfactory structures than with the amygdaloid complex, the cholinergic inputs may be modulating, such as in the Pir, the discrimination of olfactory stimuli in this nucleus.

On the other hand, ACo received projections from the basal forebrain but displayed a negative AChasa reactivity. Similar to the ACo, the Me (Chapter 2) and PMCo (Gutiérrez-Castellanos et al. 2014) also received projections from the basal forebrain, but presented a negative reaction to the AChasa. This suggests that, in addition to the possible minor cholinergic projections arising from the basal forebrain to these nuclei (ACo, Me and PMCo), non-cholinergic neurons, such as GABAergic or peptide-containing neurons, might be the major origin of these projections. It has been showed that GABAergic neurons project from the basal forebrain to the BLA (McDonald et al. 2011). These authors suggested that these neurons provide an indirect disinhibition, as well as a direct inhibition, of the pyramidal neurons in the basolateral amygdala. To our knowledge, no further studies have been reported on the possible functions of the non-cholinergic projections to the amygdala. Future studies are needed to highlight the possible modulatory role of these forebrain inputs to the corticomedial amygdala.

Projections from the thalamus

Our results showed that the thalamus did not send afferent connections to the CxA, while in contrast, the ACo received scarce projections arising from the paraventricular thalamus and Re and moderate-dense projections from the posterior intralaminar complex of the thalamus.

The projections arising from the paraventricular thalamus and Re were previously described in several works using anterograde tracers in rats (Moga et al. 1995; Turner and Herkenham, 1991; Vertes et al. 2006). Within the paraventricular thalamus, its posterior part sent the strongest projections to the ACo. The posterior paraventricular thalamic nucleus has recently been shown to be involved in the expression of learned fear in an auditory fear conditioning paradigm (Li et al. 2014). It may be possible that the projection to the ACo play a role in the expression of fear to olfactory stimuli, although experimental evidence is needed to support this possibility. The paraventricular thalamus receives dense projections arising from the locus coeruleus and dorsal and median raphe (areas that also project, in a light manner, to the ACo, see table 3) (Jones and Yang, 1985; Vertes and Martin, 1988), and therefore these modulatory systems would also influence the ACo activity via the thalamic projection.

Regarding to the posterior intralaminar complex of the thalamus, the SPF, SPFPC and PIL showed important projections to the ACo, while the MGM, PP and SG sent minor projections. The projections arising from the MGM and PIL to the ACo have been previously reported (Turner and Herkenham, 1991; LeDoux et al. 1985). These structures (MGM and PIL) receive both auditory and somatosensory inputs (LeDoux et al. 1987), and contain both tone-responding and somatosensory-responding neurons (Bordi and LeDoux, 1994). Moreover, electrical stimulation of the PIL/MGM area functions as an effective unconditioned stimulus inducing fear learning (Cruikshank et al. 1992). Therefore, although it is unknown whether the ACo plays a role in olfactory fear conditioning, it receives olfactory information from the olfactory bulb (as well as from the Pir) and somatosensory information from the posterior intralaminar thalamus, making it a good candidate to be involved in this kind of learning.

In addition to somatosensory information related to the footshock, genital somatosensory information has been proposed to reach the SPFPC (the medial aspect of the posterior intralaminar thalamus), and c-Fos studies have shown that this nucleus is activated in male hamsters when mating to ejaculation (Coolen et al. 1997). Therefore, the thalamic projection to ACo may relay both aversive and appetitive aspects of somatosensory information.

Projections from the hypothalamus

The hypothalamus is considered an essential interface between the endocrine, autonomic and somatomotor systems (Simerly, 2014). Within the variety of behaviours in which the hypothalamus is involved, it regulates aggressive-defensive responses and the expression of appropriate sexual and maternal behaviours (Simerly, 2014). In rodents, the expression of these behaviours depends to a great extent on the chemosensory systems (Brennan and Zufall, 2006) In this regard, it is surprising that the hypothalamus send moderate or minor projections to corticomedial amygdaloid nuclei, since these areas received olfactory and vomeronasal information necessary to the expression of socio-sexual behaviours.

The hypothalamus did no project to the CxA and only sent minor projections to the ACo, with the exception of the PH, which sent moderate projections (Table 3). Similarly, the hypothalamus lacks also important projections to the medial amygdaloid nucleus (see Chaper 2) and the PMCo (Gutiérrez-Castellanos et al. 2014). In addition, within the hypothalamus, only the VMH and PMV received important projections from the medial amygdaloid nucleus (Pardo-Bellver et al. 2012). Taking together, these results indicate that the hypothalamic nuclei regulating sociosexual behaviours do not exert an important direct modulation of the main area of vomeronasal-olfactory processing, namely the corticomedial amygdala.

Projections from the brainstem and midbrain

The brainstem and midbrain also showed minor projections to the CxA and ACo, with the VTA being the main afferent to the CxA and the PB to the ACo.

The VTA contains the cells of origin of the dopaminergic mesotelencephalic pathway, which also innervates several amygdaloid nuclei (Asan, 1998). In particular, the CxA shows a prominent dopaminergic innervation (Martínez-García et al., 2012). Given the paucity of afferent projections from other dopaminergic nuclei (from the thalamus, hypothalamus or brainstem), we consider most likely that the VTA input to the CxA is originated by dopaminergic cells. This raises the question of the possible role played by this dopaminergic input to the CxA. Since

dopamine in the mesolimbic pathway has been implicated in signalling the incentive salience of reward-related stimuli (Berridge and Robinson 1998), it is tempting to suggest that the dopaminergic input to the VTA may be implicated in processing the incentive salience of olfactory stimuli.

Fibres arising from the PB to the ACo have been previously reported in rat (Bernard et al. 1993). The medial part of the PB is considered to be a gustatory relay centre, implicated in processing taste information and in the learning of taste aversion, while its lateral part is implicated in cardiovascular, respiratory and nociceptive processes (Bernard et al. 1993). The PB also projects to the Me (see Chapter 2) and to the central and basolaterateral complex (Bernard et al. 1993). The PB has been shown to integrate taste and visceral sensory information in the context of taste aversion learning (Yamamoto et al. 1994). Therefore, the projection arising from the PB may send to the ACo multimodal unpleasant information related to incoming olfactory information.

Possible functional roles of the CxA and ACo

The CxA shares its majority afferent connections with the rostral Pir (see "Control injection" in the Results), with the both of them being more connected with adjacent olfactory structures and basal forebrain and to a minor extent with the amygdala. As revealed by our control injections, the rostral Pir received almost no afferents from the cortex, the hypothalamus and thalamus, similar to the CxA. This is in contrast with the more extensive connectivity of the caudal Pir with these areas and with the amygdaloid complex (Majak et al. 2004). The similar connectivity between the CxA and rostral Pir, suggest that the CxA acts like the rostral Pir, as an olfactory cortex processing the sensory information of the odorants with minor influences of the olfactory and vomeronasal amygdala.

Regarding to the ACo, the set of afferent projections described is relatively similar to that of the Me (Chapter 2). In fact, the thalamic projections to both structures are very similar, with those originated by the posterior intralaminar thalamic nuclei being almost indistinguishable. These thalamic input, together with the afferents arising from the brainstem, suggest that taste, viscerosensory, somatosensory and nociceptive information can reach the ACo, and consequently it

may be involved in a broad number of behaviours. In fact, c-Fos studies have shown activation of the ACo in both aversive and appetitive motivated tasks (Knapska et al. 2007). Since its main afference is the olfactory input from the MOB, it is clearly mainly involved in processing olfactory information, and only in a secondary way its activity would be modulated by vomeronasal information. The small influence of the vomeronasal system may be interpreted as indicative of a minor involvement of the ACo in sexual behaviour, although olfactory cues are also relevant in sexual behaviour (Baum and Cherry 2014). Thus, it seems that the ACo may play a role in most emotional behaviours as long as there is relevant olfactory information involved.

3.3.4 Reference

Asan E (1998) The catecholaminergic innervation of the rat amygdala. Adv Anat Embryol Cell Biol 142:1-118.

Baum MJ, Cherry JA (2014, in press) Processing by the main olfactory system of chemosignals that facilitate mammalian reproduction. Horm Behav doi: 10.1016/j.yhbeh.2014.06.003.

Behan M, Haberly LB (1999) Intrinsic and efferent connections of the endopiriform nucleus in rat. J Comp Neurol 408:532-548.

Bernard JF, Alden M, Besson JM (1993) The organization of the efferent projections from the pontine parabrachial area to the amygdaloid complex: a Phaseolus vulgaris leucoagglutinin (PHA-L) study in the rat. J Comp Neurol 329:201-229.

Berridge KC, Robinson TE (1998) What is the role of dopamine in reward: hedonic impact, reward learning, or incentive salience? Brain Res Brain Res Rev 28:309-369.

Bordi F, Ledoux JE (1994) Response properties of single units in areas of rat auditory thalamus that project to the amygdala. II. Cells receiving convergent auditory and somatosensory inputs and cells antidromically activated by amygdala stimulation. Exp Brain Res 98:275-286.

Brennan PA, Zufall F (2006) Pheromonal communication in vertebrates. Nature 444:308-315.

Brock O, Keller M, Douhard Q, Bakker J (2012) Female mice deficient in alpha-fetoprotein show female-typical neural responses to conspecific-derived pheromones. PLoS One 7:e39204.

Cadiz-Moretti B, Martinez-Garcia F., Lanuza E (2013) Neural Substrate to Associate Odorants and Pheromones: Convergence of Projections from the Main and Accessory Olfactory Bulbs in Mice. In: East ML, Dehnhard M (eds) Chemical Signals in Vertebrates 12. Springer Science: New York. pp 3-16.

Calu DJ, Roesch MR, Stalnaker TA, Schoenbaum G (2007) Associative encoding in posterior piriform cortex during odor discrimination and reversal learning Cereb Cortex 17:1342-1349.

Canteras NS, Simerly RB, Swanson LW (1995) Organization of projections from the medial nucleus of the amygdala: a PHAL study in the rat. J Comp Neurol 360:213-245.

Canteras NS, Simerly RB, Swanson LW (1994) Organization of projections from the ventromedial nucleus of the hypothalamus: a Phaseolus vulgaris-leucoagglutinin study in the rat. J Comp Neurol 348:41-79.

Canteras NS, Simerly RB, Swanson LW (1992) Connections of the posterior nucleus of the amygdala. J Comp Neurol 324:143-179.

Chapuis J, Wilson DA (2013) Cholinergic modulation of olfactory pattern separation. Neurosci Lett 545:50-53.

Chapuis J, Cohen Y, He X, Zhang Z, Jin S, Xu F, Wilson DA (2013) Lateral entorhinal modulation of piriform cortical activity and fine odor discrimination. J Neurosci 33:13449-13459.

Coolen LM, Peters HJ, Veening JG (1997) Distribution of Fos immunoreactivity following mating versus anogenital investigation in the male rat brain. Neuroscience 77:1151-1161.

Cousens G, Otto T. 1998. Both pre- and posttraining excitotoxic lesions of the basolateral amygdala abolish the expression of olfactory and contextual fear conditioning. Behav Neurosci 112:1092-1103.

Cruikshank SJ, Edeline JM, Weinberger NM (1992) Stimulation at a site of auditory-somatosensory convergence in the medial geniculate nucleus is an effective unconditioned stimulus for fear conditioning. Behav Neurosci 106:471-483.

Dielenberg RA, Hunt GE, McGregor IS (2001) "When a rat smells a cat": the distribution of Fos immunoreactivity in rat brain following exposure to a predatory odor. Neuroscience 104:1085-1097.

Dong HW, Swanson LW (2006a) Projections from bed nuclei of the stria terminalis, dorsomedial nucleus: implications for cerebral hemisphere integration of neuroendocrine, autonomic, and drinking responses. J Comp Neurol 494:75-107.

Dong HW, Swanson LW (2006b) Projections from bed nuclei of the stria terminalis, anteromedial area: cerebral hemisphere integration of neuroendocrine, autonomic, and behavioral aspects of energy balance. J Comp Neurol 494:142-178.

Dong HW, Swanson LW (2004) Projections from bed nuclei of the stria terminalis, posterior division: implications for cerebral hemisphere regulation of defensive and reproductive behaviors. J Comp Neurol 471:396-433.

Grove EA (1988) Efferent connections of the substantia innominata in the rat. J Comp Neurol 277:347-364.

Gutierrez-Castellanos N, Pardo-Bellver C, Martinez-Garcia F, Lanuza E (2014) The vomeronasal cortex - afferent and efferent projections of the posteromedial cortical nucleus of the amygdala in mice. Eur J Neurosci 39:141-158.

Haberly LB (2001) Parallel-distributed processing in olfactory cortex: new insights from morphological and physiological analysis of neuronal circuitry. Chem Senses 26:551-576.

Haberly LB, Price JL (1978) Association and commissural fiber systems of the olfactory cortex of the rat. J Comp Neurol 178:711-740.

Heckers S, Ohtake T, Wiley RG, Lappi DA, Geula C, Mesulam MM (1994) Complete and selective cholinergic denervation of rat neocortex and hippocampus but not amygdala by an immunotoxin against the p75 NGF receptor. J Neurosci 14:1271-1289.

Hurley KM, Herbert H, Moga MM, Saper CB (1991) Efferent projections of the infralimbic cortex of the rat. J Comp Neurol 308:249-276.

Jones BE, Yang TH (1985) The efferent projections from the reticular formation and the locus coeruleus studied by anterograde and retrograde axonal transport in the rat. J Comp Neurol 242:56-92.

Kang N, Baum MJ, Cherry JA (2009) A direct main olfactory bulb projection to the 'vomeronasal' amygdala in female mice selectively responds to volatile pheromones from males. Eur J Neurosci 29:624-634.

Kemppainen S, Jolkkonen E, Pitkanen A (2002) Projections from the posterior cortical nucleus of the amygdala to the hippocampal formation and parahippocampal region in rat. Hippocampus 12:735-755.

Knapska E, Radwanska K, Werka T, Kaczmarek L (2007) Functional internal complexity of amygdala: focus on gene activity mapping after behavioral training and drugs of abuse. Physiol Rev 87:1113-1173.

Krieger J, Schmitt A, Lobel D, Gudermann T, Schultz G, Breer H, Boekhoff I (1999) Selective activation of G protein subtypes in the vomeronasal organ upon stimulation with urine-derived compounds. J Biol Chem 274:4655-4662.

Krushel LA, van der Kooy D (1988) Visceral cortex: integration of the mucosal senses with limbic information in the rat agranular insular cortex. J Comp Neurol 270:39-54, 62-3.

Ledoux JE (2000) Emotion circuits in the brain. Annu Rev Neurosci 23:155-184.

Ledoux JE, Ruggiero DA, Reis DJ (1985) Projections to the subcortical forebrain from anatomically defined regions of the medial geniculate body in the rat. J Comp Neurol 242:182-213.

Ledoux JE, Ruggiero DA, Forest R, Stornetta R, Reis DJ (1987) Topographic organization of convergent projections to the thalamus from the inferior colliculus and spinal cord in the rat. J Comp Neurol 264:123-146.

Lehman MN, Winans SS, Powers JB (1980) Medial nucleus of the amygdala mediates chemosensory control of male hamster sexual behavior. Science 210:557-560.

Leinders-Zufall T, Lane AP, Puche AC, Ma W, Novotny MV, Shipley MT, Zufall F (2000) Ultrasensitive pheromone detection by mammalian vomeronasal neurons. Nature 405:792-796.

Li Y, Dong X, Li S, Kirouac GJ (2014) Lesions of the posterior paraventricular nucleus of the thalamus attenuate fear expression. Front Behav Neurosci 8:94.

Luskin MB, Price JL (1983) The topographic organization of associational fibers of the olfactory system in the rat, including centrifugal fibers to the olfactory bulb. J Comp Neurol 216:264-291.

Majak K, Pitkanen A (2003) Projections from the periamygdaloid cortex to the amygdaloid complex, the hippocampal formation, and the parahippocampal region: a PHA-L study in the rat. Hippocampus 13:922-942.

Majak K, Ronkko S, Kemppainen S, Pitkanen A (2004) Projections from the amygdaloid complex to the piriform cortex: A PHA-L study in the rat. J Comp Neurol 476:414-428.

Majkutewicz I, Cecot T, Jerzemowska G, Myslinska D, Plucinska K, Trojniar W, Wrona D (2010) Lesion of the ventral tegmental area amplifies stimulation-induced Fos expression in the rat brain. Brain Res 1320:95-105.

Maren S, Fanselow MS (1995) Synaptic plasticity in the basolateral amygdala induced by hippocampal formation stimulation in vivo J Neurosci 15:7548-7564.

Martel KL, Baum MJ (2009) A centrifugal pathway to the mouse accessory olfactory bulb from the medial amygdala conveys gender-specific volatile pheromonal signals. Eur J Neurosci 29:368-376.

Martínez-García F, Novejarque A, Gutiérrez-Castellanos N, Lanuza E (2012) Piriform cortex and amígdala. In: Watson C, Paxinos G, Puelles L (eds) The Mouse Nervous System. Academic Press, San Diego, pp 140-172.

Martinez-Garcia F, Martinez-Ricos J, Agustin-Pavon C, Martinez-Hernandez J, Novejarque A, Lanuza E (2009) Refining the dual olfactory hypothesis: pheromone reward and odour experience. Behav Brain Res 200:277-286.

Martinez-Ricos J, Agustin-Pavon C, Lanuza E, Martinez-Garcia F (2008) Role of the vomeronasal system in intersexual attraction in female mice. Neuroscience 153:383-395.

McDonald AJ (1998) Cortical pathways to the mammalian amygdala. Prog Neurobiol 55:257-332.

McDonald AJ, Mascagni F (1997) Projections of the lateral entorhinal cortex to the amygdala: a Phaseolus vulgaris leucoagglutinin study in the rat. Neuroscience 77:445-459.

McDonald AJ, Muller JF, Mascagni F (2011) Postsynaptic targets of GABAergic basal forebrain projections to the basolateral amygdala. Neuroscience 183:144-159.

McDonald AJ, Mascagni F, Guo L (1996) Projections of the medial and lateral prefrontal cortices to the amygdala: a Phaseolus vulgaris leucoagglutinin study in the rat. Neuroscience 71:55-75.

McIntyre CK, Ragozzino ME, Gold PE (1998) Intra-amygdala infusions of scopolamine impair performance on a conditioned place preference task but not a spatial radial maze task. Behav Brain Res 95:219-226.

Miyamichi K, Amat F, Moussavi F, Wang C, Wickersham I, Wall NR, Taniguchi H, Tasic B, Huang ZJ, He Z, Callaway EM, Horowitz MA, Luo L (2011) Cortical representations of olfactory input by trans-synaptic tracing. Nature 472:191-196.

Moga MM, Weis RP, Moore RY (1995) Efferent projection of the paraventricular thalamic nucleus in the rat. J Comp Neurol 359:221-238.

Mohedano-Moriano A, Pro-Sistiaga P, Ubeda-Banon I, Crespo C, Insausti R, Martinez-Marcos A (2007) Segregated pathways to the vomeronasal amygdala: differential projections from the anterior and posterior divisions of the accessory olfactory bulb. Eur J Neurosci 25:2065-2080.

Mohedano-Moriano A, de la Rosa-Prieto C, Saiz-Sanchez D, Ubeda-Banon I, Pro-Sistiaga P, de Moya-Pinilla M, Martinez-Marcos A (2012) Centrifugal telencephalic afferent connections to the main and accessory olfactory bulbs. Front Neuroanat 6:19.

Moncho-Bogani J, Martinez-Garcia F, Novejarque A, Lanuza E (2005) Attraction to sexual pheromones and associated odorants in female mice involves activation of the reward system and basolateral amygdala. Eur J Neurosci 21:2186-2198.

Nagai T, Kimura H, Maeda T, McGeer PL, Peng F, McGeer EG (1982) Cholinergic projections from the basal forebrain of rat to the amygdala. J Neurosci 2:513-520.

Newman SW (1999) The medial extended amygdala in male reproductive behavior. A node in the mammalian social behavior network. Ann N Y Acad Sci 877:242-257.

Ottersen OP (1982) Connections of the amygdala of the rat. IV. Corticoamygdaloid and intraamygdaloid connections as studied with axonal transport of horseradish peroxidase. J Comp Neurol 205:30-48.

Ottersen OP (1980) Afferent connections of the amygdaloid complex of the rat and cat. II. Afferents from the hypothalamus and the basal telencephalon. J Comp Neurol 194:267-289.

Ottersen OP, Ben-Ari Y (1979) Afferent connections of the amygdaloid complex of the rat and cat. I. Projections from the thalamus. J Comp Neurol 187:401-424.

Pardo-Bellver C, Cadiz-Moretti B, Novejarque A, Martinez-Garcia F, Lanuza E (2012) Differential efferent projections of the anterior, posteroventral, and posterodorsal subdivisions of the medial amygdala in mice. Front Neuroanat 6:33.

Paxinos G, Franklin K B J (2001) The Mouse Brain in Stereotaxic Coordinates. Academic Press, San Diego.

Petrovich GD, Risold PY, Swanson LW (1996) Organization of projections from the basomedial nucleus of the amygdala: A PHAL study in the rat. J Comp Neurol 374:387-420.

Pidoplichko VI, Prager EM, Aroniadou-Anderjaska V, Braga MF (2013) alpha7-Containing nicotinic acetylcholine receptors on interneurons of the basolateral amygdala and their role in the regulation of the network excitability. J Neurophysiol 110:2358-2369.

Pitkanen A, Stefanacci L, Farb CR, Go GG, Ledoux JE, Amaral DG (1995) Intrinsic connections of the rat amygdaloid complex: projections originating in the lateral nucleus. J Comp Neurol 356:288-310.

Pro-Sistiaga P, Mohedano-Moriano A, Ubeda-Banon I, Del Mar Arroyo-Jimenez M, Marcos P, Artacho-Perula E, Crespo C, Insausti R, Martinez-Marcos A (2007) Convergence of olfactory and vomeronasal projections in the rat basal telencephalon. J Comp Neurol 504:346-362.

Santiago AC, Shammah-Lagnado SJ (2004) Efferent connections of the nucleus of the lateral olfactory tract in the rat. J Comp Neurol 471:314-332.

Saper CB, Loewy AD (1980) Efferent connections of the parabrachial nucleus in the rat. Brain Res 197:291-317.

Savander V, Go G-, Ledoux JE, Pitkanen A (1996) Intrinsec connections of the rat amygdaloid complex: Projections originating in the accessory basal nucleus. J Comp Neurol 374:291-313.

Savander V, Go CG, Ledoux JE, Pitkanen A (1995) Intrinsic connections of the rat amygdaloid complex: projections originating in the basal nucleus. J Comp Neurol 361:345-368.

Scalia F, Winans SS (1975) The differential projections of the olfactory bulb and accessory olfactory bulb in mammals. J Comp Neurol 161:31-55.

Semba K (2000) Multiple output pathways of the basal forebrain: organization, chemical heterogeneity, and roles in vigilance. Behav Brain Res 115:117-141.

Shammah-Lagnado SJ, Santiago AC (1999) Projections of the amygdalopiriform transition area (APir). A PHA-L study in the rat. Ann N Y Acad Sci 877:655-660.

Shi CJ, Cassell MD (1998) Cortical, thalamic, and amygdaloid connections of the anterior and posterior insular cortices. J Comp Neurol 399:440-468.

Simerly RB (2014) Organization of the hypothalamus. In: Paxinos G (ed) The Rat Nervous System (4th edn). Academic Press, Amsterdam, pp 267-294.

Shipley MT, Adamek GD (1984) The connections of the mouse olfactory bulb: a study using orthograde and retrograde transport of wheat germ agglutinin conjugated to horseradish peroxidase. Brain Res Bull 12:669-688.

Takagishi M, Chiba T (1991) Efferent projections of the infralimbic (area 25) region of the medial prefrontal cortex in the rat: an anterograde tracer PHA-L study. Brain Res 566:26-39.

Turner BH, Herkenham M (1991) Thalamoamygdaloid projections in the rat: a test of the amygdala's role in sensory processing. J Comp Neurol 313:295-325.

Vazdarjanova A, McGaugh JL (1999) Basolateral amygdala is involved in modulating consolidation of memory for classical fear conditioning. J Neurosci 19:6615-6622.

Vertes RP, Hoover WB (2008) Projections of the paraventricular and paratenial nuclei of the dorsal midline thalamus in the rat. J Comp Neurol 508:212-237.

Vertes RP, Martin GF (1988) Autoradiographic analysis of ascending projections from the pontine and mesencephalic reticular formation and the median raphe nucleus in the rat. J Comp Neurol 275:511-541.

Vertes RP, Hoover WB, Do Valle AC, Sherman A, Rodriguez JJ (2006) Efferent projections of reuniens and rhomboid nuclei of the thalamus in the rat. J Comp Neurol 499:768-796.

Woolf NJ, Eckenstein F, Butcher LL (1984) Cholinergic systems in the rat brain: I. Projections to the limbic telencephalon. Brain Res Bull 13:751-784.

Yamamoto T, Shimura T, Sako N, Yasoshima Y, Sakai N (1994) Neural substrates for conditioned taste aversion in the rat. Behav Brain Res 65:123-137.

4. GENERAL DISCUSSION

4. General Disscussion

The projections from the MOB to the corticomedial nuclei of the amygdala lack a topographic organization. This raises the question about the nature of the olfactory inputs received by these amygdaloid nuclei. One option is that specific populations of mitral cells distributed along the mitral cell layer of the MOB, deliver specific types of semiochemical information to the amygdaloid complex. The projections from the mitral cells to the Pir, in contrast, send a broad range of general odour information from inputs originated throughout the entire mitral cell layer. For example, mitral cells that are innervated by olfactory sensory cells expressing the particular receptor OR37C, project specifically to the MePD (Bader et al. 2012). These sensory cells, respond to the presence of long-chain fatty aldehydes (Bautze et al. 2012), some of which are present in anal gland secretions (Bautze et al. 2014). Other (non-exclusive) possibility is that the same mitral cells that projects to the Pir also projects to the amygdaloid complex, delivering to both general information about an odour. Kang et al. (2011) showed that mitral axons from the MOB send collaterals to the anterior and posterior Pir, ACo, MeA and PLCo. This suggests that the same odour information is transmitted to the Pir and to these nuclei of the amygdaloid complex. Therefore, from the anatomical point of view, it is likely that the corticomedial amygdaloid nuclei play a role associating a broad range of odours with a particular emotional experience.

The MeA receives the highest degree of convergent projections arising from the main (MOB) and accessory (AOB) olfactory bulbs (Pro-Sistaga et al. 2007; Cadiz-Moretti et al. 2013). The ACo and CxA present minor convergent projections with the strongest projection arising from the main olfactory bulb. In contrast, the PMCo do not show convergent projections from the MOB and AOB and receive important projections from the latter one. Therefore, the neuroanatomical connections suggest that the MeA may be a key structure in the association of vomeronasal and olfactory information, although functional data obtained in different behavioural experiments and species are not fully consistent. Lesion studies in female mice have shown that the posterior part of the Me is more relevant for the attraction towards male volatiles (DiBenedictis et al. 2012). In contrast, in male hamsters both lesions of the anterior and posterior Me reduced the preference for male-derived odours (Maras and Petrulis, 2006). It should be taken into

account that in these studies the response of the experimental animals requires no learning. In this regard, previous results presented by Moncho-Bogani et al. (2005) on c-fos expression in the amygdala of female mice showed that the Me is activated with the exposure of male-soiled bedding (when learning takes place), but not when the olfactory-vomeronasal memory is expressed. In this case, only the anterior part of the basolateral amygdaloid nucleus (BLA) shows c-Fos expression, suggesting that the Me is involved in the learning phase but not in the expression of the acquired memory.

Regarding to the intraamygdaloid connections, the Me, ACo and PMCo (Gutierrez-Castellanos et al. 2014) are highly interconnected among them and with the rest of chemosensory amygdala, while the CxA shows less connections with the chemosensory amygdaloid nuclei. In addition, all these nuclei show poor connections with the deep amygdaloid nuclei. The only exception is the basomedial nucleus, which projects to the Me and ACo and in a minor extent to the PMCo (Gutierrez-Castellanos et al. 2014).

Regarding to the chemosensoy amygdala, the high interconnection among its nuclei suggests that the vomeronasal-olfactory information is integrated in a network-like manner within all these nuclei, with none of them being strictly involved in one particular aspect of sociosexual and reproductive behaviours. This may explain why corticomedial nuclei show an increase c-fos reactivity during the expression of a variety of sociosexual behaviours (Knapska et al. 2007), including maternal behaviours in rats (Fleming et al. 1994), exposure to chemicals cues derived from males in female mice (Moncho-Bogani et al. 2005) and following sexual experience (Pfaus et al. 1993).

With regard to the interconnections between the chemosensory and deep amygdaloid nuclei, the BMA present the strongest connections between these two systems, and may act as a link between the olfactory and vomeronasal information, on the one hand, and the emotional learning processes taking place in the BLA and lateral nucleus (La), on the other. Therefore, it is possible that the corticomedial nuclei and BLA/La play a complementary role in these associative processes. The circuitry of the amygdala may be acting similar to the other learning/memory circuits; the cortical nuclei may act as the hippocampus where instable memories are formed. Then these memories are transferred, through the BMA, to the BLA, where the stable memories are stored. In this analogy, the BMA would act as the entorhinal cortex, and the BLA would be analogous to the cortex. Further studies are needed to corroborate this hypothesis.

The amygdaloid and the BST complex seem to relay the chemosensory information to the hypothalamus, which is the main behavioural effector area (Swanson 2000). By contrast, the hypothalamus lacks an important direct feedback connection back to the amygdaloid complex, with the exception of some nuclei that project to the Me. This raises the question of whether the processing of chemical information in the amygdaloid complex is modulated by the hypothalamus. One possibility is that the information about the hypothalamic activity reaches the amygdala by means of indirect feedback projections. For example, the posterior part of the medial division of the BST (BSTMP) shows important efferent connections to the Me and ACo (Dong et al. 2004). This nucleus together with the Me and the hypothalamus are key structures related with sociosexual and defensive behaviours (Canteras 2002). Thus, it is possible that the BSTMP acts a relay centre, delivering information from the hypothalamus to the amygdala. The afferent connections of the BSTMP are unknown, so further studies are needed to corroborate this hypothesis. Other possibility is that the amygdaloid complex senses the hypothalamic activity by means of hormone receptors. The Me and ACo display high levels of receptors for steroid hormones, which may be activated by the sexual hormones influenced by the hypothalamic activity (Simerly et al. 1990). A third possibility is that the hypothalamus sends its feedback projections to the amygdala through the Me. Since this nucleus presents the highest amount of afferents arising from the hypothalamus compared to other amygdaloid nuclei, it may relay hypothalamic information to the rest of the amygdaloid complex. Further studies are needed to highlight the functional relation between the hypothalamus and the amygdala.

The Me and ACo receive important projections arising from the posterior paraventricular thalamus, posterior intralaminar thalamus and the parabrachial nucleus within the brainstem. On the other hand, other cortical nuclei such as the PMCo and CxA do not present afferent connections arising from these areas. The projections arising from the thalamus and brainstem to the Me and ACo may relay somatosensory information related to fear conditioning paradigms in the case of the paraventricular and posterior intralaminar thalamus (Cruikshank et al. 1992; Cousens et al. 2012; Rosen et al. 1998; Li et al. 2014), somatosensory information related to genital stimulation in the case of the parvicellular part of the subparafascicular thalamic nucleus (Veening and Coolen 1998; Coolen et al. 1997) and information related with gustarory/viscerosensorial stimulation for the case of the parabrachial nucleus (Bernard

et al. 1993). Regardless of the functional implication of each of these projections, which to our knowledge is unknown, it is possible that the Me and ACo function as integrative centres where vomeronasal and olfactory information is contextualized with somatosensory stimuli.

In conclusion, the ACo and Me seem to be nuclei where olfactory and vomeronasal information is integrated with highly processed somatosensory information. In addition, it is possible that they act like the first structures where synaptic plasticity takes place to associate olfactory and vomeronasal stimuli, working in synergy with the BLA where this learned association is finally stored. The CxA may be involved in odour processing similar to the olfactory processing performed by the Pir. The PMCo may function as the vomeronasal cortex of the amygdala, mainly processing the raw vomeronasal information and relaying it to the rest of the amygdaloid complex, similar to the role of the CxA/Pir with the odour stimuli within the olfactory cortex. The PLCo is the last cortical nuclei of the amygdala for which information about its connections is poorly described. It would be useful to describe its anatomical relations with the rest of the amygdala and brain structures to have a more complete picture of the amygdala connectivity.

4.1. Reference

Bader A, Breer H, Strotmann J (2012) Untypical connectivity from olfactory sensory neurons expressing OR37 into higher brain centers visualized by genetic tracing Histochem Cell Biol 137:615-628.

Bautze V, Schwack W, Breer H, Strotmann J (2014 Identification of a natural source for the OR37B ligand Chem Senses 39:27-38.

Bautze V, Bar R, Fissler B, Trapp M, Schmidt D, Beifuss U, Bufe B, Zufall F, Breer H, Strotmann J (2012) Mammalian-specific OR37 receptors are differentially activated by distinct odorous fatty aldehydes Chem Senses 37:479-493.

Bernard JF, Alden M, Besson JM (1993) The organization of the efferent projections from the pontine parabrachial area to the amygdaloid complex: a Phaseolus vulgaris leucoagglutinin (PHA-L) study in the rat. J Comp Neurol 329:201-229.

Cadiz-Moretti B, Martinez-Garcia F., Lanuza E (2013) Neural Substrate to Associate Odorants and Pheromones: Convergence of Projections from the Main and Accessory Olfactory Bulbs in Mice. In: Chemical Signals in Vertebrates 12, East ML, Dehnhard M, editors. Springer Science: New York. p 3-16.

Canteras NS. 2002. The medial hypothalamic defensive system: hodological organization and functional implications. Pharmacol Biochem Behav 71:481-491.

Coolen LM, Peters HJ, Veening JG (1997) Distribution of Fos immunoreactivity following mating versus anogenital investigation in the male rat brain. Neuroscience 77:1151-1161.

Cousens GA, Kearns A, Laterza F, Tundidor J (2012) Excitotoxic lesions of the medial amygdala attenuate olfactory fear-potentiated startle and conditioned freezing behavior. Behav Brain Res 229:427-432.

Cruikshank SJ, Edeline JM, Weinberger NM (1992) Stimulation at a site of auditory-somatosensory convergence in the medial geniculate nucleus is an effective unconditioned stimulus for fear conditioning. Behav Neurosci 106:471-483.

DiBenedictis BT, Ingraham KL, Baum MJ, Cherry JA (2012) Disruption of urinary odor preference and lordosis behavior in female mice given lesions of the medial amygdala Physiol Behav 105:554-559.

Dong HW, Swanson LW (2004) Projections from bed nuclei of the stria terminalis, posterior division: implications for cerebral hemisphere regulation of defensive and reproductive behaviors. J Comp Neurol 471:396-433.

Fleming AS, Suh EJ, Korsmit M, Rusak B (1994) Activation of Fos-like immunoreactivity in the medial preoptic area and limbic structures by maternal and social interactions in rats. Behav Neurosci 108:724-734.

Gutierrez-Castellanos N, Pardo-Bellver C, Martinez-Garcia F, Lanuza E (2014) The vomeronasal cortex - afferent and efferent projections of the posteromedial cortical nucleus of the amygdala in mice. Eur J Neurosci 39:141-158.

Kang N, Baum MJ, Cherry JA (2011) Different profiles of main and accessory olfactory bulb mitral/tufted cell projections revealed in mice using an anterograde tracer and a whole-mount, flattened cortex preparation Chem Senses 36:251-260.

Knapska E, Radwanska K, Werka T, Kaczmarek L (2007) Functional internal complexity of amygdala: focus on gene activity mapping after behavioral training and drugs of abuse. Physiol Rev 87:1113-1173.

Li Y, Dong X, Li S, Kirouac GJ (2014) Lesions of the posterior paraventricular nucleus of the thalamus attenuate fear expression. Front Behav Neurosci 8:94.

Maras PM, Petrulis A (2006) Chemosensory and steroid-responsive regions of the medial amygdala regulate distinct aspects of opposite-sex odor preference in male Syrian hamsters. Eur J Neurosci 24:3541-3552.

Moncho-Bogani J, Martinez-Garcia F, Novejarque A, Lanuza E (2005) Attraction to sexual pheromones and associated odorants in female mice involves activation of the reward system and basolateral amygdala. Eur J Neurosci 21:2186-2198.

Pfaus JG, Kleopoulos SP, Mobbs CV, Gibbs RB, Pfaff DW (1993) Sexual stimulation activates c-fos within estrogen-concentrating regions of the female rat forebrain Brain Res 624:253-267.

Pro-Sistiaga P, Mohedano-Moriano A, Ubeda-Banon I, Del Mar Arroyo-Jimenez M, Marcos P, Artacho-Perula E, Crespo C, Insausti R, Martinez-Marcos A (2007)

Convergence of olfactory and vomeronasal projections in the rat basal telencephalon. J Comp Neurol 504:346-362.

Rosen JB, Fanselow MS, Young SL, Sitcoske M, Maren S (1998) Immediate-early gene expression in the amygdala following footshock stress and contextual fear conditioning. Brain Res 796:132-142.

Simerly RB, Chang C, Muramatsu M, Swanson LW (1990) Distribution of androgen and estrogen receptor mRNA-containing cells in the rat brain: an in situ hybridization study. J Comp Neurol 294:76-95.

Swanson LW (2000) Cerebral hemisphere regulation of motivated behavior. Brain Res 886:113-164.

Veening JG, Coolen LM (1998) Neural activation following sexual behavior in the male and female rat brain Behav Brain Res 92:181-193.

5. GENERAL CONCLUSIONS

5. General Conclusions

1. The main (MOB) and accessory (AOB) olfactory bulbs send convergent projections to a restricted area of the anterior piriform (Pir) cortex, which is part of the olfactory cortex.

2. Within the amygdaloid complex, both olfactory bulbs project to the ventral part of the anterior amygdaloid area (AAV), the anterior (MeA) and posterodorsal (MePD) subdivisions of the medial amygdaloid nucleus, the bed nucleus of the accessory olfactory tract (BAOT), the anterior cortical amygdaloid nucleus (ACo), the cortex-amygdala transition zone (CxA) and the nucleus of the lateral olfactory tract (LOT). The ACo, CxA and LOT receive a predominant olfactory input, whereas the MeA, MePD, BAOT and AAV receive a predominant vomeronasal input.

3. Among the nuclei of the chemosensory amygdala, the MeA, MePD, ACo and CxA receive projections from the MOB and AOB that reach their layer II, and therefore may have a major functional relevance. The MeA display the highest amount of convergent projections from both olfactory bulbs.

4. The three subdivisions of the medial amygdaloid nucleus, the MeA, MePV and MePD, show in general a similar pattern of afferent connections, although minor differences were present among them.

5. The afferent connections to the MePD display the most important differences compared to the MeA and MePV, while these last two subdivisions are more similar between them. The MePD is more connected with the sexually dimorphic brain circuit, while the MeA

and MePV are, in a less specific manner, connected with areas related with reproductive and defensive behaviours.

6. The projections arising from the bulbs to the Me, ACo and CxA lack a topographic organization, with the exception of the projections originated by AOB to the MePD. In this case, the rostral part of the AOB sends more projections to the MePD than the caudal part of the AOB.

7. The three subdivisions of the medial amygdaloid nucleus (Me) and the ACo show an important afferent connection from the chemosensory amygdala, while the deep amygdaloid nuclei present minor afferent connections, with the exception of the basomedial nucleus. In addition, the subdivisions of the Me present a strong interconnection between them. On the other hand, the CxA shows moderate to scarce projections arising from the chemosensory amygdala, while the deep nuclei of the amygdala do not project to the CxA.

8. The bed nucleus if the stria terminalis (BST) does not send projections to the CxA and only the posterior part of the medial division and the intraamygdaloid division (BSTIA) of the BST present important projections to the Me and ACo. The posteriointermediate part of the medial division of the BST (BSTMPI) and BSTIA send more projections to the MeA, MePV and ACo compared to the MePD. On the other hand, the posteriomedial part of the medial division of the BST (BSTMPM) display more projections to the MePD than to the other corticomedial amygdaloid nuclei mentioned above.

9. The basal forebrain is a common input to the corticomedial nucleus of the amygdala. In general, the medial septum, diagonal band and striato-pallidum regions send afferent connections to the three subdivisions of the Me and to the ACo and CxA (with the exception of the medial septum which does not project to the CxA).

10. The hypothalamus sends, with few exceptions, minor projections to the Me and the ACo and does not send projections to the CxA. The ventral part of the premmamillary nucleus showed strong afferent connections to the posterior Me. The ventromedial hypothalamic nucleus mainly projects to the MeA and MePV, while the medial preoptic nucleus mainly projects to the MePD. Finally, the posterior hypothalamic area sends a moderate afferent projection to the MeA, MePV and ACo.

11. Within the thalamus and brainstem, the Me and ACo receive important projections arising from the posterior part of the paraventricular thalamus, posterior intralaminar thalamus and the parabrachial nucleus.

6. RESUMEN EN CASTELLANO

Del REGLAMENT SOBRE DIPÒSIT, AVALUACIÓ I DEFENSA DE LA TESI DOCTORAL de la Universitat de València:

Article 7.

Tesi doctoral presentada en una llengua diferent que les oficials de la Universitat de València

1. La Subcomissió de Doctorat pot autoritzar la lectura d'una tesi doctoral que haja estatredactada en qualsevol llengua d'ús científic, tècnic o artístic diferent de les oficials a laUniversitat de València.

2. En tot cas, a més de la documentació assenyalada d'aquesta normativa, el doctorand o doctoranda ha d'incloure en la tesi doctoral un resum ampli redactat en una de les llengües que són oficials a la Universitat de València, en el qual en tot cas ha de constar ***els objectius, la metodologia i les conclusions de la tesi****, amb una extensió màxima de 8.000 paraules.*

6.1 Objetivos

El objetivo de este proyecto de tesis es estudiar en ratones las bases neuroanatómicas del aprendizaje emocional apetitivo en el que se asocian olores con feromonas sexuales, las cuales son estímulos vomeronasales en estos animales. Los olores y feromonas sexuales son detectados por el epitelio olfatorio principal (MOE) y el órgano vomeronasal (VNO), respectivamente. El MOE proyecta al bulbo olfatorio principal (MOB) y el VNO proyecta al bulbo olfatorio accesorio (AOB). Estos bulbos mandan proyecciones directas a la amígdala, las cuales convergen o se solapan en algunos de los núcleos que la componen. Esta convergencia de la información vomeronasal y olfatoria en núcleos amigdalinos los convierte en posibles candidatos en donde podría ocurrir la asociación de olores y feromonas sexuales. Este tipo de aprendizaje emocional apetitivo juega un papel esencial en el correcto desarrollo de conductas sexuales relacionadas con la reproducción (Martínez-García et al. 2009; Griffiths and Brenan, 2014).

Para estudiar las bases anatómicas de este tipo de aprendizaje, nos planteamos los siguientes objetivos específicos:

Objetivo 1: trazado de conexiones de las proyecciones desde el MOB y AOB en núcleos corticales y no corticales de la amígdala e identificación de las posibles áreas de convergencia de estas proyecciones.

Los resultados de los experimentos llevados acabo para lograr este objetivo, indicaron que, de los núcleos corticales de la amígdala, la parte anterior de la amígdala medial (MeA), la parte posterodorsal de la amígdala medial (MePD), el área de transición córtico-amigdalina (CxA) y la amígdala cortical anterior (ACo) reciben proyecciones convergentes del AOB y MOB. A la luz de estos resultados, nos planteamos los dos siguientes objetivos de la tesis:

Objetivo 2: descripción de las proyecciones aferentes a las tres divisiones de la amígdala medial: la parte anterior (MeA), la parte posterodorsal (MePD) y la parte posteroventral (MePV).

El núcleo medial de la amígdala es, desde el punto de vista cualitativo, el mayor receptor de proyecciones convergentes de ambos sistemas olfatorios. Es por tanto

el principal candidato para jugar un papel clave en el aprendizaje olfativo-vomeronasal. Para poder interpretar el papel de este núcleo es necesario conocer el resto de sus aferencias, y en particular el detalle de dichas aferencias a sus diferentes subdivisiones, para las que se han propuesto diferentes funciones (Choi et al. 2005). Este estudio completa la descripción del patrón de conexiones de las subdivisiones de la amígdala medial, dado que las proyecciones eferentes se han estudiado previamente en nuestro laboratorio (Pardo-Bellver et al. 2012)

Objetivo 3: descripción del las aferencias de CxA y ACo.

Las dos estructuras de la amígdala cortical olfativa que reciben también una proyección desde el AOB son CxA y ACo. Ambas son estructuras para las que se desconoce su patrón de conexiones. Como primer paso para evaluar desde el punto de vista anatómico el posible papel de CxA y ACo en el aprendizaje olfativo-vomeronasal, y en coherencia con el Objetivo 2, describimos el patrón de aferencias de estas dos estructuras.

Los resultados de los experimentos realizados para alcanzar el objetivo 1 han sido ya publicados (Cádiz-Moretti et al. 2013). Los resultados relacionados con el Objetivo 2 se han remitido como manuscrito para su evaluación a la revista *Brain, Structure and Function*, y se encuentran en segunda revisión. Los resultados relacionados con el Objetivo 3 han dado lugar a un manuscrito que se remitirá en breve a la misma revista.

6.2 Metodología

Animales

Para este trabajo, utilizamos 105 ratones hembra (*Mus musculus*, CD1) de entre 8-27 semanas de edad que pesaban entre 24,7-53,2 g. Fueron estabuladas en cajas con comida y agua *ad libitum,* bajo un ciclo 12h día:noche a 25-26°C.

Cirugía e inyecciones de trazadores

Los primeros 29 animales fueron anestesiados con inyecciones intraperitoneales (IP) de una solución 3:2 de ketamina y medotomedina (76mg/kg), complementada con una inyección de atropina (0,04mg/kg, IP) para reducir la depresión cardio-

respiratoria. Los 76 animales restantes fueron operados usando un sistema de anestesia gaseosa en donde, a través de una mascara anestésica, los ratones inhalaban el anestésico isofluorano (2-2.5%) disuelto en oxígeno (1-1.3 L/min). Todos los animales recibieron una inyección subcutánea del analgésico butorfanol (5mg/kg). Después de fijar la cabeza en el aparato estereotáxico, realizamos un pequeño agujero en el cráneo sobre la estructura diana.

Experimento 1: Para estudiar las proyecciones eferentes desde el bulbo olfatorio accesorio (AOB) y el bulbo olfatorio principal (MOB), 37 animales recibieron inyecciones iontoforéticas de una dextranamina conjugada con tetrametilrodamina y biotina (TBDA) diluida al 5% en tampón fosfato (PB; 0,01M, pH 8,0)

Experimento 2: Para estudiar las aferencias a las tres subdivisiones de la amígdala medial, 28 animales recibieron inyecciones iontoforéticas del trazador retrogrado fluorescente Fluoro-Gold (FG) diluido al 2% en agua destilada.

Experimento 3: Para estudiar las aferencias a la zona de transición cortico-amigdalina (CxA) y a la amígdala cortical anterior (ACo), 40 ratones recibieron inyecciones iontoforéticas del trazador retrógrado FG. Adicionalmente, para minimizar el uso de ratones y estudiar las proyecciones eferentes de CxA y ACo, inyectamos en el hemisferio contralateral, el trazador anterógrado dextranamina conjugado con biotina (BDA) diluido al 5% en PB (0,01M, pH 8,0) (los resultados de las proyecciones eferentes de estos núcleos serán analizados en un estudio posterior).

Los trazadores fueron inyectados a través de micropipetas de vidrio aplicando pulsos de corriente positiva. Para evitar la difusión del trazador a lo largo del recorrido de la pipeta, aplicamos corriente de retención al introducir y extraer la micropipeta. Adicionalmente, dejamos la punta en el lugar de la inyección durante 5-10 minutos para evitar el reflujo del trazador. Las coordenadas de inyección para el AOB, MOB, MeA, MePD, MePV, CxA y ACo fueron modificadas para la cepa CD1 a partir del atlas de ratón (Paxinos y Franklin, 2004).

Después de finalizar las inyecciones, cerramos la piel del cráneo con Histoacryl y en el caso de aquellos animales que operamos con ketamina/medotomedina,

colocamos una inyección intramuscular de atipamezol (1ml/Kg) para revertir los efectos de la medotomedina. Durante todo el procedimiento, mantuvimos el calor corporal de los ratones operándolos sobre una manta térmica y hidratamos sus ojos con gotas oculares.

Histología

Después de 3-5 días de supervivencia para el experimento 1 y 6-8 días para los experimentos 2 y 3, les inyectamos a los ratones una sobredosis de pentobarbital sódico (90 mg/kg, IP) y los perfundimos transcardialmente con suero salino (0,9%) y una solución de fijadora de paraformaldehído al 4% en PB (0,01M, pH 7,6). Tras la perfusión, extrajimos los cerebros del cráneo, los post-fijamos en la misma solución fijadora y los crioprotegimos en una solución de sacarosa al 30% en PB (0,01M, pH 7,6). Con un microtomo de congelación, cortamos secciones parasagitales de los bulbos (30 μm) y coronales (40 μm) del resto de encéfalo obteniendo cuatro series paralelas.

Para visualizar la TBDA y BDA, primero inactivamos las peroxidasas endógenas del tejido con una solución de H_2O_2 al 1% en tampón Tris salino (TBS; 0,05M, ph 7,6) durante 15 minutos y luego las incubamos en el complejo ABC diluido 1:50 en TBS-Tx (Triton X-100 0.3% en TBS 0.05 M pH 7.6) a temperatura ambiente durante 90 minutos. Posteriormente, lavamos las secciones con TBS y revelamos la actividad peroxidada con una solución de diaminobenzidina al 0,025%, H_2O_2 al 0,01% y sulfato de amonio y níquel al 0,1% en PB (0.1 M, pH 8.0), obteniendo un precipitado negro.

En los casos en los que realizamos inyecciones de FG, primero visualizamos la localización de la inyección mirando las series en un microscopio de fluorescencia para posteriormente proceder a detección del FG a través de una inmunoperoxidasa. Para hacer esto, primero inactivamos la peroxidada endógena del tejido como describimos anteriormente para la BDA. En aquellos casos en donde realizamos una inyección contralateral de BDA, no repetimos este paso ya que la detección de la BDA la realizamos previamente como describimos en el párrafo anterior. Luego, incubamos las series en una solución de bloqueo de TBS-Tx que contenía suero normal de cabra (NGS) al 8% y seroalbumina bovina (BSA)

al 4% durante dos horas a temperatura ambiente. A continuación, incubamos las secciones secuencialmente en: el anticuerpo primario anti-FluoroGold diluido a 1:3000 en TBS-Tx con NGS al 4% y BSA al 2% durante la noche a 4°C; el anticuerpo secundario (IgG de cabra anti-conejo) biotinilado diluido 1:200 en TBS-Tx con NGS al 4% durante dos horas a temperatura ambiente; y ABC elite diluido 1:50 en TBS-Tx durante 2 horas a temperatura ambiente. Finalmente revelamos la peroxidada en una solución de diaminobenzidina al 0,025% y H_2O_2 al 0,01% en PB (0.1 M, pH 8.0), obteniendo un precipitado café.

Montamos las series en portas gelatinizados y luego las deshidratamos gradualmente en alcoholes, las aclaramos en xileno y las cubrimos con Entellan. Para facilitarnos la identificación de las estructuras que mostraban marcaje anterógrado o retrógrado, en el experimento 1 antes de cubrir los portas contrastamos el tejido con la tinción de Nissl. En los experimentos 2 y 3, en la mayoría de los casos, procesamos una segunda serie para la inmunohistoquímica del FG y las contrastamos con la tinción de Nissl (experimento 2) o, en algunos casos, procesamos una segunda serie con el método de Nissl con el objetivo visualizar la citoarquitectura (experimento 3).

Adquisición y procesamiento de imágenes

Observamos las secciones utilizando un microscopio Olympus CX41RF-5 y las fotografiamos con una cámara digital Olympus XC50. Las imágenes fluorescentes de los sitios de inyección de FG las tomamos con un microscopio de fluorescencia equipado con una cámara digital. Las imágenes fueron procesadas con Adobe Photoshop y las ilustraciones y paneles de figuras las hicimos en Adobe PhotoShop e Illustrator.

6.3 Conclusiones

1. El bulbo olfatorio principal (MOB) y accesorio (AOB) proyectan convergentemente a un área del córtex olfatorio. Ésta es una área restringida del la corteza piriforme (Pir) anterior.
2. Dentro del complejo amigdalino, ambos bulbos olfatorios proyectan a la amígdala anterior ventral (AAV), a la subdivisión anterior (MeA) y posterodorsal (MePD) de la amígdala medial, al núcleo del tracto olfatorio

accesorio (BAOT), a la amígala cortical anterior (ACo), a la corteza de transición amigdalina (CxA) y al núcleo del tracto olfatorio lateral (LOT). Las estructuras ACo, CxA y LOT reciben proyecciones predominantemente olfatorias, mientras que MeA, MePD, BAOT y AAV reciben proyecciones predominantemente vomeronasales.

3. Dentro de los núcleos amigdalinos quimiosensoriales, la MeA, MePD, ACo y CxA reciben proyecciones provenientes tanto del MOB como del AOB, que terminan en su capa II y por lo tanto es probable que sean funcionalmente relevantes. La MeA presenta el mayor grado de convergencia de las proyecciones provenientes de ambos bulbos olfatorios.
4. Las tres subdivisiones de la amígdala medial (Me), que corresponden a la MeA, MePV y MePD presentan, en general, un patrón de aferencias similar con algunas diferencias menores entre ellas.
5. Al comparar las aferencias a las tres subdivisiones de la Me, la MePD muestra los inputs más diferentes entre ellas mientras que las aferencias a la MeA y MePV son similares entre sí. La MePD está más conectada con el circuito cerebral sexualmente dimórfico, mientras que la MeA y la MePV están, de una manera menos específica, conectadas con áreas relacionadas a conductas reproductivas y defensivas.
6. Las proyecciones provenientes del los bulbos a la Me, ACo y CxA no están organizadas de una manera topográfica, con la excepción de las proyecciones originadas desde el AOB al MePD. En este caso, la parte rostral de AOB envía mas proyecciones al MePD que la parte caudal del AOB.
7. Las tres subdivisiones de la Me y el ACo reciben una conexión aferente importante desde la amígdala quimiosensorial, mientras que las proyecciones de la amígdala profunda hacia estos núcleos son menores, con la excepción del núcleo basomedial. Adicionalmente, las tres subdivisiones de la Me están fuertemente interconectadas. Por otro lado, la CxA muestra proyecciones moderadas o escasas provenientes de la amígdala quimiosensorial, mientras que los núcleos amigdalinos profundos no proyectan a CxA.
8. El núcleo de la estría terminalis (BST) no proyecta a CxA y solo la parte posterior de su división medial y su división intraamigdalina (BSTIA)

presentan aferencias importantes a la Me y ACo. La parte posterointermedia de la división medial de BST (BSTMPI) y BSTIA proyectan mas a MeA, MePV y ACo comparada con su proyección a MePD. Por el contrario, la parte posteromedial de la división medial del BST (BSTMPM) proyecta más a MePD que a los otros núcleos corticoamigdalinos mencionados anteriormente.

9. El prosencéfalo basal proyecta de manera común a los núcleos amigdalinos. En general, el septum medial, la banda diagonal y las regiones striato-palidales presentan aferencias a las tres subdivisiones de la Me y en menor grado al ACo y la CxA (con excepción del septum medial, que no proyecta a la CxA).
10. El hipotálamo, no proyecta a CxA, mientras que presenta proyecciones menores a Me y ACo, con algunas excepciones. La parte ventral del núcleo premamilar muestra aferencias importantes a la parte posterior de Me. El núcleo ventromedial hipotalámico proyecta principalmente a la MeA y MePV, mientras que el núcleo medial preóptico proyecta principalmente a la MePD. Finalmente, el área hipotalámica posterior presenta aferencias moderadas a la MeA, MePV y ACo.
11. Respecto al tálamo y al tronco del encéfalo, la Me y ACo reciben proyecciones importantes provenientes del la parte posterior del tálamo paraventricular, así como de la parte posterior del tálamo intralaminar

6.4 Bibliografía

Cadiz-Moretti B, Martinez-Garcia F., Lanuza E (2013) Neural Substrate to Associate Odorants and Pheromones: Convergence of Projections from the Main and Accessory Olfactory Bulbs in Mice. In: Chemical Signals in Vertebrates 12, East ML, Dehnhard M, editors. Springer Science: New York. p 3-16.

Choi GB, Dong HW, Murphy AJ, Valenzuela DM, Yancopoulos GD, Swanson LW, Anderson DJ (2005) Lhx6 delineates a pathway mediating innate reproductive behaviors from the amygdala to the hypothalamus. Neuron 46:647-660.

Griffiths PR, Brennan PA (2014) Roles for learning in mammalian chemosensory responses. Horm Behav .

Martínez-García F, Novejarque A, Lanuza E (2009) Evolution of the amygdala in vertebrates. In: Evolutionary Neuroscience, J Kaas, editor. Elsevier Academic Press: Oxford (U.K.). p 313-392.

Pardo-Bellver C, Cadiz-Moretti B, Novejarque A, Martinez-Garcia F, Lanuza E (2012) Differential efferent projections of the anterior, posteroventral, and posterodorsal subdivisions of the medial amygdala in mice. Front Neuroanat 6:33.